A LABORATORY INVESTIGATION OF THE STRUCTURAL DESIGN OF BITUMINOUS MIXTURES

SEPTEMBER, 1966

NO. 15

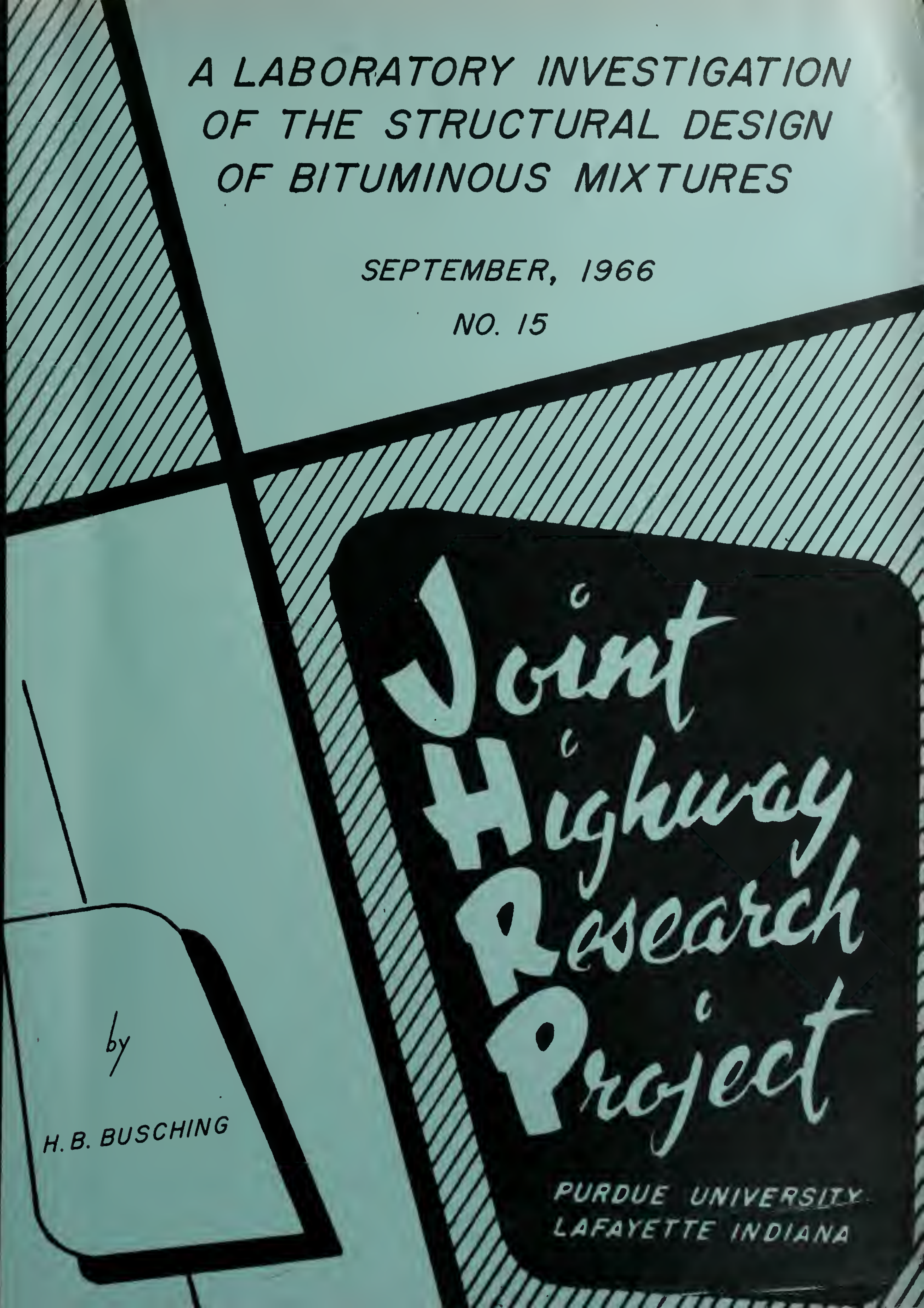

by

H. B. BUSCHING

Joint
Highway
Research
Project

PURDUE UNIVERSITY
LAFAYETTE INDIANA

Progress Report

A LABORATORY INVESTIGATION OF THE STRUCTURAL DESIGN OF BITUMINOUS MIXTURES

TO: G. A. Leonards, Director
Joint Highway Research Project

August 10, 1966

FROM: H. L. Michael, Associate Director
Joint Highway Research Project

File: 2-5-23
Project: C-36-8W

Attached is a report entitled "A Laboratory Investigation of the Structural Design of Bituminous Mixtures." The report was prepared by Mr. H. W. Busching under the direction of Professor W. H. Goetz and with the assistance of Professor M. E. Harr. Mr. Busching used this report as his thesis for the Ph.D. degree.

The report will be transmitted to the Bureau of Public Roads for their review, comments and approval. This report constitutes the Final Report on Phase I of the Structural Design HPR project.

It is proposed that a paper and an oral presentation of material from this report be given at the annual meeting of the Association of Asphalt Paving Technologists in Denver, Colorado in February, 1967. It is requested that project funds be made available to cover transportation and per diem expenses incurred during presentation of the paper.

The report is submitted to the Board for the record, and for action on the above request.

Respectfully submitted,

Harold L. Michael

Harold L. Michael
Associate Director

HLM:jgs

Attachment

Copy:
F. L. Ashbaucher
J. R. Cooper
J. W. Delleur
W. L. Dolch
W. H. Goetz
W. L. Grecco
G. K. Hallock
F. S. Hill
J. F. McLaughlin
F. B. Mendenhall
R. D. Miles
J. C. Oppenlander
W. P. Privette
M. B. Scott
F. W. Stubbs
K. B. Woods
E. J. Yoder

Digitized by the Internet Archive
in 2011 with funding from
LYRASIS members and Sloan Foundation; Indiana Department of Transportation

http://www.archive.org/details/laboratoryinvest00busc

Progress Report

A LABORATORY INVESTIGATION OF THE STRUCTURAL DESIGN OF BITUMINOUS MIXTURES

By

H. W. Busching, Graduate Assistant

and

W. H. Goetz, Professor of Highway Engineering

Joint Highway Research Project

Project: C-36-8W

File: 2-5-23

Prepared as Part of an Investigation

Conducted by

Joint Highway Research Project
Engineering Experiment Station
Purdue University

in cooperation with

Indiana State Highway Commission

and the

Bureau of Public Roads
U.S. Department of Commerce

Not Released for Publication

Subject to Change

Not Reviewed by
Indiana State Highway Commission
or the
Bureau of Public Roads

Purdue University
Lafayette, Indiana
August 10, 1966

ACKNOWLEDGMENTS

The author is indebted to several persons who provided assistance during the course of this research. Professor W. H. Goetz and Professor M. E. Harr, who were the author's thesis advisors, provided counsel and encouragement that was appreciated throughout the study.

Particularly stimulating and helpful during various portions of the research were conversations with Professor R. A. Schapery, Professor E. O. Stitz and Professor S. K. Suddarth.

Special thanks also go to the author's wife whose patience and understanding aided the successful completion of this investigation.

TABLE OF CONTENTS

Page

LIST OF TABLES.................................. v

LIST OF FIGURES................................. vii

ABSTRACT.. ix

INTRODUCTION.................................... 1

REVIEW OF LITERATURE............................ 5

    General References.......................... 5
    Specific Research........................... 9

DEVELOPMENT OF THEORY........................... 13

    General Assumptions......................... 13
    Material Coefficients for Transverse Anisotropy... 16
    Evaluation of Material Coefficients......... 22

EXPERIMENTAL INVESTIGATION OF THEORY............ 27

    Uniaxial Compression Tests.................. 28
    Direct Shear Test........................... 30
    Uniaxial Compression with Volume Change Measurements............ 30
    Torsion Test................................ 36

RESULTS OF TESTS AND DISCUSSION................. 41

    Uniaxial Compression Test Results........... 41
        Stiffness Moduli, E_1 and E_3 41
        Poisson's Ratio......................... 48
    Uniaxial Compression Test Results with Volume Change Measurements........ 60
    Direct Shear Test Results................... 64
    Comparison of Shear and Torsion Test Results...... 68

SUMMARY OF RESULTS AND CONCLUSIONS.............. 78

SUGGESTIONS FOR FURTHER RESEARCH................ 81

LIST OF REFERENCES.............................. 83

Page

APPENDIX A: NOTATION.................................... 87

APPENDIX B: MATERIALS AND PREPARATION OF SPECIMENS..... 91

APPENDIX C: INSTRUMENTATION............................ 103

APPENDIX D: TABULATED TEST RESULTS..................... 110

APPENDIX E: STRESS-STRAIN RELATIONSHIPS................ 113

VITA... 114

LIST OF TABLES

Table | Page

1. Typical Data Sheet for Uniaxial Compression Test.......... 32
2. Typical Data Sheet for Shear Test.......... 33
3. Sample Calculation of the Coefficient of Linear Correlation for Log $E_3(t)$ on Log t.......... 46
4. Sample Calculation of the Coefficient of Linear Correlation for Transverse Strain on Longitudinal Strain (Poisson's Ratio).......... 50
5. Poisson's Ratios Obtained from Uniaxial Compression Tests.......... 51
6. Poisson's Ratios, $\mu_{21} + \mu_{31}$, Obtained from Uniaxial Compression Test with Volume Change Measurement.......... 57
7. Poisson's Ratio, μ_{13}, Obtained from Uniaxial Compression Test with Volume Change Measurement.......... 58
8. Torsion Modulus (psi x 10^{-4}).......... 70
9. Shear Modulus (psi x 10^{-4}).......... 71
10. Intercepts of Torsion and Shear Moduli for Loading Time of Thirty Seconds.......... 75
11. Least Squares Logarithmic Slopes of Torsion and Shear Moduli on Time.......... 76
12. 95% Confidence Intervals for Shear and Torsion Moduli.......... 77
13. Sieve Analysis of Aggregates.......... 93
14. Results of Tests on Asphalt Cement.......... 94
15. Sample Calculations for Cantilever Transducer.... 105

Table Page

16. Typical Format for Transducer Calibration Metal Foil Strain Gages)........................ 109

17. Stiffness Moduli ($x10^{-4}$psi)........................ 110

18. Shear Moduli ($x10^{-4}$psi)........................ 112

LIST OF FIGURES

Figure Page

1. Schematic Diagram of Deterministic Process....... 14

2. Typical Element and Coordinate System............ 18

3. Uniaxial Compression Specimen with Transducers and Holders.......................... 29

4. Typical Graphical Data for Compression, Shear and Torsion Tests........................ 31

5. Direct Shear Specimen and Specimen Holder........ 34

6. Shear Specimen and Holder........................ 35

7. Triaxial Cell with Pipet and Recorder............ 37

8. Torsion Specimen Holders......................... 39

9. Torsion Specimen and Displacement Transducer..... 40

10. Compression and Shear Moduli vs. Time, 70°, 80°, 90°F.................................. 42

11. Shearing Strain vs. Time (0.5 Sec. ≤ Time ≤ 30 Sec.)...................... 44

12. E_3/E_1 vs. Time.................................. 47

13. Transverse Strain vs. Longitudinal Strain and Slopes Defining Poisson's Ratio.............. 49

14. Histrogram for Poisson's Ratio Obtained from Uniaxial Compression Tests................. 53

15. Possible Loading That Changes Original Transverse Gage Length.......................... 54

16. Surface Irregularities after Compression......... 56

17. Poisson's Ratio vs. Time from Volume Change Measurements......................... 59

18. Shear Modulus vs. Time, 70°F..................... 65

Figure Page

19. Shear Modulus vs. Time, 80°F.................... 66

20. Shear Modulus vs. Time, 90°F.................... 67

21. Comparison of Torsion and Shear Moduli - 23.1 psi.......................... 72

22. Comparison of Torsion and Shear Moduli - 40.8 psi.......................... 73

23. Comparison of Torsion and Shear Moduli - 58.3 psi.......................... 74

24. Orientation of Beam of Compacted Bituminous Material Showing Notation Convention............ 88

25. Gradation Curve for Bituminous Mixture.......... 92

26. Mold and Tamping Foot for Compacting Beam of Bituminous Mixture...................... 95

27. Uniaxial Compression Specimens with Jig for Sizing................................ 97

28. Jig for Specimen Alignment...................... 98

29. Uniaxial Compression Specimen with Base, Top and Alignment Jig........................... 100

30. Interior of Constant Temperature Room Showing Test Stand and Recorder................. 101

31. Schematic Diagram of Displacement Transducer and Wheatstone Bridge........................... 106

32. Displacement Transducer......................... 108

ABSTRACT

Busching, Herbert William. Ph.D., Purdue University, January, 1967. A Laboratory Investigation of the Structural Design of Bituminous Mixtures. Major Professor: William H. Goetz.

This research was undertaken to investigate theory and tests that would be useful in describing the behavior of transversely anisotropic bituminous mixtures. It was also the purpose of this study to instrument a typical element of bituminous mixture to obtain measurements that could be used in describing the stress-deformation behavior of the material tested. The theory and testing procedures were complementary and provided quantitative parameters that describe the response of a bituminous mixture subjected to creep loading.

Laboratory tests undertaken to substantiate the theory include uniaxial compression, direct shear, uniaxial compression with volume change measurements and torsion tests.

The matrix equation that was derived and can be used to describe the behavior of transversely anisotropic, nonconservative, statistically homogeneous materials subject to small strains is as follows:

$$\begin{bmatrix} \epsilon_1 \\ \epsilon_2 \\ \epsilon_3 \\ \epsilon_4 \\ \epsilon_5 \\ \epsilon_6 \end{bmatrix} = \begin{bmatrix} \frac{1}{E_1} & \frac{\mu_{21}}{E_1} & \frac{\mu_{13}}{E_3} & 0 & 0 & 0 \\ \frac{\mu_{21}}{E_1} & \frac{1}{E_1} & \frac{\mu_{13}}{E_3} & 0 & 0 & 0 \\ \frac{\mu_{31}}{E_1} & \frac{\mu_{31}}{E_1} & \frac{1}{E_3} & 0 & 0 & 0 \\ 0 & 0 & 0 & \frac{1}{G_{13}} & 0 & 0 \\ 0 & 0 & 0 & 0 & \frac{1}{G_{13}} & 0 \\ 0 & 0 & 0 & 0 & 0 & \frac{2(1-\mu_{21})}{E_1} \end{bmatrix} \begin{bmatrix} \sigma_1 \\ \sigma_2 \\ \sigma_3 \\ \sigma_4 \\ \sigma_5 \\ \sigma_6 \end{bmatrix}$$

Torsion and shear tests were performed to determine the invariance of one element of the material coefficient matrix. Good agreement was noted for the moduli obtained from these two tests with different boundary conditions.

Stiffness and shear moduli as well as values of Poisson's ratios were obtained for various orientations within the mixture. Testing results for the mixture compacted in the laboratory substantiated the anisotropic nature of the material. Three loads applied at three test temperatures were utilized in determining the coefficients that could be used to describe behavior of the material.

Mixture stiffness was found to be greater in the direction of the applied compactive forces than in orthogonal directions. Additional work is necessary to measure Poisson's ratios accurately by means of volume change measurements when small strains prevail.

The results of this investigation indicate that the concepts of the research have potential application when utilized in the design of bituminous mixtures. The concepts and parameters verified in laboratory testing have possible use in proportioning constituents of bituminous mixtures as well as in unifying mixture design and pavement design procedures.

INTRODUCTION

Bituminous mixtures are being used in modern highways as wearing courses as well as load-distributing layers. In these applications both the bituminous material and the aggregate serve as structural elements. Recent emphasis (35) (23) has been placed upon specifying more exactly the role of bituminous materials and mixtures when used in any position in a layered system.

Currently used design methods (30) employ stability numbers that may provide some measure of statistical quality control, but do not relate mixture constituents to loads imposed on the pavement. Moreover, the response of the mixture to load in useful engineering units such as stress and strain is not considered.

At the present time no single theory of material behavior which considers time-dependent characteristics of bituminous mixtures is widely used in the design of flexible pavements. Actually, bituminous mixtures exhibit both time- and temperature-dependent behavior. Evaluation of the dependence of bituminous mixtures on time and temperature is important in predicting mixture behavior under traffic-load-associated stresses as well as non-traffic-load-associated stresses.

Approximate analyses of the time-dependent deformation of bituminous mixtures have been made within the theory of linear viscoelasticity. The difficulties associated with nonlinear behavior of the material and the inversion of transformed viscoelastic solutions, however, have been deterrents to the general application of this theory to the design of flexible pavements and bituminous mixtures. In addition to this, the correspondence principle requires that before the viscoelastic solution can be obtained, the associated elastic problem must be amenable to solution. It should be noted from this discussion that viscoelasticity solutions depend on elasticity solutions while elasticity solutions, in turn, depend on conditions and assumptions related to the mechanical response of the material under consideration. Therefore, a basic approach in describing the mechanical behavior of material starts with the laws of physics applicable to continuous media.

Physical testing of typical material elements is required for determining what constitutive mechanical relations exist for particular materials. The typical element may or may not be statistically homogeneous and isotropic. In addition, phenomena at the atomic and molecular levels which contribute to the complex mechanisms that relate input and output for a typical element may be evaluated quantitatively, provided these phenomena contribute some measureable mechanical response.

Hence, the theory of mechanics of deformable bodies provides a sufficiently general framework within which constituents

of bituminous mixtures can be evaluated and pavement response to traffic- and temperature-induced stress can be predicted.

The general theory of continuum mechanics incorporates the general equations of motion in three dimensions and the mathematical definitions of strain which are valid for all materials. Besides this, some approximation of material behavior is used to relate material response to stress. The theory of elasticity is often used to analyze materials that are assumed to be homogeneous, isotropic and time-independent; however, this is merely a special case of the general theory of the mechanical behavior of materials.

Cauchy's generalized statement of material behavior which is utilized in this study states that a relationship between stress and strain exists. It is possible to evaluate the time and temperature dependence of stress and strain within the framework of this general statement.

Because bituminous mixtures are placed in layers that differ on the basis of composition, thickness and state of compaction, it is reasonable to hypothesize that the material will behave as a transversely anisotropic material. A transversely anisotropic, or hexagonal, material (20) has one axis of rotational symmetry. Hence, deformation response of the material to stress will be direction-dependent.

Material coefficients similar to those of the hexagonal system may be used to describe layered systems of this type. Six material coefficients exist for a statistically homogeneous, nonconservative and transversely anisotropic material

analogous to the two material constants that exist for homogeneous, elastic isotropic bodies.

This investigation was undertaken to instrument a typical element of bituminous mixture and to evaluate the six material coefficients for a bituminous mixture compacted in the laboratory. Since the material coefficients are functions of time and temperature, they may be used to relate stresses and strains that develop in transversely anisotropic material subject to loads of varying duration applied throughout a range of temperatures.

REVIEW OF LITERATURE

This review of literature presents two aspects of mechanistic description and evaluation of materials. The first portion summarizes some important observations from continuum mechanics and general material behavior, while the second portion presents a resumé of some contributions to the evaluation of bituminous mixture behavior.

General References

Initial investigations of the mechanical behavior of materials are centuries old. The theory of elasticity as it is utilized today received important experimental and theoretical contributions from Hooke, Cauchy, Navier, and others (9) (12) (27). Todhunter and Pearson (46) have summarized the historical development of the theory of elasticity and Love (27) has presented a classic account of mathematical aspects of many problems in elasticity. Several texts concerning elasticity (9) (14) (42) present ample theory and applications requisite to an understanding of the deformation of homogenous, isotropic, elastic bodies under applied stresses.

In reality, however, the materials that are used in structural applications are not completely homogeneous, isotropic or elastic. Freudenthal (15) writes "...the assumptions of homogeneity, isotropy and time-independent elasticity are irreconcilable with the phenomena of fatigue, time- and temperature-

sensitive cohesive strength and creep of real materials." Even materials that are apparently elastic reveal inelastic behavior when subject to closer examination (10) (33) (51).

Although the solution of elastic stress distribution problems in isotropic material has been considered in great detail, until recent time comparatively little work has been done on similar problems in anisotropic materials. One reason why only limited data are available for anisotropic materials is given by Hearmon (20):

> The solutions in anisotropic elasticity often lead to calculations which are extremely difficult or even prohibitively difficult by hand methods. The increasing availability of electronic computers may enable these calculations to be carried out more readily in the future...

Many of the materials that exist in nature, however, exhibit anisotropy. Voigt (47), Cady (5) and others (22) describe the anisotropic behavior of some classes of crystals. Barden (1) cites reports of anisotropy in geologic formations such as shales and mudstones and some natural deposits of clays. Roscoe and Schofield (40) and others (26) (39) have promoted concepts of anisotropic behavior in soils and bituminous mixtures. Orthotropic anisotropy has been recognized for several decades by researchers in forestry. Jayne and Suddarth (21) state that, "With but few exceptions fibrous materials, whether of natural origin or reconstituted can be classified physically as orthogonally anisotropic or, more commonly, as orthotropic." More recent experimental investigations (8) (17) (18) (44) have indicated the validity of

anisotropic material analyses for wood and filament-reinforced materials.

Michell (29) and Wolf (49) made early contributions to the theory of anisotropic elasticity by determining deflections of a transversely anisotropic material loaded on its surface. Both Lehknitskii (25) and Hearmon (20) present solutions to broad classes of problems in the theory of anisotropic elasticity.

Elliott (11) presents solutions of problems in three dimensions that can be found in terms of two harmonic functions. He gives expressions for displacements and stresses in elastic crystals in terms of harmonic functions and elastic moduli. Elliott represents stress distributions in various metals in a radius vector plot where the length of the vector is proportional to the magnitude of stress.

A summary of three-dimensional stress distributions for various loadings on a homogeneous anisotropic elastic half-space is presented in Mededelingen (28). The effect of various values of Poisson's ratios on the stress distribution is shown.

Considerations of material dependence on time and temperature are well documented in the literature of viscoelastic analysis (3) (10). Schapery (41), Williams (48), Perloff and Moavenzadeh (36) and others present viscoelasticity solutions for time-dependent stress distributions.

Although time- and temperature-dependent behavior of materials is discussed within the framework of a viscoelastic analysis, the correspondence principle requires that the

corresponding elasticity problem be amenable to analysis before the viscoelastic or time-dependent solution assumes a time-dependent form. Inversion of the transform is not always easy or even possible; however, Schapery (41) has presented methods of inversion that permit approximate solutions to be obtained for many problems.

While current literature contains few references to the use of the general theory of elasticity in time- and temperature-dependent problems, some researchers (16) (45) have reported marked variations in the elastic constants for isotropic materials when time and temperature conditions are changed during testing. Everett and Miklowitz (13) present data that show changes in Young's modulus and Poisson's ratio for metals tested to 1500°F.

Van der Poel (37) records the time-dependent stiffnesses of bituminous mixtures. Polakowski and Ripling (38) recognize the time and temperature dependence of materials and present graphical data for stress-strain-time relationships for high impact polystyrene at room temperature and 125°F.

Classical derivations of the elastic constants by Love (27) and Filonenko-Borodich (14) have utilized the strain-energy function to establish relationships among the constants. Derivations of elastic constants which utilize the strain-energy function involve assumptions that the work of deformation is conserved when deforming forces are removed. This precludes the use of these elasticity coefficients in describing the behavior of nonconservative material. Bolotin (4) states

that internal strain energy is not a state function for inelastic materials.

To avoid application of a theory based on strain-energy concepts to the behavior of nonconservative materials requires the derivation of coefficients as presented in the next section - development of theory. The coefficient matrix described in the next section is not identical with that obtained by Love (27) and others (5) (47) for transversely anisotropic material because it is not symmetric and the elements of the matrix may assume forms that, in contradistinction to the approach utilizing strain-energy concepts, permit accumulation of permanent deformation.

Specific Research

The second portion of the review of literature presents a resumé of some specific developments in bituminous mixture evaluation. Emphasis is placed on those tests in which evaluation of material behavior is made with recognition of temporal and thermal dependence.

The purposes for which materials are tested are given by Nijboer (34) as follows:

1. To recognize the material
2. To control its manufacture
3. To determine the properties which are decisive for its application

Present design methods and associated tests (30) do not consider material response over a range of loading times and temperatures and hence no quantitative descriptive parameter

is provided by these design methods. Although the test results may be independent of the boundary conditions, no measure of this independence is assessed.

Lee and Marwick (24) showed that a bituminous mixture deforms at different rates. The intial, secondary and tertiary portions of the strain vs. time curve for a particular mixture might be used as descriptive parameters for the mixture. This hypothesis was substantiated by the results of several different types of tests on bituminous mixtures. Because tests with different boundary conditions yielded similar strain vs. time relationships, the authors inferred that the deformation vs. time relationship was a unique parameter of the mixture.

Van der Poel (37) noted that at low temperatures and short times of loading the stiffnesses of the bituminous materials he tested were asymptotic to approximately the same value. He stated:

> Under these conditions the material is purely elastic in the sense of classical mechanics and consequently the stiffness can be termed Young's modulus in this case.

For a limited range, Wood and Goetz (50) found that a linear relationship existed between log-permanent deformation and log-number of load repetitions. Other researchers (31) have verified a linear log-strain vs. log-time relationship for bituminous mixtures. It is possible that the slopes of these lines reflect the response of the mixture to different loads; however, invariance of the response to boundary conditions was not evaluated.

Lal (23) found that for several different temperatures and loads, deformation vs. time relationships were linear on log-log plots. By utilizing several different tests, he determined invariant properties of a sheet asphalt mixture. The invariant functions found by Lal describe stresses as functions of time, temperature, strain and strain rate. The invariance of the resulting expressions was determined to be valid for strains up to 0.4 percent.

Monismith (31) presented creep data obtained from both tension and compression tests at 40°F. The strains obtained from the two types of tests were similar for a loading time of five minutes. Invariance of strain was noted for axial stresses up to 77 psi and axial strains of approximately 0.1 percent.

Other researchers (35) have used the complex modulus to characterize bituminous mixtures, but tests with different boundary conditions were not considered.

This brief review of literature indicates that the response of bituminous mixtures has been widely investigated in the laboratory and several parameters have been established which might be used to characterize mixture behavior. Only a few researchers have established invariant properties of bituminous mixtures that could be utilized for the prediction of performance. It appears, however, that experimental and theoretical justification exists for investigating bituminous mixture behavior for the purpose of establishing invariant parameters

that may be used to predict mixture performance. The mathematical theory of contiuum mechanics appears to be a sufficiently general framework within which experimental investigations can be made.

DEVELOPMENT OF THEORY

The development of theory concerns three specific areas. The presentation in this section includes general assumptions, material coefficients for transverse anisotropy and evaluation of material coefficients.

General Assumptions

The theory underlying the experimental work is based on the assumption that a bituminous mixture will behave as a mechanically deterministic system. In this particular case, a determinable relationship between strains and imposed stresses is sought. Figure 1 shows schematically the relationship that is hypothesized.

The transfer functions or operators that are sought are the $C_{ij}(t, T, \sigma_{ij}, \ldots)$ that allow determination of the output if the input conditions are known. This is of particular interest at the present time since recent research projects have been concerned with description of pavement behavior as well as boundary loading conditions.

The mechanical response to be measured is deformation. The expression of small deformations in differential form enables one to note the range and variety of variables that might be studied by this type of investigation. Hence:

$$du(t,T,\sigma,\ldots) = \frac{\partial u}{\partial t}dt + \frac{\partial u}{\partial T}dT + \frac{\partial u}{\partial \sigma}d\sigma + \ldots$$

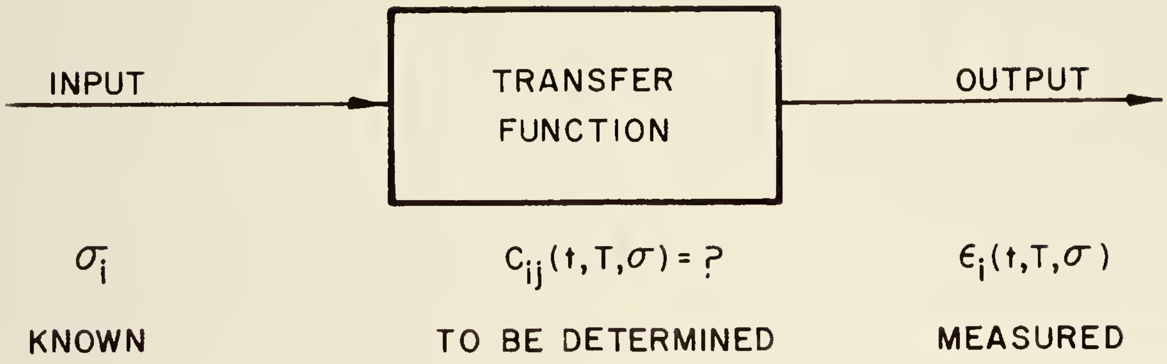

FIGURE I. SCHEMATIC DIAGRAM OF DETERMINISTIC PROCESS

The three dots indicate a continuation of the terms in the total differential and may include consideration of terms such as dependence of the deformation of the mixture upon moisture, steric hardening, cycle of loads and other factors. In this study, deformation was related specifically to stress magnitude, time and temperature. It is recognized that truncation of the series that describes the differential deformation would introduce some error into the validity of applying the relations obtained in the laboratory to field problems. The discrepancies are admitted and further studies will be needed to evaluate them quantitatively. As far as possible, other factors that might influence deformation were kept constant. Hence, the interval between cycles, specimen size and other factors were kept uniform throughout testing in order to obtain as closely as possible the relationship:

$$du(t,T,\sigma,\cdots) = \frac{\partial u}{\partial t}\,dt + \frac{\partial u}{\partial T}\,dT + \frac{\partial u}{\partial \sigma}\,d\sigma + \cdots \Big|_{*}$$

Other limitations that should be recognized are the assumptions that the typical element is statistically homogeneous and transversely anisotropic. The typical element that is considered in the course of testing has finite dimensions although it is assumed that infinitesimal differential theories of material will hold for this element as well as for a body composed of many identical elements.

Sokolnikoff (42) and Love (27) present derivations of the material coefficients that describe deformation of elastic, anisotropic materials. In these derivations a strain-energy

---

*Effect of other factors = constant.

function is assumed to exist and hence the reversibility of material behavior is assumed. DeGroot (19) and others have developed a symmetric matrix of material coefficients by utilizing the theory of thermodynamics of irreversible processes, but this was done with the assumption that the material being described possessed microscopic reversibility and obeyed linear phenomenological laws.

Because bituminous mixtures are generally recognized as nonlinear (23) in their stress-deformation behavior and because strain energy is not conserved, a new derivation of material coefficients for a statistically homogeneous, transversely anisotropic, nonconservative material is presented here.

Material Coefficients for Transverse Anisotropy

For a transversely anisotropic material, a rotation transformation about one axis of the material element establishes congruence between the edges and faces of the element in its initial and final positions. The matrix of material coefficients for a transversely anisotropic, statistically homogeneous, nonconservative material is obtained by methods considered here.

Although several authors (47) (5) (20) present matrices of material coefficients which describe various types of elastic symmetry, these matrices are symmetric by virtue of identities established with the aid of strain-energy functions.

The derivation of material coefficients given here is made without use of a strain-energy function. From this derivation it is possible to obtain coefficients that describe the

behavior of materials in which internal strain-energy is not conserved. In addition to this, coefficients presented here differ from those used in transversely anisotropic elastic materials in that the number of independent coefficients is six for the nonsymmetric case vs. five for the symmetric case.

A typical element of material is located at the origin of the x_1, x_2, x_3 coordinate system shown in Figure 2. If the material is transversely anisotropic, then its deformation response to stress will be the same everywhere in the x_1x_2 plane, but dissimilar in the x_1x_3 and x_2x_3 planes. Consequently, the material properties of the typical element should be invariant with respect to arbitrary rotations about the x_3 axis in the x_1x_2 plane.

For small strains, Cauchy's generalized statement of Hooke's law (see Appendix E) may be written:

$$\begin{bmatrix} \epsilon_1 \\ \epsilon_2 \\ \epsilon_3 \\ \epsilon_4 \\ \epsilon_5 \\ \epsilon_6 \end{bmatrix} = \begin{bmatrix} c_{11} & c_{12} & c_{13} & c_{14} & c_{15} & c_{16} \\ c_{21} & c_{22} & c_{23} & c_{24} & c_{25} & c_{26} \\ c_{31} & c_{32} & c_{33} & c_{34} & c_{35} & c_{36} \\ c_{41} & c_{42} & c_{43} & c_{44} & c_{45} & c_{46} \\ c_{51} & c_{52} & c_{53} & c_{54} & c_{55} & c_{56} \\ c_{61} & c_{62} & c_{63} & c_{64} & c_{65} & c_{66} \end{bmatrix} \begin{bmatrix} \sigma_1 \\ \sigma_2 \\ \sigma_3 \\ \sigma_4 \\ \sigma_5 \\ \sigma_6 \end{bmatrix}$$

where σ_i and ϵ_i are related to the stresses and strains,

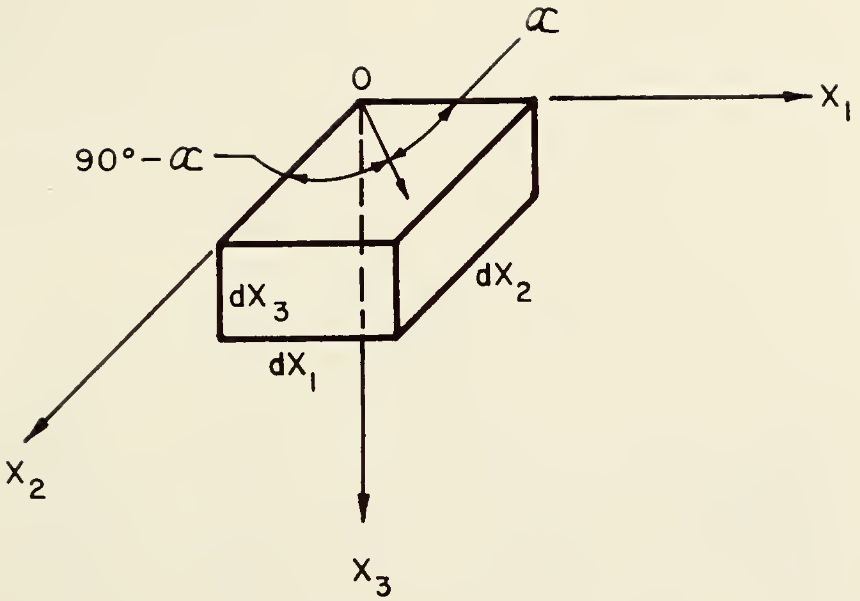

FIGURE 2. TYPICAL ELEMENT AND COORDINATE SYSTEM

σ_{ij} and ϵ_{ij}, as shown in Appendix A.

If the typical element is subjected to stresses and strains σ_{ij} and ϵ_{ij} in the original coordinate system, the stresses and strains, σ_{ij} and ϵ_{ij} for a rotated element may be described by use of equations of rotation transformation:

$$\sigma'_{ij} = a_{ik}a_{jl}\,\sigma_{kl}$$

$$\gamma'_{ij} = a_{ik}a_{jl}\,\gamma_{kl}$$

or, equivalently,

$$S' = ASA^T$$

$$E' = AEA^T$$

where

$$a_{ij} = \text{direction cosine} = \cos\,(x'_i,\ x_j);$$

$$A = \begin{bmatrix} a_{11} & a_{12} & a_{13} \\ a_{21} & a_{22} & a_{23} \\ a_{31} & a_{32} & a_{33} \end{bmatrix}; \qquad S' = \begin{bmatrix} \sigma'_{11} & \sigma'_{12} & \sigma'_{13} \\ \sigma'_{21} & \sigma'_{22} & \sigma'_{23} \\ \sigma'_{31} & \sigma'_{32} & \sigma'_{33} \end{bmatrix};$$

$$E' = \begin{bmatrix} \epsilon'_{11} & \frac{1}{2}\epsilon'_{12} & \frac{1}{2}\epsilon'_{13} \\ \frac{1}{2}\epsilon'_{21} & \epsilon'_{22} & \frac{1}{2}\epsilon'_{23} \\ \frac{1}{2}\epsilon'_{31} & \frac{1}{2}\epsilon'_{32} & \epsilon'_{33} \end{bmatrix};$$

and A^T is the transposed direction cosine matrix.

For an arbitrary rotation, α, in the x_1x_2 plane the direction cosine matrix will be of the form:

		Original Coordinates		
		x_1	x_2	x_3
Rotated Coordinates	x_1'	$\cos\alpha$	$-\sin\alpha$	0
	x_2'	$\sin\alpha$	$\cos\alpha$	0
	x_3'	0	0	1

or

$$A = \begin{bmatrix} \cos\alpha & -\sin\alpha & 0 \\ \sin\alpha & \cos\alpha & 0 \\ 0 & 0 & 1 \end{bmatrix}$$

To calculate the values of the coefficients and to relate the original and rotated coordinate systems necessitates the determination of the following relations:

$$\sigma'_{ij} = \sigma'_{ij}\left[\epsilon'_{ij}(\epsilon_{ij})\right] \quad \text{and} \quad \sigma'_{ij} = \sigma'_{ij}\left[\sigma_{ij}(\epsilon_{ij})\right]$$

From these relations it is possible to make identifications between invariant functions involving strains in the original coordinate system.

As an example of how coefficients may be evaluated, consider the rotation transformations that reduce the coefficient matrix of equation (1) to that matrix which characterizes the transverse anisotropy hypothesized for compacted bituminous mixtures. Because the operations are lengthy in their detail, only a summary of the equivalence transformations and their associated matrix elements are shown.

A 180° rotation about the x_3 axis yields:

$$\begin{bmatrix} C_{11} & C_{12} & C_{13} & 0 & 0 & C_{16} \\ C_{21} & C_{22} & C_{23} & 0 & 0 & C_{26} \\ C_{31} & C_{32} & C_{33} & 0 & 0 & C_{36} \\ 0 & 0 & 0 & C_{44} & C_{45} & 0 \\ 0 & 0 & 0 & C_{54} & C_{55} & 0 \\ C_{61} & C_{62} & C_{63} & 0 & 0 & C_{66} \end{bmatrix} \qquad (2)$$

A 60° rotation about the x_3 axis will result in the following matrix:

$$\begin{bmatrix} C_{11} & C_{12} & C_{13} & 0 & 0 & 0 \\ C_{12} & C_{11} & C_{13} & 0 & 0 & 0 \\ C_{31} & C_{31} & C_{33} & 0 & 0 & 0 \\ 0 & 0 & 0 & C_{44} & C_{45} & 0 \\ 0 & 0 & 0 & -C_{45} & C_{44} & 0 \\ 0 & 0 & 0 & 0 & 0 & 2(C_{11}-C_{12}) \end{bmatrix} \qquad (3)$$

From a 120° rotation about the x_3 axis one obtains:

$$\begin{bmatrix} C_{11} & C_{12} & C_{13} & 0 & 0 & 0 \\ C_{12} & C_{11} & C_{13} & 0 & 0 & 0 \\ C_{31} & C_{31} & C_{33} & 0 & 0 & 0 \\ 0 & 0 & 0 & C_{44} & C_{45} & 0 \\ 0 & 0 & 0 & -C_{45} & C_{44} & 0 \\ 0 & 0 & 0 & 0 & 0 & 2(C_{11}-C_{12}) \end{bmatrix} \qquad (4)$$

Further rotations of 90°, 240° and 300° about the x_3 axis yield no new relations. A 180° rotation about the x_1 axis reduces the matrix in (4) to that shown in (5):

$$\begin{bmatrix} C_{11} & C_{12} & C_{13} & 0 & 0 & 0 \\ C_{12} & C_{11} & C_{13} & 0 & 0 & 0 \\ C_{31} & C_{31} & C_{33} & 0 & 0 & 0 \\ 0 & 0 & 0 & C_{44} & 0 & 0 \\ 0 & 0 & 0 & 0 & C_{44} & 0 \\ 0 & 0 & 0 & 0 & 0 & 2(C_{11}-C_{12}) \end{bmatrix} \qquad (5)$$

This matrix of coefficients differs from that given by Love (27) and Hearmon (20) for transversely anisotropic

elastic crystals. It will be noted that the matrix is not symmetric, hence, six, rather than five, independent coefficients are needed to describe material behavior. Because the derivation presented here did not involve a strain-energy equation, the elements of the matrix may be used to characterize the deformation-stress response of inelastic materials for which a strain-energy function is not well defined.

The coefficients may be functions of time, temperature, or other inputs; however, to conserve space, the coefficients are written with a single symbol although the functional dependence of the coefficients is understood. Consequently, the following equivalence is to be observed:

$$C_{ij}(t, T, \sigma, \ldots) = C_{ij}$$

Although the matrix (5) relates strains to known stresses, the inverse problem, i.e. the relation of stresses to known strains, is also amenable to solution, hence:

$$\begin{aligned} E &= CS \\ C^{-1} E &= C^{-1}CS \\ C^{-1} E &= S \end{aligned}$$

The inverse of matrix (5), C^{-1}, contains coefficients which enable stresses to be predicted if input strains are known.

Evaluation of Material Coefficients

The stress-strain relationships of equation (1) when the coefficient matrix (5) is used now become:

$$\begin{aligned} \epsilon_1 &= C_{11}\,\sigma_1 + C_{12}\,\sigma_2 + C_{13}\,\sigma_3 \\ \epsilon_2 &= C_{12}\,\sigma_1 + C_{11}\,\sigma_2 + C_{13}\,\sigma_3 \\ \epsilon_3 &= C_{31}\,\sigma_1 + C_{31}\,\sigma_2 + C_{33}\,\sigma_3 \qquad (6) \end{aligned}$$

$$\epsilon_4 = C_{44}\,\sigma_4$$

$$\epsilon_5 = C_{44}\,\sigma_5 \qquad (6,\ \text{cont.})$$

$$\epsilon_6 = 2(C_{11}-C_{12})\,\sigma_6$$

These stress-strain constitutive relations have been derived on the basis of three assumptions, namely transverse anisotropy, small strains and the statistical homogeneity of the material.

It will now be demonstrated that the determination of the coefficients, C_{ij}, can be made from uniaxial tests in tension and/or compression and direct shear tests. Consider uniaxial compression tests when either σ_1 or σ_3 acts. When σ_1 acts alone it is found from (6) that

$$C_{11} = \frac{\epsilon_1}{\sigma_1} = \frac{1}{E_1}$$

$$C_{12} = \frac{\epsilon_2/\ \epsilon_1}{\sigma_1/\ \epsilon_1} = \frac{\mu_{21}}{E_1}$$

$$C_{31} = \frac{\epsilon_3/\ \epsilon_1}{\sigma_1/\ \epsilon_1} = \frac{\mu_{31}}{E_1}$$

From the condition that σ_3 acts alone it is found that

$$C_{13} = \frac{\epsilon_1}{\sigma_3} = \frac{\epsilon_1/\ \epsilon_3}{\sigma_3/\ \epsilon_3} = \frac{\mu_{13}}{E_3}$$

$$C_{13} = \frac{\epsilon_2/\ \epsilon_3}{\sigma_3/\ \epsilon_3} = \frac{\mu_{23}}{E_3}$$

$$C_{33} = \frac{\epsilon_3}{\sigma_3} = \frac{1}{E_3}$$

When either σ_4 or σ_5 acts the following relations are found:

$$C_{44} = \frac{\epsilon_4}{\sigma_4} = \frac{\epsilon_5}{\sigma_5} = \frac{1}{G_4} = \frac{1}{G_5}$$

When matrix (5) is rewritten using Poisson's ratio and the moduli defined in Appendix A, matrix (7) results:

$$\begin{bmatrix} 1/E_1 & \mu_{21}/E_1 & \mu_{13}/E_3 & 0 & 0 & 0 \\ \mu_{21}/E_1 & 1/E_1 & \mu_{13}/E_3 & 0 & 0 & 0 \\ \mu_{31}/E_1 & \mu_{31}/E_1 & 1/E_3 & 0 & 0 & 0 \\ 0 & 0 & 0 & 1/G_4 & 0 & 0 \\ 0 & 0 & 0 & 0 & 1/G_4 & 0 \\ 0 & 0 & 0 & 0 & 0 & \frac{2}{E_1}(1-\mu_{21}) \end{bmatrix} \qquad (7)$$

It can be noted from the preceding development that the material coefficients can be evaluated from tests in which linear dimension changes are measured directly. It is also possible to demonstrate the evaluation of some material coefficients from uniaxial compression tests in a triaxial cylinder in which volume change measurements can be made. The coefficients C_{21}, C_{31} and C_{13} can be evaluated in this manner. Consider a uniaxial test in which only σ_3 acts. From the first invariant of strain when small strains prevail:

$$\epsilon_1 + \epsilon_2 + \epsilon_3 = \frac{\Delta V}{V} = \sigma_3 (2C_{13} + C_{33})$$

or noting that

$$C_{33} = \frac{1}{E_3} \quad \text{and} \quad C_{13} = \frac{\mu_{13}}{E_3} \, .$$

$$\frac{\Delta V}{2V\,\epsilon_3} - \frac{1}{2} = \mu_{13}$$

For an incompressible material this expression reduces to $\mu_{13} = -\frac{1}{2}$. If only σ_1 acts then

$$\frac{\Delta V}{V} = \sigma_1 (C_{11} + C_{12} + C_{31})$$

$$\frac{\Delta V E_1}{V \sigma_1} = 1 + \mu_{21} + \mu_{31}$$

or

$$\frac{\Delta V}{V \sigma_1} - 1 = \mu_{21} + \mu_{31}$$

For an anisotropic material it should be noted that μ_{21} and μ_{31} are not necessarily equal when there is no volume change. As in the previous relations, when the material is isotropic and incompressible this relation reduces to $\mu_{21} = \mu_{31} = -\frac{1}{2}$.

Because only the sum of μ_{21} and μ_{31} can be determined from a test in a triaxial cylinder, an additional defining relation is necessary to find the magnitudes of μ_{21} and μ_{31} separately. It is possible to obtain the value of μ_{21} from the sixth relationship in (6). This is accomplished in the following manner:

From the last equation of (6) we note

$$\epsilon_6 = C_{66} \sigma_6 = 2(C_{11} - C_{12}) \sigma_6$$

or

$$\frac{1}{2} \epsilon_{12} = \left(\frac{1}{E_1} - \frac{\mu_{21}}{E_1}\right) \sigma_{12}$$

Hence,

$$\frac{\epsilon_{12} \; E_1}{2 \sigma_{12}} = 1 - \mu_{21} \qquad \text{or}$$

$$\mu_{21} = -\frac{E_1}{2G_{12}} + 1$$

For an isotropic incompressible material, G = E/3 and hence

$$\mu_{21} = 1-\frac{3E}{2E} = 1-\frac{3}{2} = -\frac{1}{2}$$

It should be noted here that $\frac{E_3}{E_1}$ might be used as a measure of the anisotropy of the material. In this ratio only the two moduli are represented and because no transverse strains need be measured these moduli could be determined reliably.

A summary of the stress-strain consitutive relations obtained from the assumptions and results of this section is given by the following:

$$\epsilon_1 = \frac{1}{E_1}\sigma_1 + \frac{\mu_{21}\sigma_2}{E_1} + \frac{\mu_{13}\sigma_3}{E_3}$$

$$\epsilon_2 = \frac{\mu_{21}\sigma_1}{E_1} + \frac{\sigma_2}{E_1} + \frac{\mu_{13}\sigma_3}{E_3}$$

$$\epsilon_3 = \frac{\mu_{31}\sigma_1}{E_1} + \frac{\mu_{31}\sigma_2}{E_1} + \frac{1}{E_3}\sigma_3$$

$$\epsilon_4 = \frac{1}{G_4}\sigma_4$$

$$\epsilon_5 = \frac{1}{G_4}\sigma_5$$

$$\epsilon_6 = \frac{2}{E_1}(1-\mu_{21})\ \sigma_6$$

EXPERIMENTAL INVESTIGATION OF THEORY

The tests described in detail in this section were performed to investigate the theory of material behavior introduced in the preceding section. Four tests are described: they include uniaxial compression, direct shear, uniaxial compression with volume change measurements and torsion tests.

The testing procedures were selected as ones that could be used to evaluate mixtures that are compacted in the laboratory as well as those that are obtained from pavements in service. Although the results presented were obtained from laboratory-compacted specimens, similar compression, shear and torsion specimens could be obtained from highway pavements. Mixture constituents, compaction and cutting procedures and dimensions of the specimens tested are described in Appendix B.

In an attempt to simulate loading conditions that are among the most severe encountered in service, the loads applied to test specimens were static loads applied for a period of 30 seconds. It was thought that this would be representative of the duration of load that might be expected at signalized intersections where rutting and shoving sometimes occur.

Static loads imposed on test specimens were of magnitudes representative of those that would be encountered in pavements

loaded by tires of highway vehicles. In all tests except the uniaxial compression test with volume change measurements, stresses were 23.1, 40.8 and 58.3 psi, in that order. Testing was undertaken at temperatures of 70, 80 and 90° F, in that order, for the compression, direct shear and torsion tests. The test temperature for the uniaxial compression test with volume change measurement was 95°F.

To avoid discrepancies that might be introduced by using varying cycle times, each specimen was loaded for 30 seconds and then the specimen was allowed to relax for $14\frac{1}{2}$ minutes prior to the next load application. This procedure was repeated for each specimen at three different temperatures and for three different loads. The minimum length of time between different test temperatures was four hours.

Uniaxial Compression Test

Compression specimens 1 x 1 x 2.05 inches were bonded to the specimen holder shown in Figure 3 with Eastman 910 adhesive. The specimen holders were bolted to the concrete and steel test stand and a 2.5 kg. seating load was placed on the specimen prior to compression loading. Specimens with their long axis coincident with both the x_1 and the x_3 directions were tested in this manner. From tests of this type the coefficients C_{11}, C_{12}, C_{31}, C_{33} and C_{13} were determined.

Cantilever beam type displacement transducers placed against the four sides of the specimen as well as on top of the specimen were used to measure the deformation of the specimen. The transducers and a schematic diagram of the

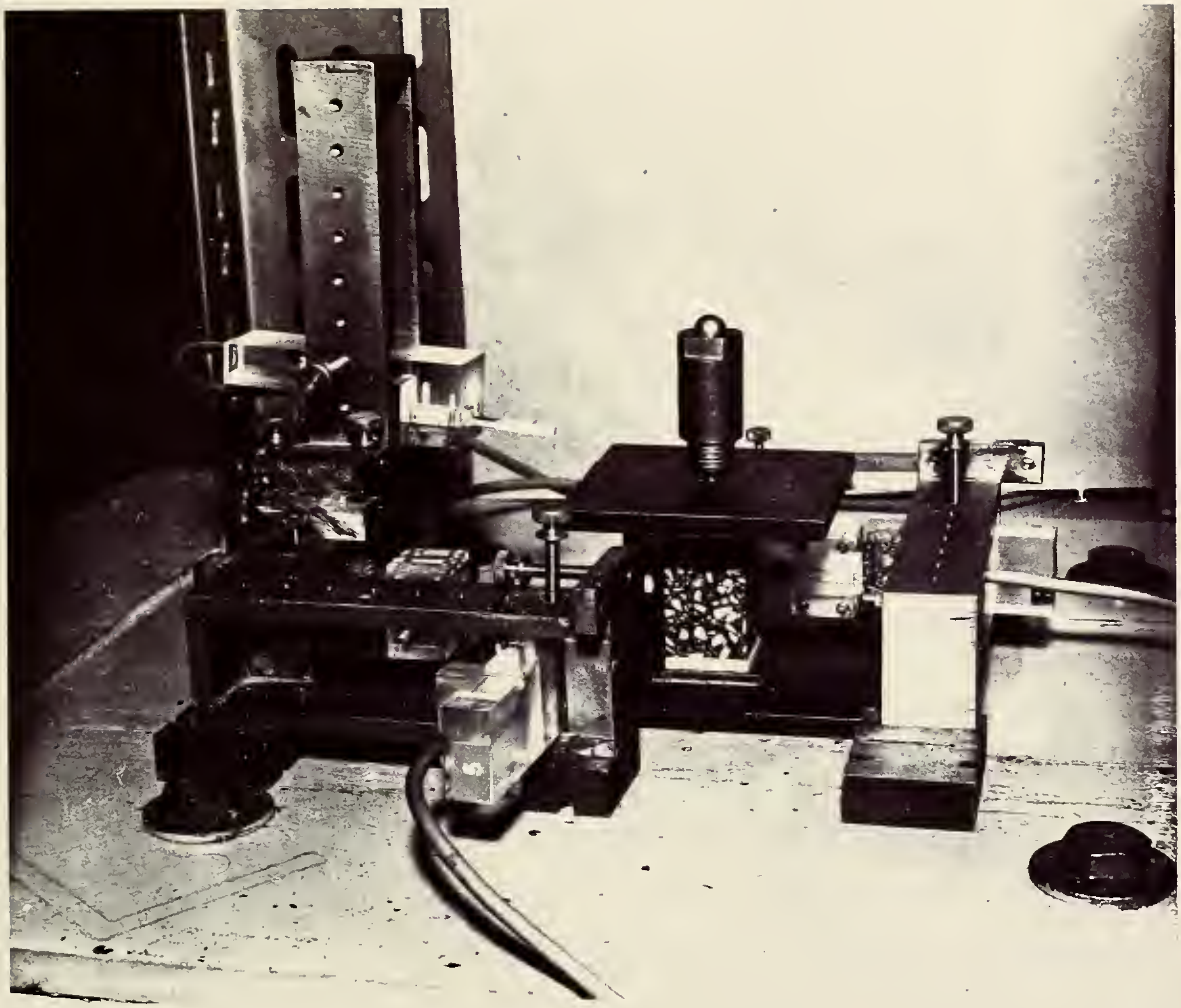

FIGURE 3. UNIAXIAL COMPRESSION SPECIMEN WITH TRANSDUCERS AND HOLDERS

circiutry involved are shown in Appendix C. A typical data channel from the recorder and a data sheet used in reducing the graphic data are shown in Figure 4 and Table 1, respectively.

Cutting and polishing of specimens prior to testing was accomplished as described in Appendix B.

Direct Shear Test

Direct shear test specimens were tested by applying a stress, σ_{13}, to a specimen cut from a beam of bituminous mixture. As for the uniaxial compression test specimens, the direct shear test specimens were secured to their holders by means of either Eastman 910 adhesive or the formulation of epoxy resins described in Appendix B.

Shear specimen deformation was measured by either one or two displacement transducers. Pictures of the shear specimen and holder are shown in Figures 5 and 6.

Prior to testing, the shear specimen holder was bolted to the concrete and steel test stand. Loads were applied to test specimens through a wire and pulley loading system. A shear specimen ready for testing is shown in Figure 6. Typical graphical and numerical data are shown in Figure 4 and Table 2, respectively. The direct shear test was used to evaluate the coefficient C_{44}.

Uniaxial Compression with Volume Change Measurements

Specimens of the same size as those used in the uniaxial compression test were used in the compression testing with volume change measurement. Each specimen was coated with a

SPECIMEN: DIRECT SHEAR
STRESS: σ_{12} = 40.8 psi

CHART SPEED: 0.5 cm/sec
POWER AMPLIFIER: X .02
PREAMPLIFIER: 5 mv/cm
TEMPERATURE: 70°F

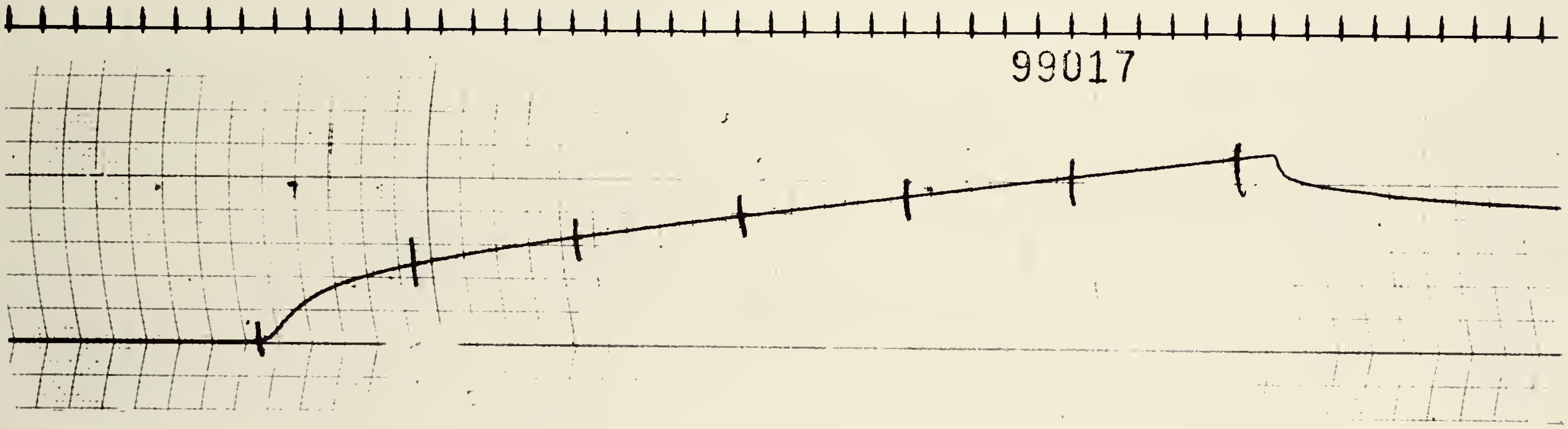

FIGURE 4. TYPICAL GRAPHICAL DATA FOR COMPRESSION, SHEAR AND TORSION TESTS

TABLE 1

Typical Data Sheet for Uniaxial Compression Test

Specimen N3
70°F, 23.1 psi

Time (sec)	Pen Displacement (mm) Gage (1)	Gage (2)	Gage (3)	Gage (5)	Gage (6)
5	1.5	4.0	-0.5	3.5	-1.0
10	2.5	5.5	-1.0	4.5	-1.5
15	3.5	6.0	-1.5	4.0	-1.5
20	4.5	6.5	-1.5	4.0	-1.5
25	5.0	7.0	-1.5	4.0	-1.5
30	5.5	7.5	-2.0	4.0	-1.5

Time (sec)	Long. Deformation (0.0001 in)	Transverse Deformations (0.0001 in)			
	x .476*	x .189*	x .213*	x .228*	x .466*
5	0.72	0.76	-0.11	0.80	-0.47
10	1.19	1.04	-0.21	0.91	-0.70
15	1.67	1.13	-0.32	0.91	-0.70
20	2.15	1.23	-0.32	0.91	-0.70
25	2.38	1.32	-0.32	0.91	-0.70
30	2.62	1.42	-0.42	0.91	-0.70

Strains (0.0001 in/in)

Time (sec)	$\epsilon_3=\frac{1}{2}(1)$	$\epsilon_t=(2)+(3)$	$\epsilon_t=(5)+(6)$	$E_3(t)=\frac{23.1}{\epsilon_3}$ psi
5	0.37	0.65	0.33	62.4
10	0.60	0.83	0.21	38.5
15	0.84	0.81	0.21	27.5
20	1.07	0.91	0.21	21.6
25	1.19	1.00	0.21	19.4
30	1.31	1.00	0.21	17.6

*Deformation Conversion Factors

TABLE 2

Typical Data Sheet for Shear Test

Specimen S1
70°F, 23.1 psi

Pen Displacement (mm)		Deformation (0.0001 inches)	
Time (sec)	Gage (1)	Time (sec)	Gage x 1.19* (1)
5	3.5	5	4.17
10	4.0	10	4.76
15	4.5	15	5.35
20	5.0	20	5.95
25	5.5	25	6.55
30	6.0	30	7.14

Strains (0.0001 in/in)

Time (sec)	$\epsilon_{13} = 2x(1)$	$G_{13}(t) = \frac{23.1}{\epsilon_{13}}$ psi x 10^{-4}
5	8.34	2.77
10	9.52	2.42
15	10.70	2.16
20	11.90	1.94
25	13.10	1.76
30	14.28	1.62

*Deformation Conversion Factor

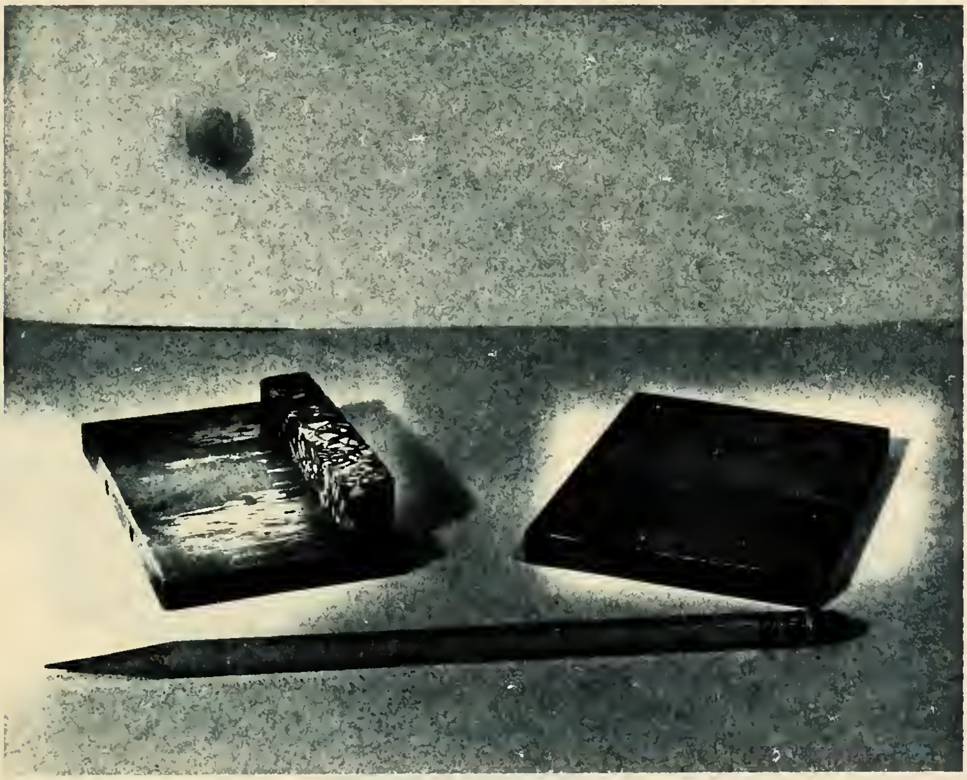

FIGURE 5. DIRECT SHEAR SPECIMEN AND SPECIMEN HOLDER

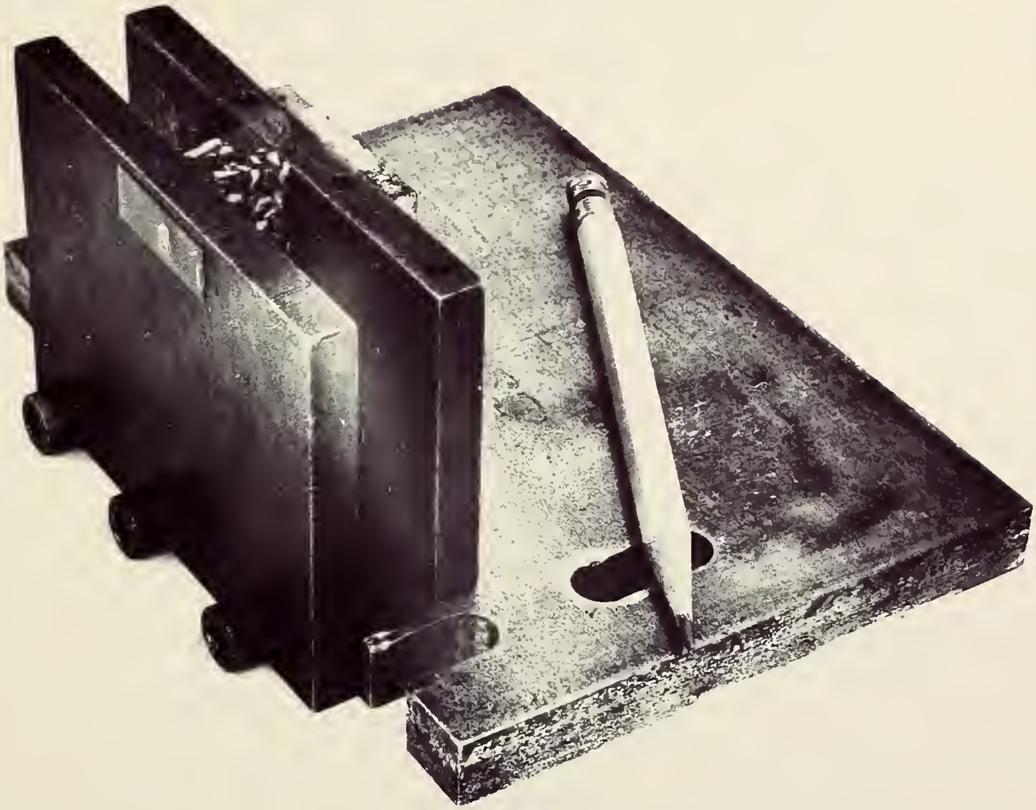

FIGURE 6. SHEAR SPECIMEN AND HOLDER

latex waterproofing compound and tested in uniaxial compression in a water- and oil-filled triaxial cell. The triaxial cell was equipped with a pipet that permitted the determination of volume changes as small as 0.001 ml. Axial strains were detected by a spring-loaded linear variable differential transformer and recorded on an electronic recorder. A photograph of the testing apparatus and a typical graphical data sheet are shown in Figure 7.

Because volume changes were so small, the conditions of loading in this test were different from those described in previous paragraphs. A seating load of 8.8 psi was applied for one minute prior to the beginning of each test. After one minute the height of water in the pipet was recorded and an additional 52.8 psi was placed on the sample. The height of water in the pipet was noted and axial strains were recorded every five minutes for one hour. At the end of one hour the test was terminated.

Torsion Test

To determine the shear moduli and the coefficient C_{44} obtained from the direct shear test, torsion tests were performed on a right circular cylinder cut from the beam of compacted bituminous material. The circular section was chosen to avoid warping of the cross-section that would be expected from the theory of torsion of noncircular prismatic shapes. The torsion test was chosed to verify the invariance of the coefficients found from the direct shear test. If the

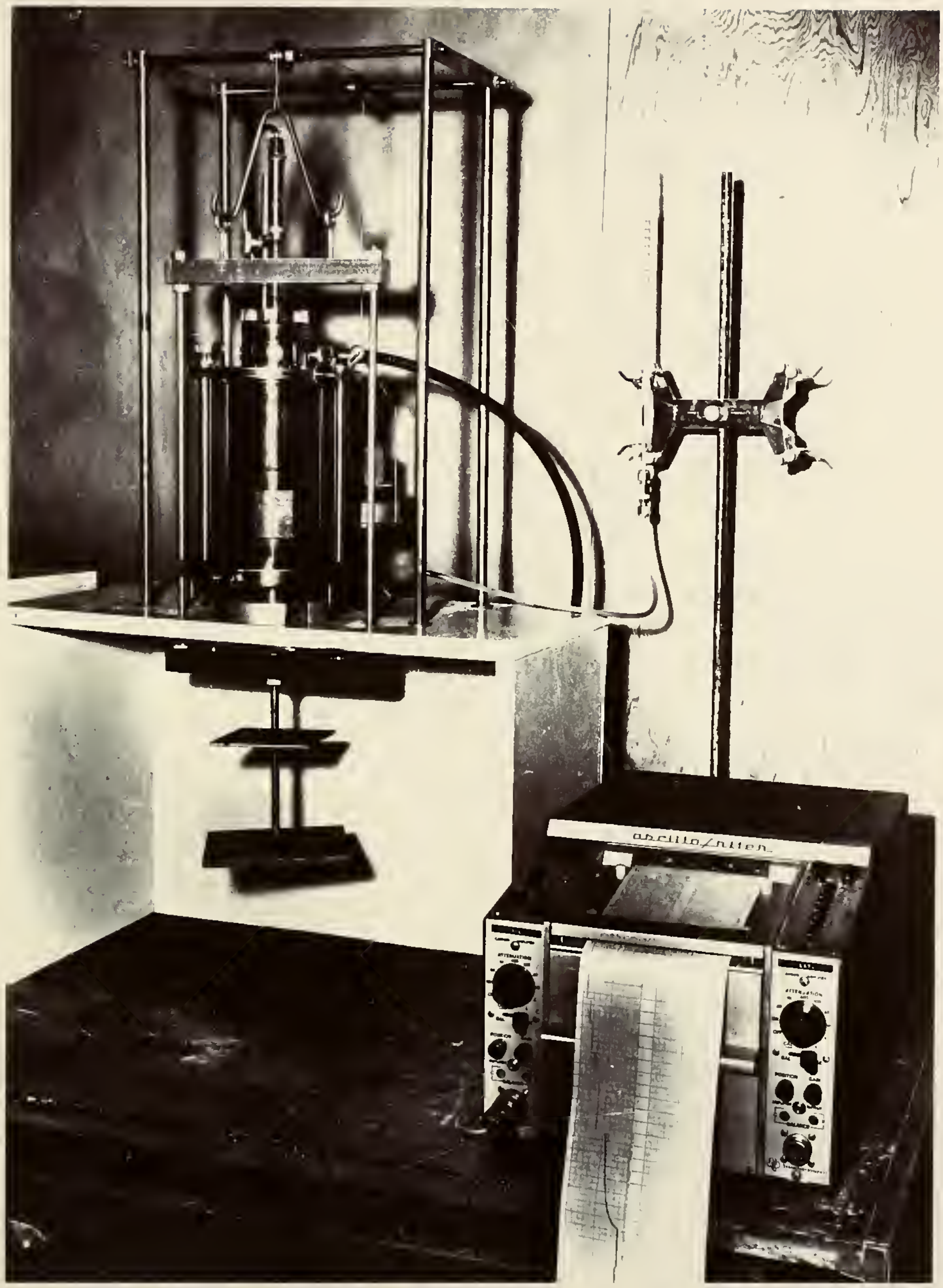

FIGURE 7. TRIAXIAL CELL WITH PIPET AND RECORDER

coefficients found from the direct shear test are properties of the mixture they should be independent of the test used to define them. The torsion specimen holders, test apparatus and a typical graphical data sheet are shown in Figures 8, 9 and 4, respectively.

Loading conditions and temperatures during testing were the same for the torsion test as for the uniaxial compression and direct shear tests.

The stress equation used in the torsion test was:

$$\sigma_{13} = Tr/J \quad \text{where}$$

T is the applied torsional moment, r is the radius of the test cylinder and J is the polar moment of the cross-section. Hence: $C_{44} = 1/G_{13} = J\,\epsilon_{13}/Tr$.

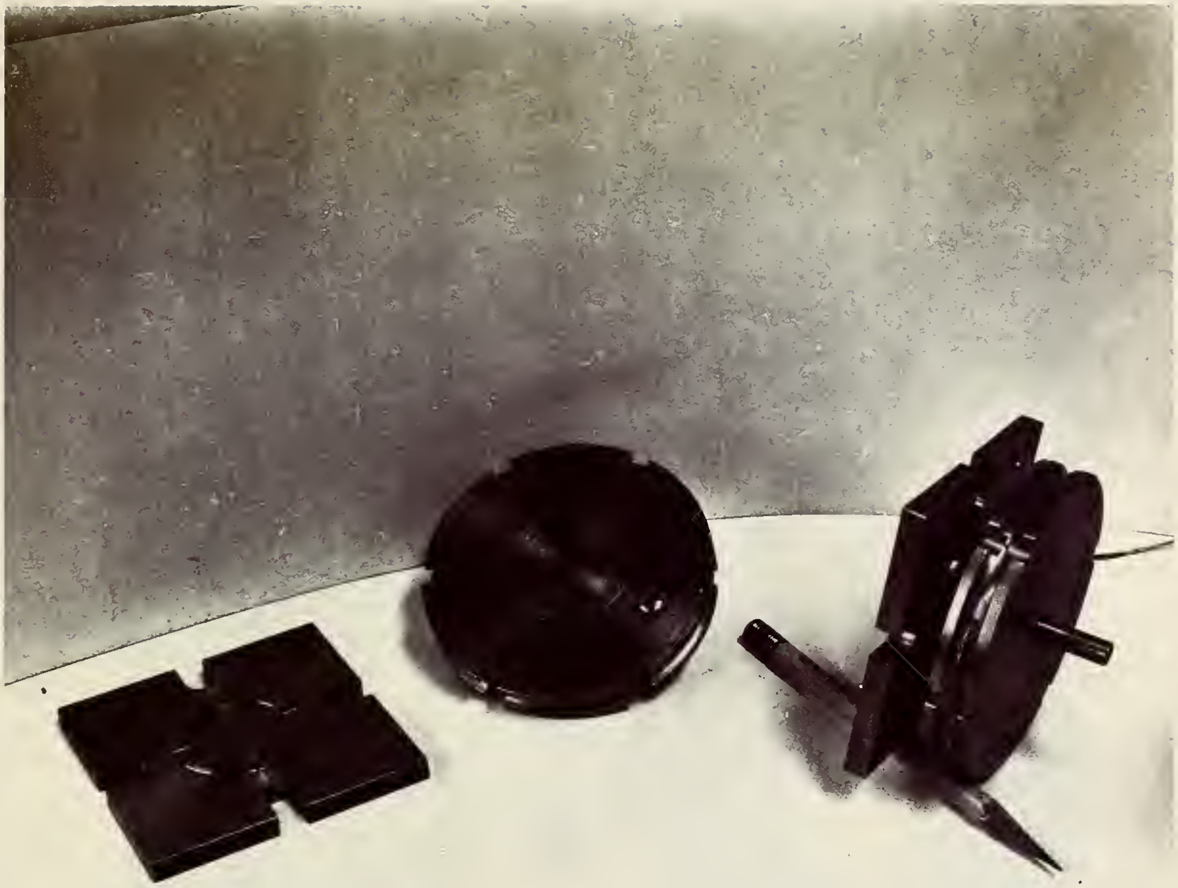

FIGURE 8. TORSION SPECIMEN HOLDERS

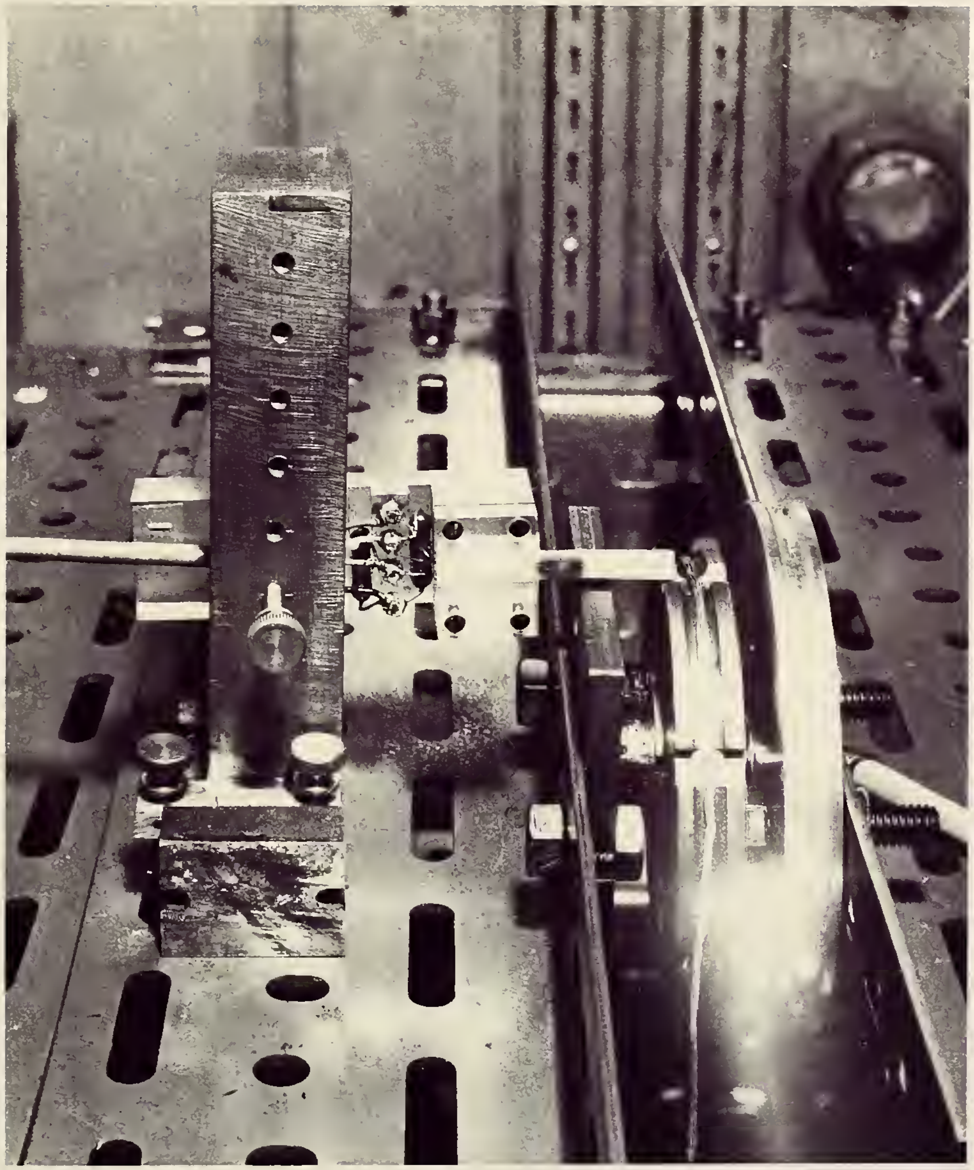

FIGURE 9. TORSION SPECIMEN AND DISPLACEMENT TRANSDUCER

RESULTS OF TESTS AND DISCUSSION

The results of laboratory tests are presented here together with comments on trends and relationships indicated by the data. The presentation of data is organized in the following sequence:

1. Uniaxial Compression Test Results
    a. Stiffness Moduli
    b. Poisson's Ratios
2. Uniaxial Compression Test Results with Volume Change Measurements
3. Direct Shear Test Results
4. Comparison of Shear and Torsion Test Results

Uniaxial Compression Test Results

Results discussed in this section were obtained from data taken during uniaxial compression testing. Values of the stiffness moduli and Poisson's ratios presented were obtained from linear deformations.

Stiffness Moduli, E_1 and E_3

Tabular data from uniaxial compression tests are shown in Appendix D. Plots of these data for specimens obtained from the same compacted beam are shown in the upper portion of Figure 10. Data indicate that the stiffness moduli, E_1

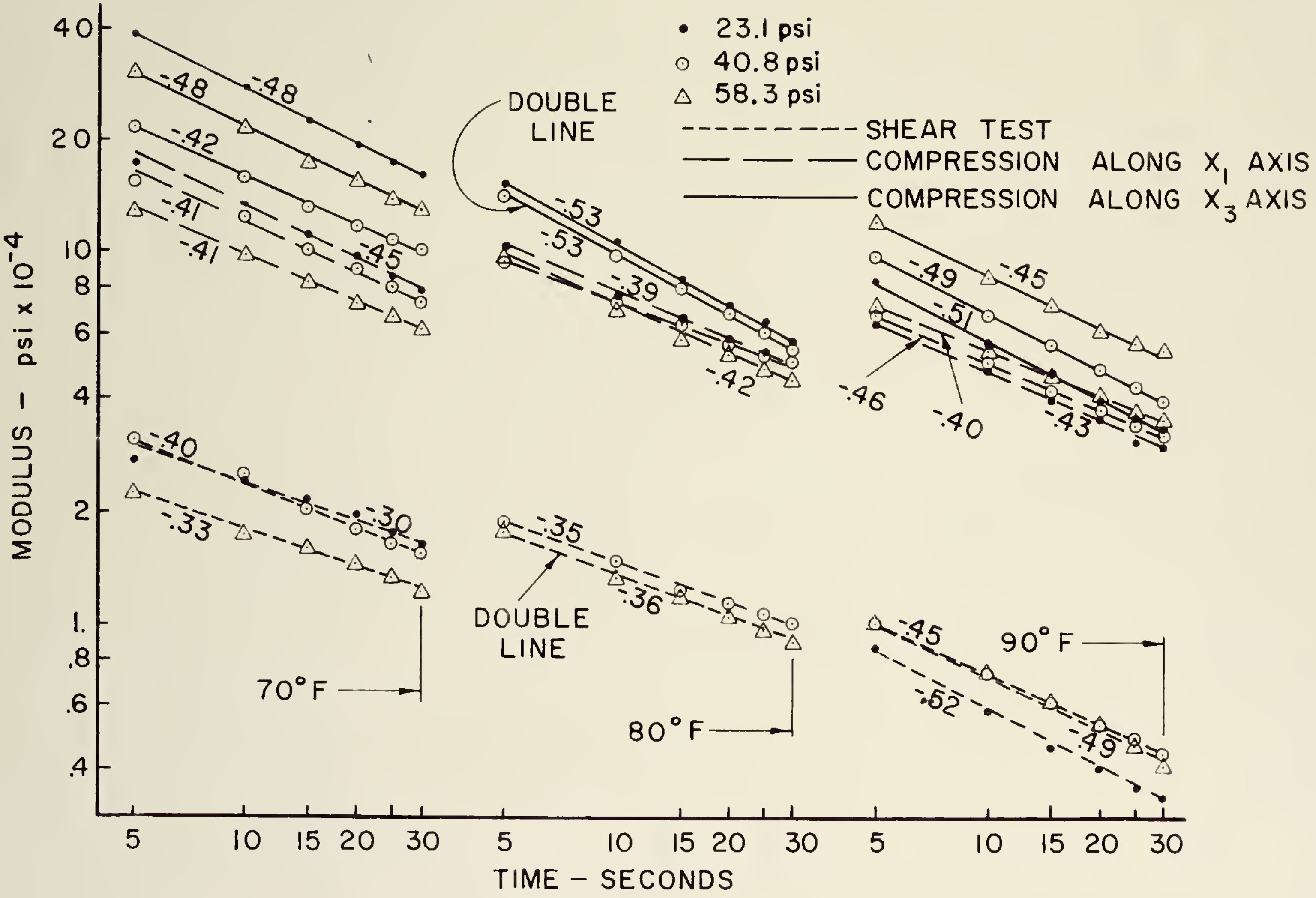

FIGURE 10. COMPRESSION AND SHEAR MODULI VS. TIME, 70°, 80°, 90° F

and E_3, are linear on a log-modulus vs. log-time plot. Data are presented for uniaxial tests along both the x_1 and x_3 axes and for test temperatures of 70, 80 and 90°F.

The numbers associated with each curve in Figure 10 are least square slopes computed on an electronic computer. In all cases, the slopes of the lines are negative and hence mixture stiffness, as defined by E_1 and E_3, decreases with time. The trend of behavior indicates that the moduli determined from compression tests decrease with increases in temperature.

It will be noted that data are recorded only for the time range of from five seconds to thirty seconds. Although it was anticipated that data for time values of less than five seconds might yield relations similar to those shown, experimental error was considered excessive for loading times less than five seconds. Error was introduced, in part, by deviations in placing the load on the specimen and uncertainty in interpreting from the graphic data where the initial time, $t = 0$, was located. Initial seating of the load and inertia effects at small values of time would also add to erroneous determination of stiffness for small strains. Figure 11 shows a plot of log-shear strain vs. log-time which indicates that extrapolation to smaller values of time might be realistic; however, throughout the remainder of this section, records of the moduli are presented only for time values greater than or equal to five seconds.

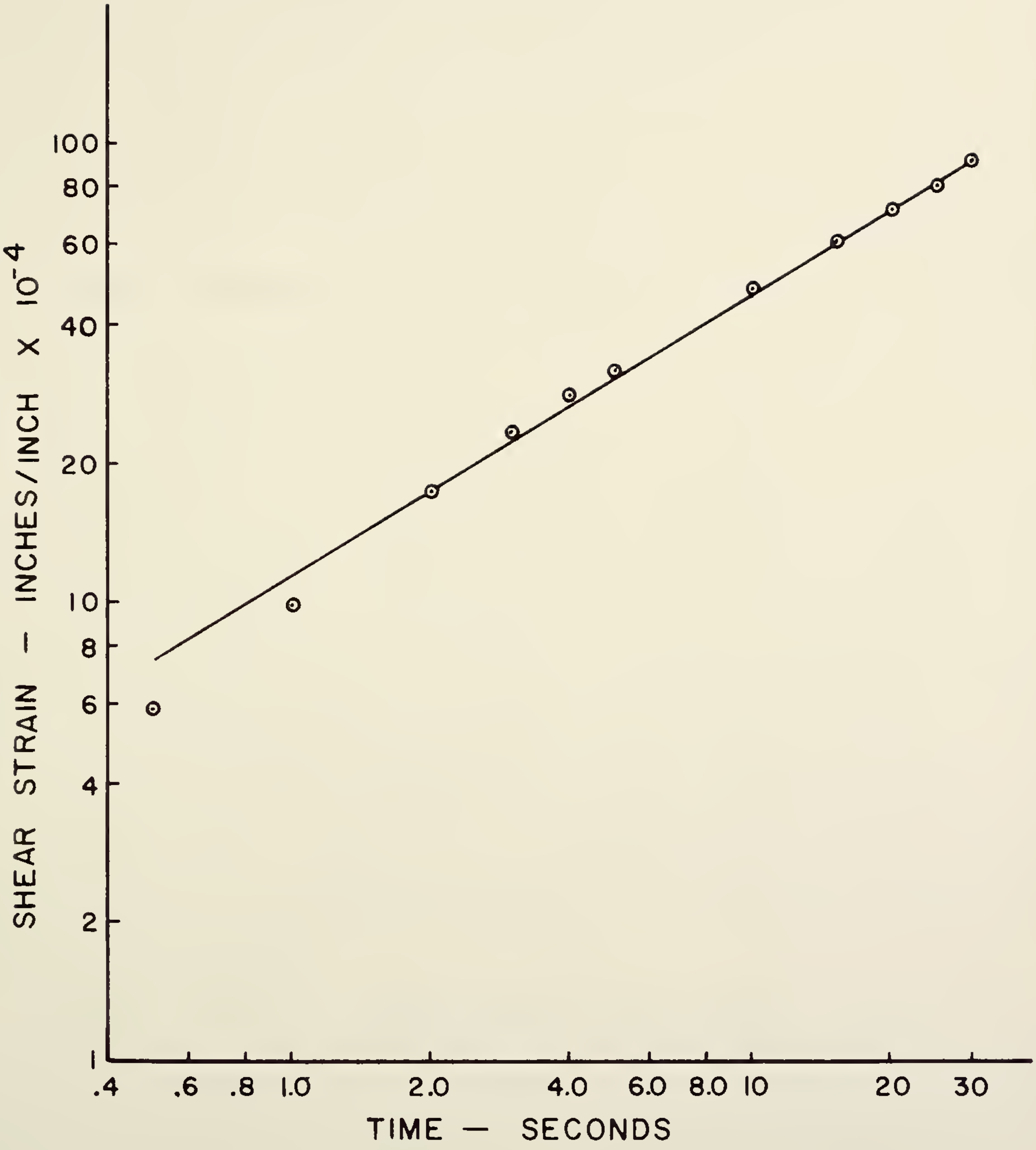

FIGURE 11. SHEARING STRAIN VS TIME
(0.5 SEC. ≤ TIME ≤ 30 SEC.)

Initially, data were to be collected for the evaluation of stiffness moduli by means of uniaxial tension tests. Difficulty in obtaining consistent results, particularly transverse strain measurements, motivated the use of compression tests for determination of stiffnesses. It was hypothesized that the non-rigid nature of the tension test loading apparatus and the nonhomogeneous strength characteristics of the bituminous mixture caused excessive stresses and strains that resulted in bending of the specimen and hence an indication of strain that was erratic.

Although plots of the log-modulus vs. log-time appeared linear, several coefficients of linear correlation were computed to obtain a measure of how well the data could be approximated by a straight line. All the linear correlation coefficients were greater than 0.95 and most were very close to 1.0. In Table 3 are typical computations for the determination of this coefficient. Linearity on a log-log plot, based on the magnitude of the correlation coefficients, assists description of material behavior.

A measure of the anisotropy of the mixture tested is given by the ratio E_3/E_1. Figure 12 shows plots of this ratio obtained from data of Figure 10. It should be noted from this figure that for the highest stress level and for all three test temperatures used in this study, anisotropy is essentially constant over the time range considered. The data indicate that assumptions of isotropy for laboratory-compacted mixtures may be seriously questioned. The same behavior may be present

TABLE 3

Sample Calculation of the Coefficient of Linear Correlation for Log $E_3(t)$ on Log t

Uniaxial Compression Test
Specimen N3
$70^{o}F$, 40.8 psi

	Log t	Log $E_3(t)$	log t = Log t-$\overline{\text{Log t}}$	log $E_3(t)$ = Log $E_3(t)$-$\overline{\text{Log }E_3\text{t}}$	$(\log t)^2$	log t log $E_3(t)$	$(\log E_3(t))^2$
	0.70	1.33	-0.48	-0.21	0.230	0.101	0.404
	1.00	1.19	-0.18	-0.07	0.032	0.013	0.005
	1.18	1.12	0.00	0.00	0.000	0.000	0.000
	1.30	1.06	0.12	0.06	0.014	0.007	0.004
	1.40	1.03	0.22	0.09	0.048	0.020	0.008
	1.48	1.00	0.30	0.12	0.090	0.036	0.014
Sums	7.06	6.73			0.414	0.177	0.075

$\overline{\text{Log t}}$=1.18 $\overline{\text{Log E}}$-1.12

$$r = \frac{\sum \log t \log E_3(t)}{\sqrt{(\Sigma \log t^2)\ (\Sigma \log E_3(t)^2)}} = \frac{0.177}{\sqrt{(0.414)(0.075)}} = \underline{\underline{1.0}} = \text{Coefficient of linear correlation}$$

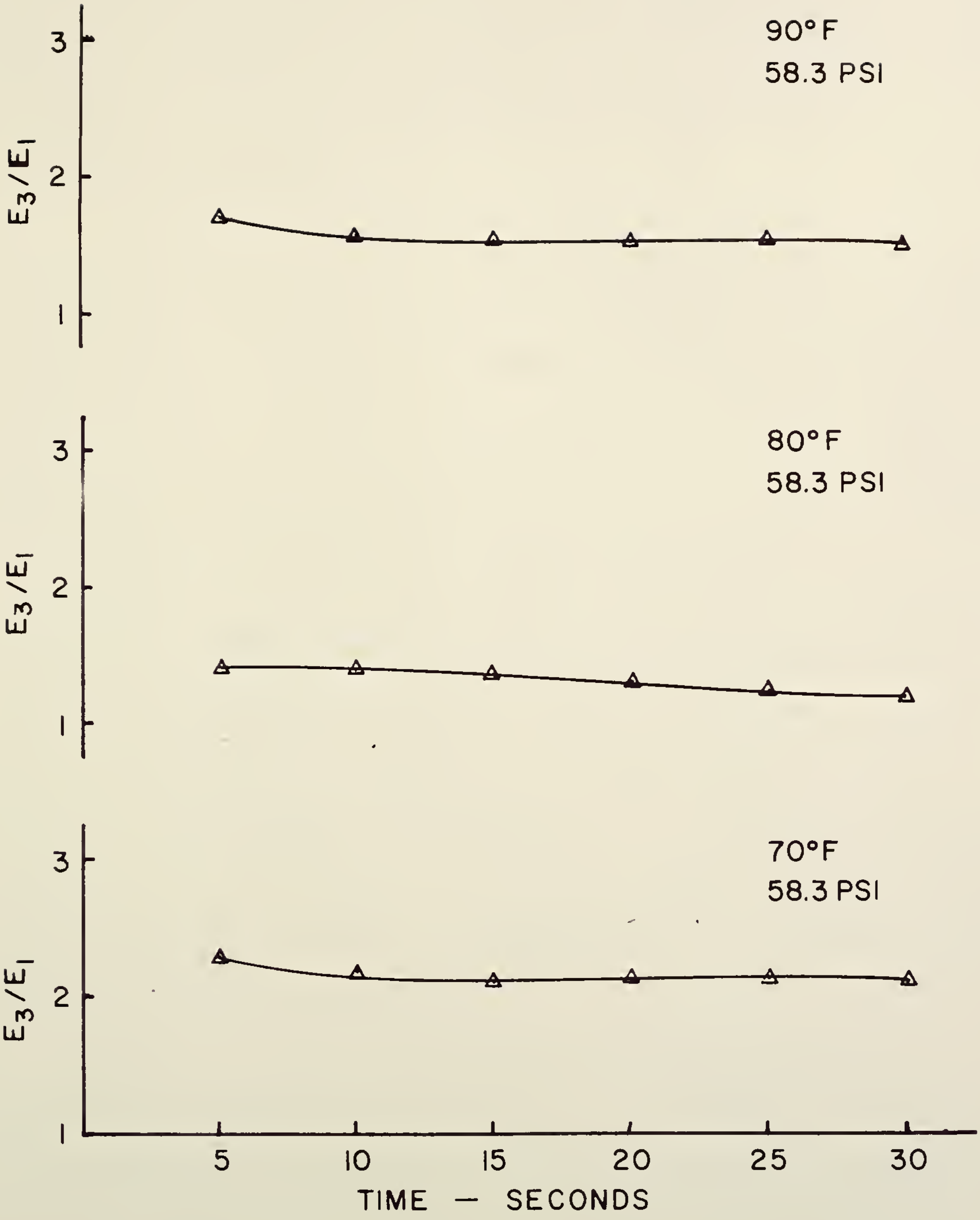

FIGURE 12. E_3/E_1 VS. TIME

in field-compacted mixtures. In all cases shown in Figure 12 the value of E_3 is greater than E_1 and the ratio E_3/E_1 for all data of Figure 10 has the approximate range 1.8 to 1.1. From this it can be noted that the mixture is stiffer in the direction of applied compactive forces than it is in orthogonal directions.

Poisson's Ratios

Because Poisson's ratios were necessary for the determination of some material coefficients, plots of transverse strain vs. longitudinal strain were made from data obtained from uniaxial compression tests. Poisson's ratio is defined as (transverse strain)/(longitudinal strain).

Several coefficients of linear correlation were computed to obtain a measure of the linearity of Poisson's ratios for the loading conditions utilized in this research. A sample calculation is shown in Table 4. Representative plots of transverse strain, ϵ_t, vs. longitudinal strain, ϵ_l, are shown in Figure 13. The slopes of the lines shown in this figure are Poisson's ratios and may be considered to be constant for the duration of loading involved.

Efforts to obtain the values of Poisson's ratios by inspection of graphs were found to be inaccurate and hence a least squares slope was calculated for each of the specimens by use of a computer program for the IBM 7094 computer. A tabulation of some values of Poisson's ratios determined from uniaxial compression tests is shown in Table 5. The

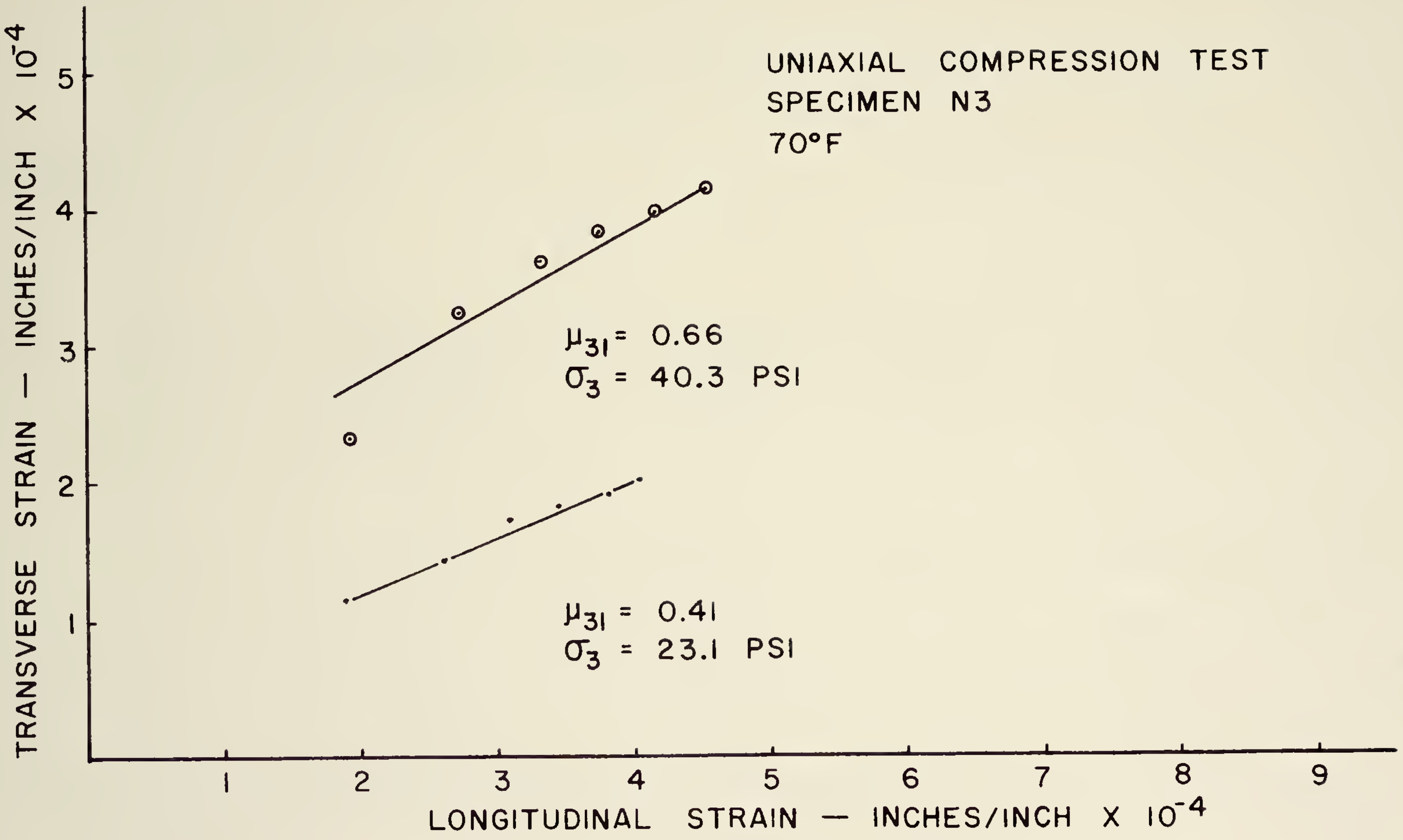

FIGURE 13. TRANSVERSE STRAIN VS. LONGITUDINAL STRAIN AND SLOPES DEFINING POISSON'S RATIO

TABLE 4

Sample Calculation of the Coefficient of Linear Correlation for Transverse Strain on Longitudinal Strain (Poisson's Ratio)

Uniaxial Compression Test
Specimen N3
70°F, 40.8 psi

ϵ_ℓ	ϵ_t	$e_\ell = \epsilon_\ell - \bar{\epsilon}_\ell$	$e_t = \epsilon_t - \bar{\epsilon}_t$	e_ℓ^2	$e_\ell e_t$	e_t^2
1.90	1.13	-1.26	-0.54	1.59	0.68	0.29
2.62	1.43	-0.54	-0.24	0.29	0.13	0.06
3.10	1.72	-0.06	0.05	0.00	0.00	0.00
3.46	1.81	0.30	0.14	0.09	0.04	0.02
3.81	1.91	0.65	0.24	0.42	0.16	0.06
4.05	2.00	0.89	0.33	0.79	0.29	0.11
Sums 18.94	10.00			3.18	1.30	0.54

$\bar{\epsilon}_\ell = 3.16$ $\bar{\epsilon}_t = 1.67$

$$r = \frac{\sum e_\ell e_t}{\sqrt{(\sum e^2)(\sum e_t^2)}} = \frac{1.30}{\sqrt{(3.18)(0.54)}} = \underline{\underline{0.99}} = \text{Coefficient of linear correlation}$$

TABLE 5

Poisson's Ratios Obtained from Uniaxial Compression Tests

Temperature: 80°F

Stress, psi	(-) μ_{21}	(-) μ_{31}
23.1	1.33	0.21
	0.25	0.45
	0.48	0.40
	0.44	0.24
	0.66	0.47
	1.26	0.27
	0.31	
40.8	0.47	0.28
	0.47	0.43
	0.40	0.59
	0.46	0.31
	0.42	0.81
	0.68	0.33
	0.42	0.50
	0.63	0.37
	0.52	
58.3	0.45	0.40
	0.41	0.25
	0.30	0.50
	0.27	0.34
	0.78	0.79
	0.38	0.35

variability in the magnitude of Poisson's ratio is evident from observations of data in this table.

The measurement of Poisson's ratios in particular directions is required for the evaluation of several material coefficients, namely C_{12}, C_{13} and C_{31}. Figure 14 shows a histogram of the values of Poisson's ratios made from 165 determinations. Although the larger portion of the values of Poisson's ratio measured lies between 0.0 and 0.5, it is not possible to observe from this plot or from tabular data what value of Poisson's ratio is measured most consistently for particular conditions of load and temperature. No trends of uniformity were evident in values of this ratio obtained from uniaxial compression tests without volume change measurement.

Several hypotheses are advanced to explain the apparent randomness of the observed values of Poisson's ratio. The first of these hypotheses is related to the small size of the strains being measured. Figure 15 shows by means of arrows the positions of the transverse gages in their assumed initial position. In reality, the test may have proceeded as shown in B, in which case the eccentricity of the specimen would obscure the measurement of transverse strains be altering the gage length. Since the order of magnitude of transverse strains was approximately 1 to 5 x 0.0001 inch, the eccentricity shown would distort the observed values of Poisson's ratio significantly. A second reason that is hypothesized for the erratic behavior of measurements of Poisson's ratio is that nonhomogeneities in the strength of the bituminous mixture might have

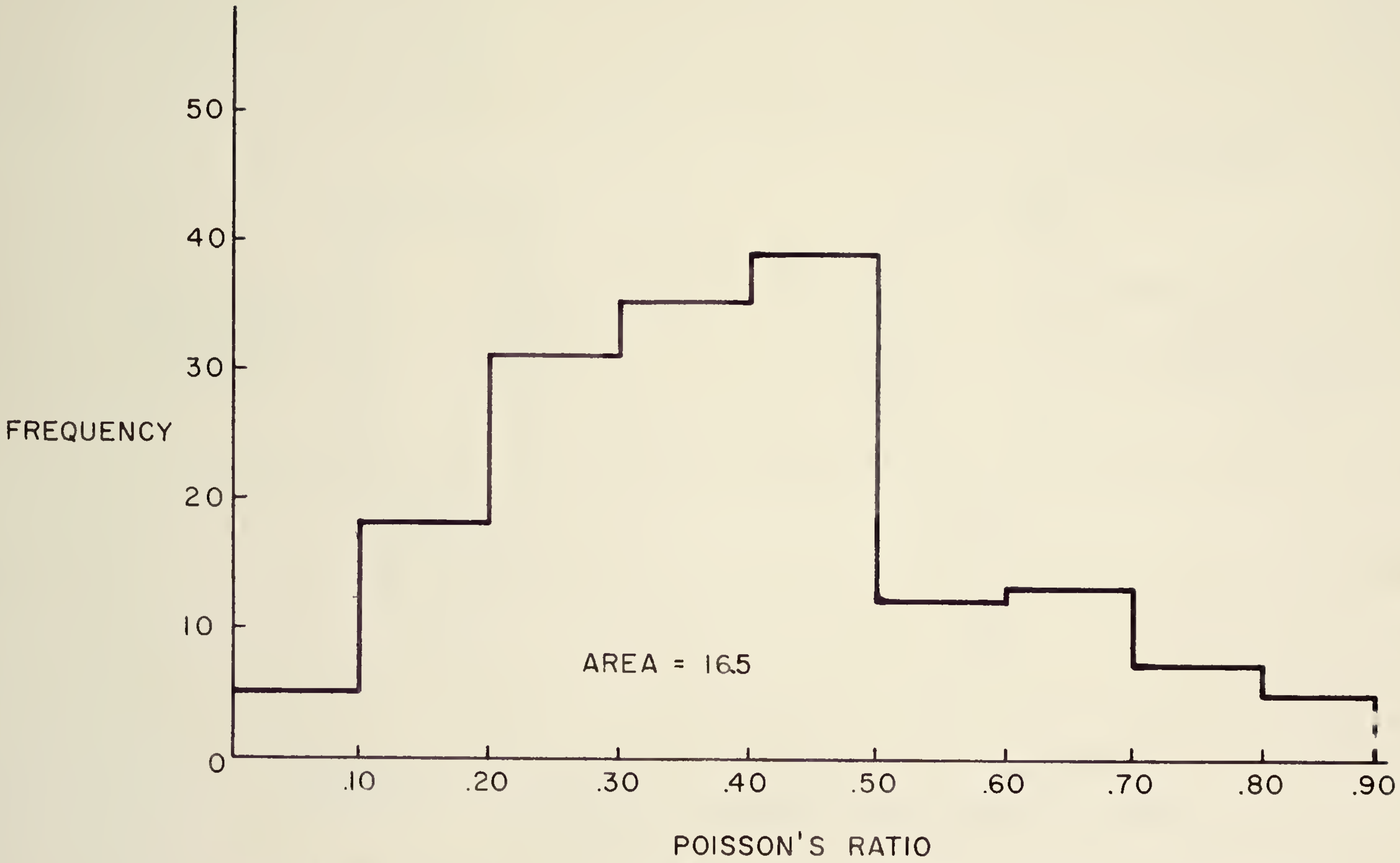

FIGURE 14. HISTOGRAM FOR POISSON'S RATIO OBTAINED FROM UNIAXIAL COMPRESSION TESTS

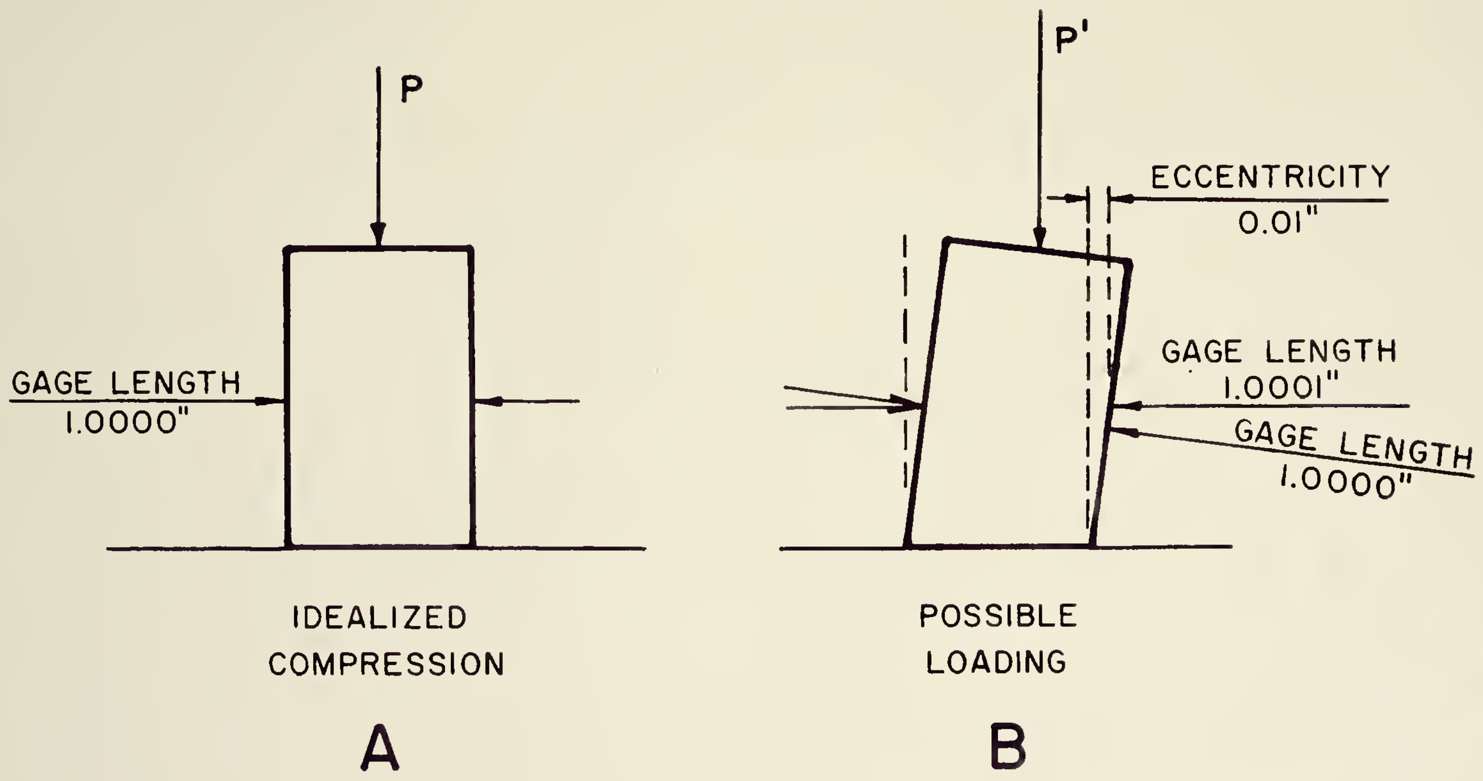

FIGURE 15. POSSIBLE LOADING THAT CHANGES ORIGINAL TRANSVERSE GAGE LENGTH

contributed to bending of the specimens and also to observed randomness of transverse strains.

Although specimen faces were polished with an 800 mesh grinding compound, surface rugosity was a factor possibly contributing to the discrepancies that are reported here. The contact points of the transducers may have moved relative to their initial positions during the course of compression testing and hence may have moved into or out of small depressions in the surface of the specimens. Surface voids in the bituminous mixture, although minimal in this instance, would apparently preclude the definition of Poisson's ratio by measurements of the change in linear dimensions. This consideration is especially pertinent in testing more open-graded mixtures.

In addition to these reasons, it is possible that the values of Poisson's ratios measured were correct values of the ratio for the points where these measurements were taken. Since the mode of development of small deformations is not well understood, it is possible that the position of the transducers on either a stone face or on the bituminous material matrix are reflected in widely differing values of Poisson's ratio. Figure 16 shows a photograph of the relief of a compression specimen in which stone particles have begun to project from the originally smooth surface. It is probable that movement of these discrete particles obscures the distribution of Poisson's ratio which exists for bulk volume.

In addition to this, it is probable that the distribution

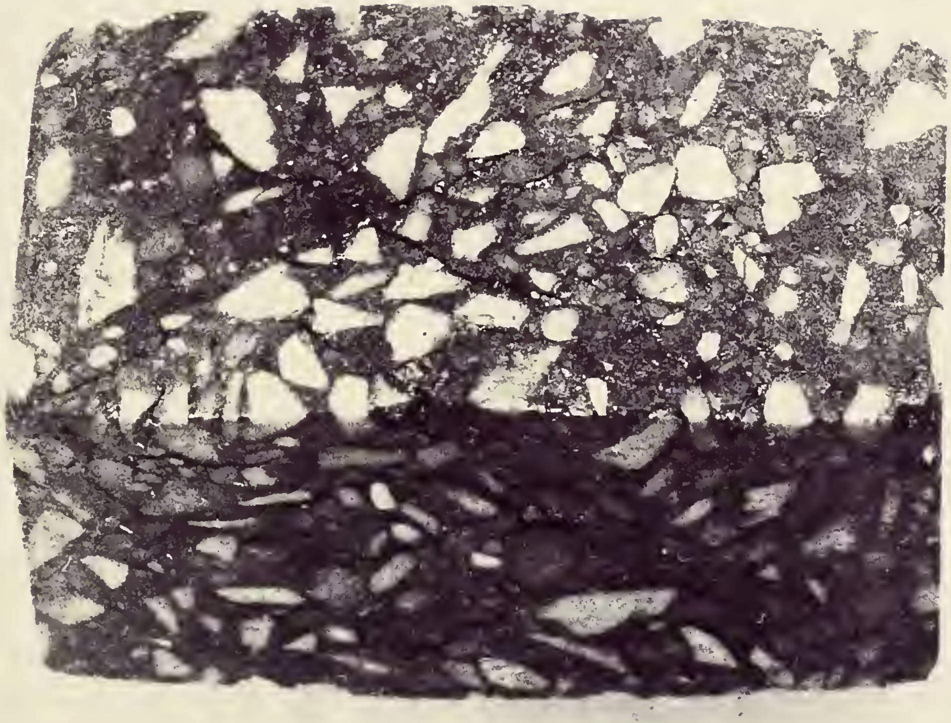

FIGURE 16. SURFACE IRREGULARITIES AFTER COMPRESSION

TABLE 6

Poisson's Ratios, $\mu_{21} + \mu_{31}$, Obtained from Uniaxial Compression Test with Volume Change Measurement

Specimen N1
95°F, 6117 psi
Volume = V = 33.6 cc
Length = L_1 = 5.2 cm

Time (min)	ΔV(cc)	ΔL_1(cm)	$\frac{\Delta V L_1}{V \Delta L_1}$	$\mu_{21} + \mu_{31} = \frac{\Delta V L_1}{V \Delta L_1} - 1$
1	-0.0165	-0.0216	0.1182	-0.8818
5	-0.0209	-0.0484	0.0668	-0.9332
10	-0.0136	-0.0585	0.0360	-0.9640
20	0.0003	-0.0712	-0.0010	-1.0010
25	0.0105	-0.0763	-0.0212	-1.0212
30	0.0114	-0.0827	-0.0214	-1.0214
35	0.0161	-0.0877	-0.0284	-1.0284
40	0.0196	-0.0915	-0.0332	-1.0332
45	0.0210	-0.0978	-0.0332	-1.0332
50	0.0216	-0.0940	-0.0322	-1.0322
55	0.0275	-0.1079	-0.0394	-1.0394
60	0.0370	-0.1105	-0.0518	-1.0518

TABLE 7

Poisson's Ratio, μ_{13}, Obtained from Uniaxial Compression Test with Volume Change Measurement

Specimen N3
95°F, 61.7 psi
Volume = V = 33.6 cc
Length = L_3 = 5.2 cm

Time (min)	ΔV(cc)	ΔL_3(cm)	$\frac{\Delta V L_3}{2V\Delta L_3}$	$\mu_{13} = \frac{\Delta V L_3}{2V\Delta L_3} - \frac{1}{2}$
1	-0.0323	-0.0355	0.0704	-0.43
5	-0.0323	-0.0559	0.0464	-0.45
10	-0.0337	-0.0686	0.0380	-0.46
15	-0.0294	-0.0762	0.0298	-0.47
20	-0.0264	-0.0826	0.0247	-0.48
25	-0.0230	-0.0890	0.0199	-0.48
30	-0.0149	-0.0915	0.0126	-0.49
35	-0.0109	-0.0978	0.0086	-0.49
40	-0.0067	-0.1017	0.0051	-0.49
45	-0.0011	-0.1054	0.0005	-0.50
50	0.0022	-0.1092	-0.0016	-0.50
55	0.0055	-0.1130	-0.0038	-0.50
60	0.0110	-0.1169	-0.0094	-0.51

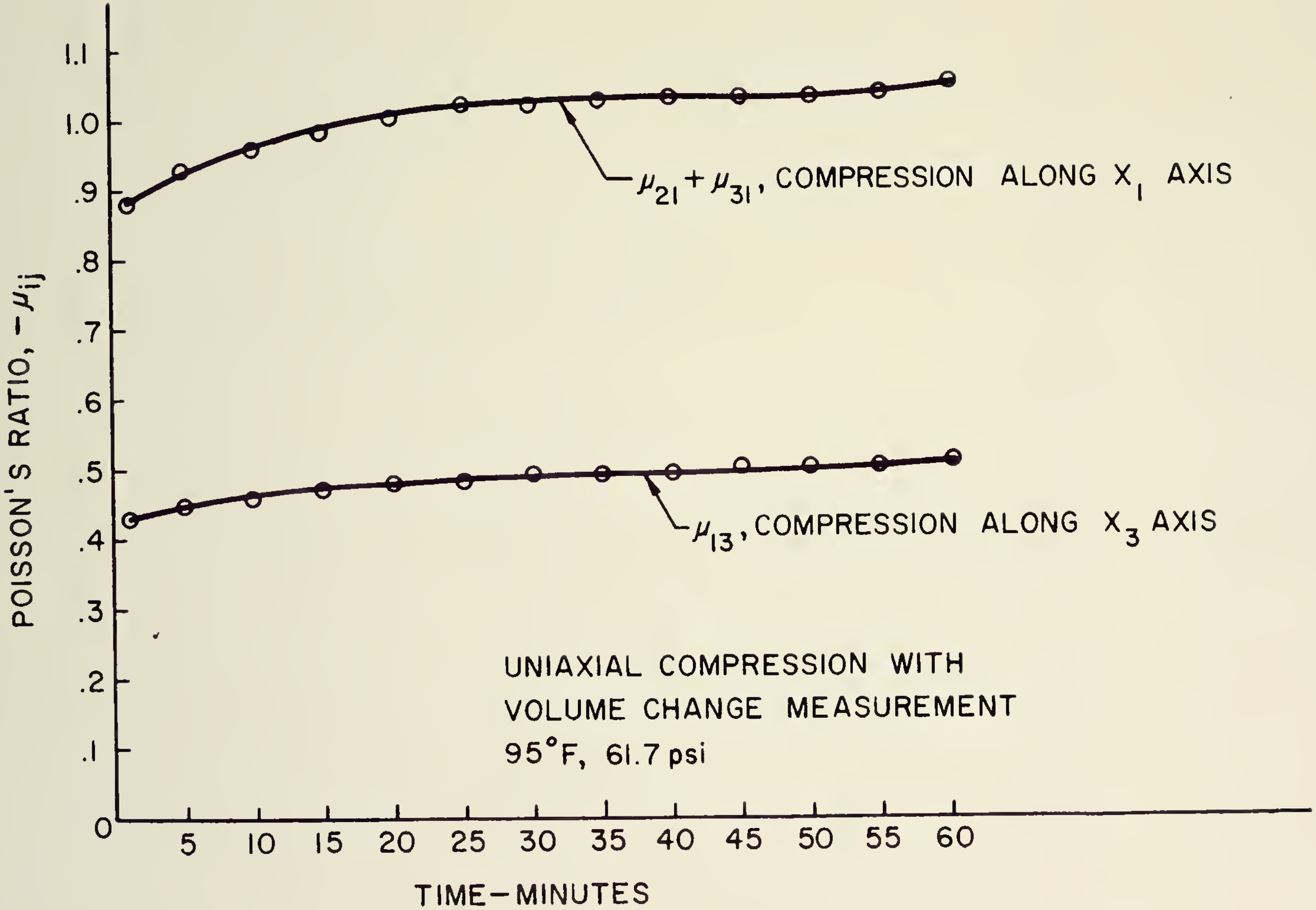

FIGURE 17. POISSON'S RATIO VS TIME FROM VOLUME CHANGE MEASUREMENTS

of Poisson's ratio shown in Figure 14 would be different had the transverse strains been measured at some location other than at the midpoint of the specimen sides. Hence, it is not unreasonable to find that Poisson's ratios obtained from dimension change measurements and from volume change measurements do not agree.

Uniaxial Compression Test Results with Volume Change Measurements

Poisson's ratio was also obtained from uniaxial compression tests with volume change measurements. These tests were performed to circumvent the difficulties involved in measuring Poisson's ratio by linear dimension change. Results from uniaxial compression tests with volume change measurements are presented in Tables 6 and 7. Figure 17 shows graphically the data from Tables 6 and 7 when Poisson's ratios are plotted as functions of time. The specimens used in these tests were prepared from the same beam and from the same orientations as the specimens tested in uniaxial compression tests without volume change measurements.

Data presented graphically indicate Poisson's ratios are slowly varying functions of time of loading for the time interval of one hour. For short durations of load the assumption that Poisson's ratio does not vary appears to be justified. Poisson's ratio varies in these particular tests from approximately 0.43 to 0.52. The maximum axial strain in these tests is approximately two percent whereas the maximum strain per load in uniaxial compression tests without volume change measurements was approximately 0.2 percent. It should be noted that this latter maximum value of strain is only approx-

mate since it was obtained from a test specimen that had been loaded several times and had probably acquired some permanent deformation that was not included in strain computations.

The determination of Poisson's ratios by volume change measurements appears to be a satisfactory mode of measurement although extrapolation to smaller time values is presently required. It is apparent that more experimental work needs to be devoted to the determination of Poisson's ratios for short durations of load. The possibility of using air-gap capacitance measurements was considered; however, resolution of the small deformations expected was not considered adequate at this time for the conditions of the study.

It should be noted from Tables 6 and 7 that volume change from compression tests is negative for small strains for both specimens.

Stiffness moduli were not computed from this test since sufficiently accurate moduli were determined previously from the uniaxial compression test without volume change measurement. The smallest value of Poisson's ratio in the tabular data was selected as that most representative of the ratio that existed during shorter loading times. Hence, the value of μ_{13} was -0.43 as shown after the one minute reading in Table 7.

The sum of μ_{21} and μ_{31} can be determined by considering some relations obtained from volume change measurements.

The volume dilation expressed as a function of strain

invariants is:

$$\frac{\Delta V}{V} = \sqrt{1 + 2J_1 - 4J_2 + 8J_3} - 1$$

where J_1, J_2 and J_3 are the first, second and third invariants of strain, respectively. For small strains this expression reduces to:

$$\frac{\Delta V}{V} = \sigma_1(C_{11} + C_{12} + C_{31})$$

or

$$\frac{\Delta V}{V\epsilon_1} - 1 = \mu_{21} + \mu_{31} = \frac{\epsilon_2}{\epsilon_1} + \frac{\epsilon_3}{\epsilon_1}$$

From Figure 12 it can be noted that the degree of anisotropy can be characterized by the ratio E_3/E_1. It is also noted from the figure that this ratio varies; however, it appears that a representative value of this quantity might be in the approximate range 1.1 to 1.8. If $E_3/E_1 = 1.5$ is selected as a representative value of this ratio for the duration of loads and the range of temperature investigated, then

$E_3 = 1.5E_1$ and

$E_3 = 1.5E_2$ for transverse anisotropy.

In the absence of other relationships it was assumed that the strain ratio ϵ_3/ϵ_2, which involves strains in directions orthogonal to the applied stress, could be approximated by E_2/E_3. Hence,

$$\frac{\Delta V}{V\epsilon_1} - 1 = \frac{\epsilon_2}{\epsilon_1} + \frac{\epsilon_3}{\epsilon_1}$$

may be written

$$\frac{\Delta V}{V\epsilon_1} - 1 = \frac{1.5\epsilon_3 + \epsilon_3}{1} = 2.5\mu_{31}$$

From Table 6 it is found that after one minute

$$\frac{\Delta V}{V\epsilon_1} - 1 = -0.88$$

hence:

$$2.5\mu_{31} = -0.88 \quad \text{and}$$

$$\mu_{31} = -0.35$$

$$\mu_{21} = -0.53$$

From the two compression tests it has been possible to determine five of the six material coefficients. Writing these coefficients in functional notation gives:

$$C_{11}(t,T,\sigma) = \frac{1}{E_1(t,T,\sigma)}$$

$$C_{12}(t,T,\sigma) = \frac{-0.53}{E_1(t,T,\sigma)}$$

$$C_{13}(t,T,\sigma) = \frac{-0.35}{E_3(t,T,\sigma)}$$

$$C_{33}(t,T,\sigma) = \frac{1}{E_3(t,T,\sigma)}$$

$$C_{31}(t,T,\sigma) = \frac{-0.43}{E_1(t,T,\sigma)}$$

Because Poisson's ratio varies slowly over a relatively long time interval in testing, these ratios are assumed to be constant for the material. Additional experimental work will be necessary to refine these measurements. The stiffness moduli, E_1 and E_3, are characterized by the logarithmic slope, m, and the 30 second intercept; hence E_1 may be written:

$$\log E_1(t,T,\sigma) = \log E_1(30,T,\sigma) + m(t,T,\sigma) \log t \Bigg|_{T,\sigma}$$

A similar expression holds for the modulus E_3.

The next two sections present results of the determination of the sixth material coefficient, C_{44}, as well as a test of necessity for establishing invariance of the coefficients.

Direct Shear Test Results

Shear test results from specimens cut from the same beam of compacted bituminous material are shown in the lower portion of Figure 10. Tabular data are shown in Appendix D. The results show that the moduli defined from shear tests behave in approximately the same way as the moduli determined from compression tests. Hence the shear modulus has the form:

$$\log G_{13}(t,T,\sigma) = \log G_{13}(30,T,\sigma) + m'(t,T,\sigma) \log t \Big|_{T,\sigma}$$

where, as in the preceding section, the quantities $G_{13}(30,T,\sigma)$ and $m'(t,T,\sigma)$ characterize the deformation response of the mixture to specific inputs.

It should be noted that in all cases shear test moduli are less than compression moduli. Some questions arose concerning the appropriate thickness of test specimen for obtaining shear without bending. The criterion for selecting ½-inch thick specimens was that this thickness permitted the least interference of boundary conditions with the maximum size particles since smaller thicknesses would not be at least two multiples of the nominal maximum size aggregate. Specimens of ¼-inch thickness were also tested in direct shear and results for some of these tests are shown in Figure 18, 19 and 20. Because the thinnner test specimens yielded an increase of the moduli of only several percent rather than a many-fold increase, it was decided that bending influences were minimal in the ½-inch thick specimen and hence this specimen size was satisfactory for the determination of shear moduli.

It is suggested that an alternate method of determining

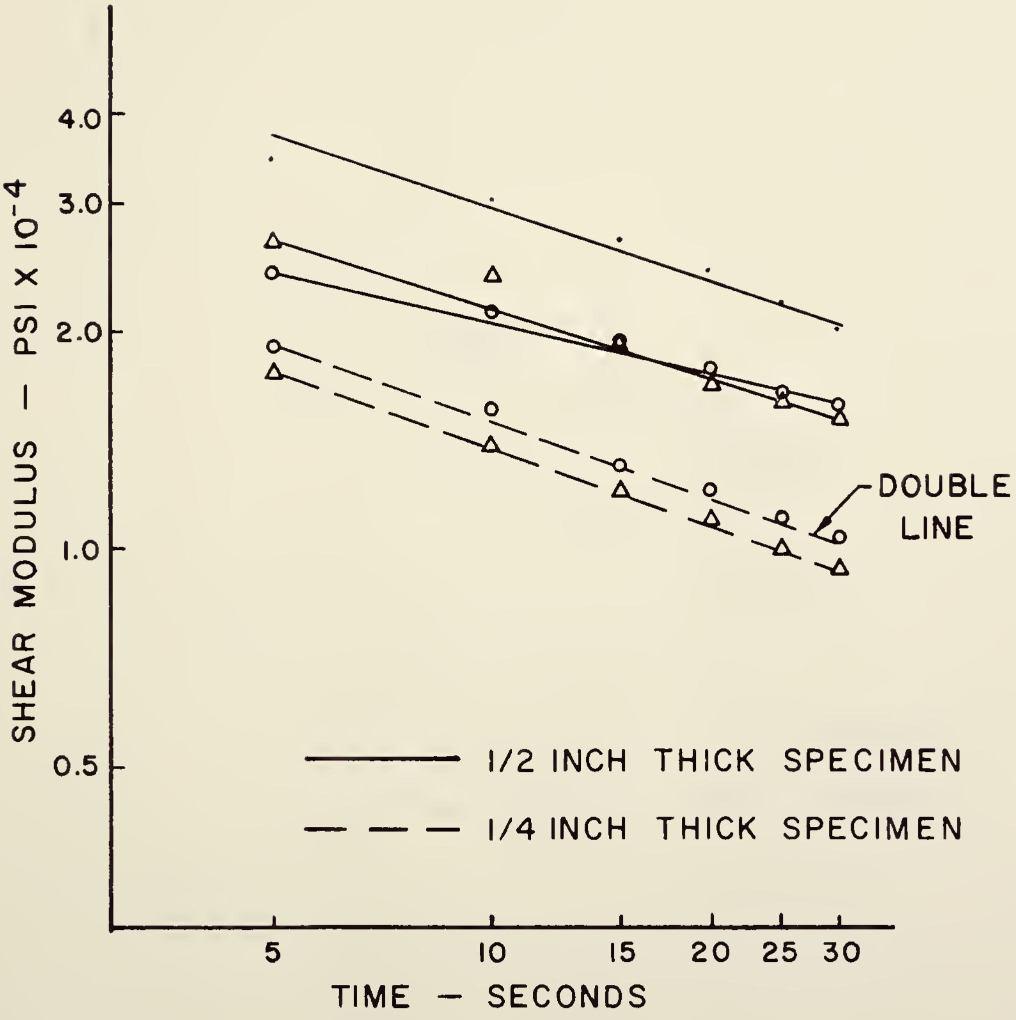

FIGURE 18. SHEAR MODULUS VS. TIME, 70°F

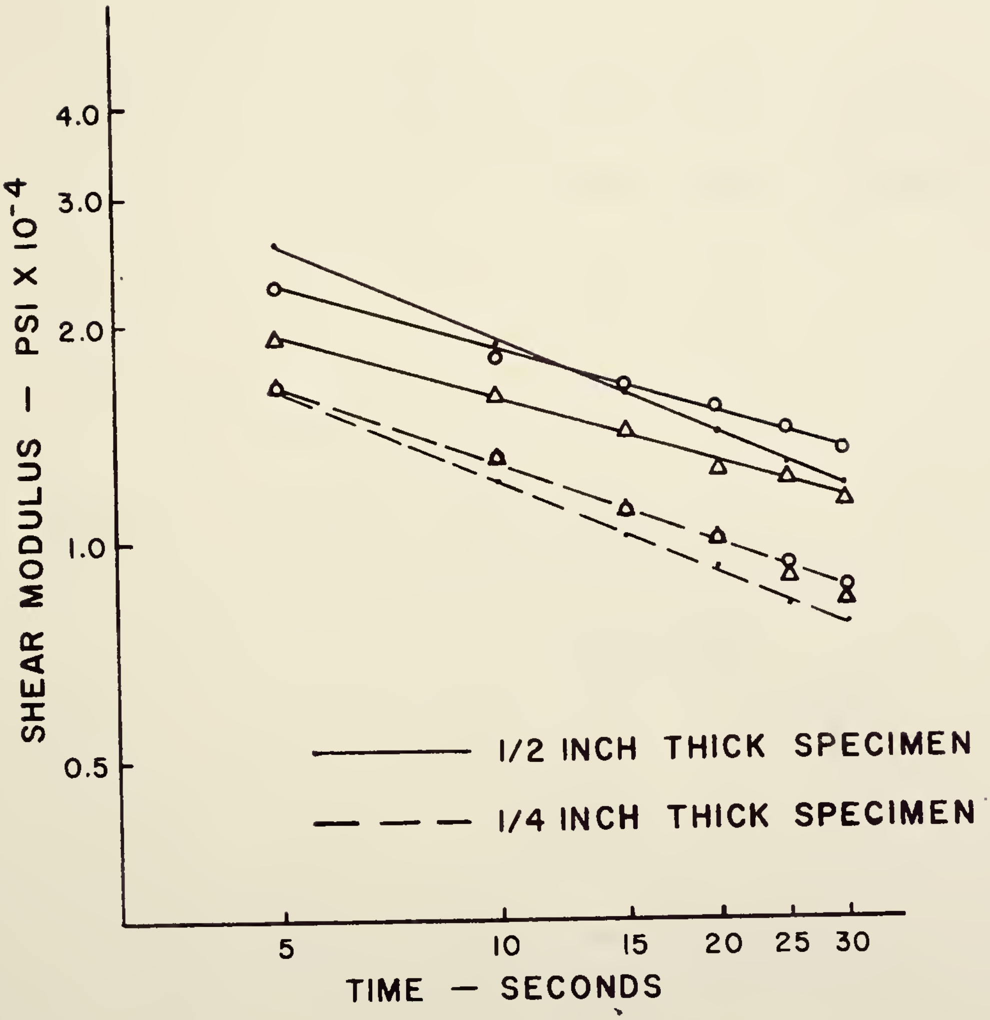

FIGURE 19. SHEAR MODULUS VS. TIME, 80°F

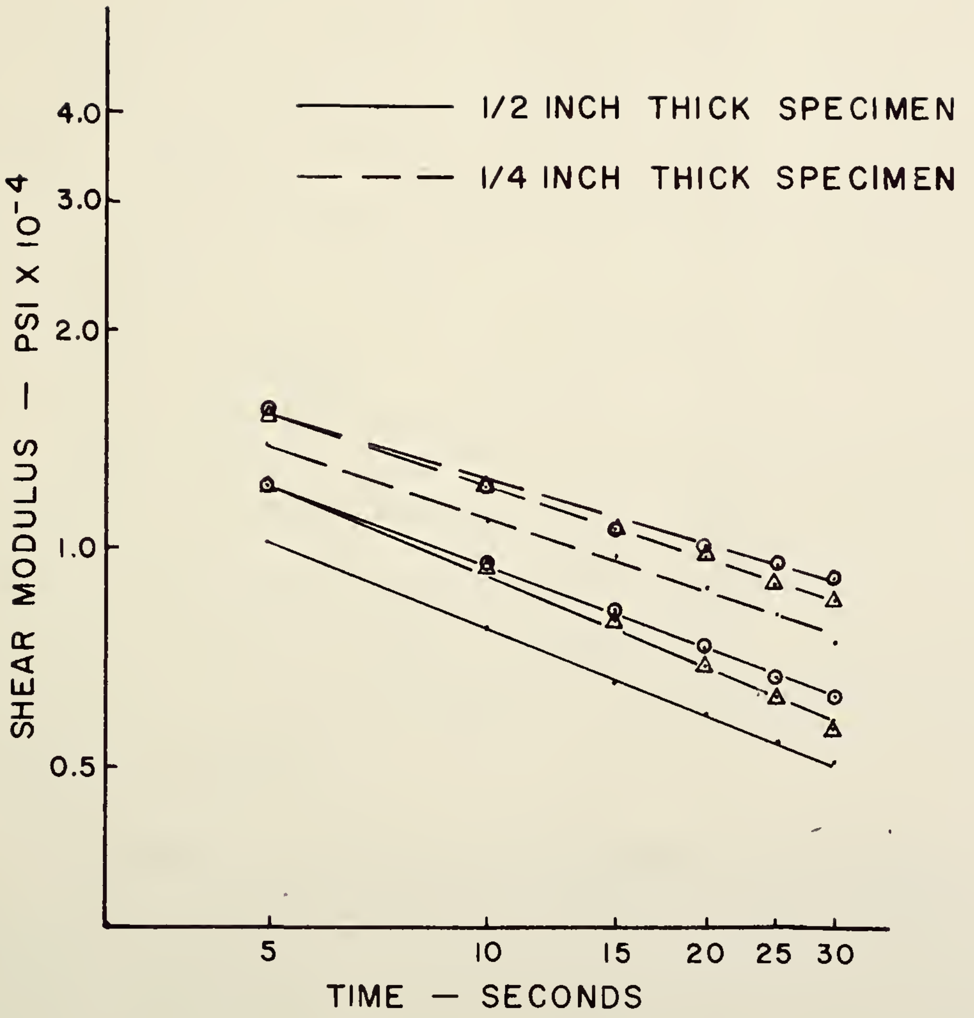

FIGURE 20. SHEAR MODULUS VS. TIME, 90°F

the proper thickness for direct shear specimens can be obtained from considerations of relations involving Poisson's ratio. From the last equation of material behavior, i.e.

$$\tfrac{1}{2}\epsilon_6 = \sigma_6(C_{11} - C_{12}),$$

$$\frac{\epsilon_{12}}{2\sigma_6} = \frac{1}{E_1} - \frac{\mu_{21}}{E_1}$$

or

$$\frac{E_1}{2G_1} = 1 - \mu_{21}$$

Hence, from the knowledge of E_1 and μ_{21} it is possible to select as the correct thickness of the direct shear specimen that thickness for which

$$G_{12} = \frac{E_1}{2(1 - \mu_{21})}$$

From Figure 10 it can be seen that the slopes of the compression moduli and shear moduli are approximately equal. This implies that the ratio $E_1/2G_{12}$ and $1 - \mu_{21}$ will be constant over the time range considered here. This is another indication of the independence of Poisson's ratio with respect to time of loading.

Comparison of Shear and Torsion Test Results

Comparison of shear moduli obtained from tests with different boundary conditions was required to determine whether a necessary condition for the invariance of the material coefficients was satisfied. Six specimens for direct shear testing and six specimens for torsion testing were cut from the same beam of compacted bituminous mixture. The volumes and loaded areas of the specimens tested in direct

shear and torsion were as follows:

	Direct Shear	Torsion
Volume of Material, in^3	0.53	0.50
Loaded Area, in^2	1.06	0.98

It should be noted that the volumes and loaded areas of the test specimens are nearly equal. Results of the tests are presented in Tables 8 and 9 and in Figures 21, 22 and 23. The logarithmic slopes and intercepts at 30 seconds of loading for each stress are presented in Tables 10 and 11. Ninety-five percent confidence intervals given in Table 12 and plotted in Figures 21, 22 and 23 show that the two tests with different boundary conditions yield essentially the same value for the moduli even though experimental deviations exist for results from each test. Consequently, it can be concluded that the values of the moduli obtained are, of necessity, invariant material moduli.

The area of the two overlapping confidence intervals is shaded in Figures 21, 22 and 23. This overlap further demonstrates that the moduli obtained are independent of the boundary conditions of the tests. From Tables 10 and 11 it can be noted that average logarithmic slopes and intercepts at 30 seconds decrease with increasing stress for both shear and torsion tests.

TABLE 8

Torsion Modulus
(psi x 10^{-4})

Specimen No.	Time (Seconds)						
	5	10	15	20	25	30	
1	2.06	1.38	1.12	1.02	0.90	0.84	
2	1.38	1.07	0.90	0.78	0.71	0.67	
3	2.14	1.52	1.31	1.07	0.98	0.90	
4	1.82	1.47	1.24	1.12	1.05	0.98	Stress = 23.1 psi
5	1.96	1.31	1.05	0.90	0.80	0.72	
6	2.14	1.63	1.32	1.18	1.05	0.98	
Avg.	1.92	1.40	1.16	1.01	0.92	0.85	
1	2.14	1.43	1.15	0.97	0.88	0.80	
2	1.54	1.12	0.94	0.85	0.78	0.73	
3	1.66	1.22	1.01	0.87	0.77	0.70	
4	1.66	1.26	1.04	0.92	0.83	0.77	Stress = 40.8 psi
5	1.89	1.38	1.12	0.98	0.88	0.83	
6	1.38	0.99	0.83	0.73	0.66	0.61	
Avg.	1.71	1.23	1.02	0.89	0.80	0.74	
1	1.98	1.29	1.06	0.90	0.78	0.71	
2	1.64	1.19	0.99	0.87	0.78	0.72	
3	1.99	1.10	0.93	0.80	0.72	0.64	
4	1.52	1.06	0.85	0.72	0.65	0.61	Stress = 58.3 psi
5	1.35	0.93	0.76	0.66	0.59	0.54	
6	1.35	0.96	0.80	0.69	0.63	0.58	
Avg.	1.64	1.09	0.90	0.77	0.69	0.63	

TABLE 9

Shear Modulus
(psi x 10^{-4})

Specimen No.	Time (Seconds)						
	5	10	15	20	25	30	
1	1.70	1.22	0.95	0.84	0.76	0.69	
2	1.56	1.22	1.00	0.90	0.81	0.75	
3	1.56	1.16	0.95	0.84	0.75	0.69	
4	1.83	1.46	1.22	1.10	0.99	0.92	Stress = 23.1 psi
5	1.46	1.16	0.95	0.88	0.81	0.73	
6	1.56	1.22	1.05	0.92	0.81	0.75	
Avg.	1.61	1.23	1.02	0.91	0.82	0.75	
1	1.42	1.04	0.86	0.74	0.66	0.60	
2	1.56	1.20	1.00	0.89	0.80	0.74	
3	1.42	1.04	0.86	0.74	0.68	0.62	
4	1.73	1.56	1.07	0.94	0.84	0.80	Stress = 40.8 psi
5	1.42	1.11	0.91	0.80	0.71	0.66	
6	1.56	1.11	0.94	0.82	0.74	0.68	
Avg.	1.52	1.18	0.94	0.82	0.74	0.68	
1	1.24	0.89	0.72	0.62	0.56	0.51	
2	1.39	1.06	0.89	0.79	0.72	0.66	
3	1.48	1.06	0.85	0.74	0.66	0.59	
4	1.39	1.06	0.89	0.77	0.67	0.62	Stress = 58.3 psi
5	1.27	0.93	0.78	0.68	0.62	0.56	
6	1.39	1.01	0.85	0.74	0.66	0.60	
Avg.	1.36	1.00	0.83	0.72	0.61	0.59	

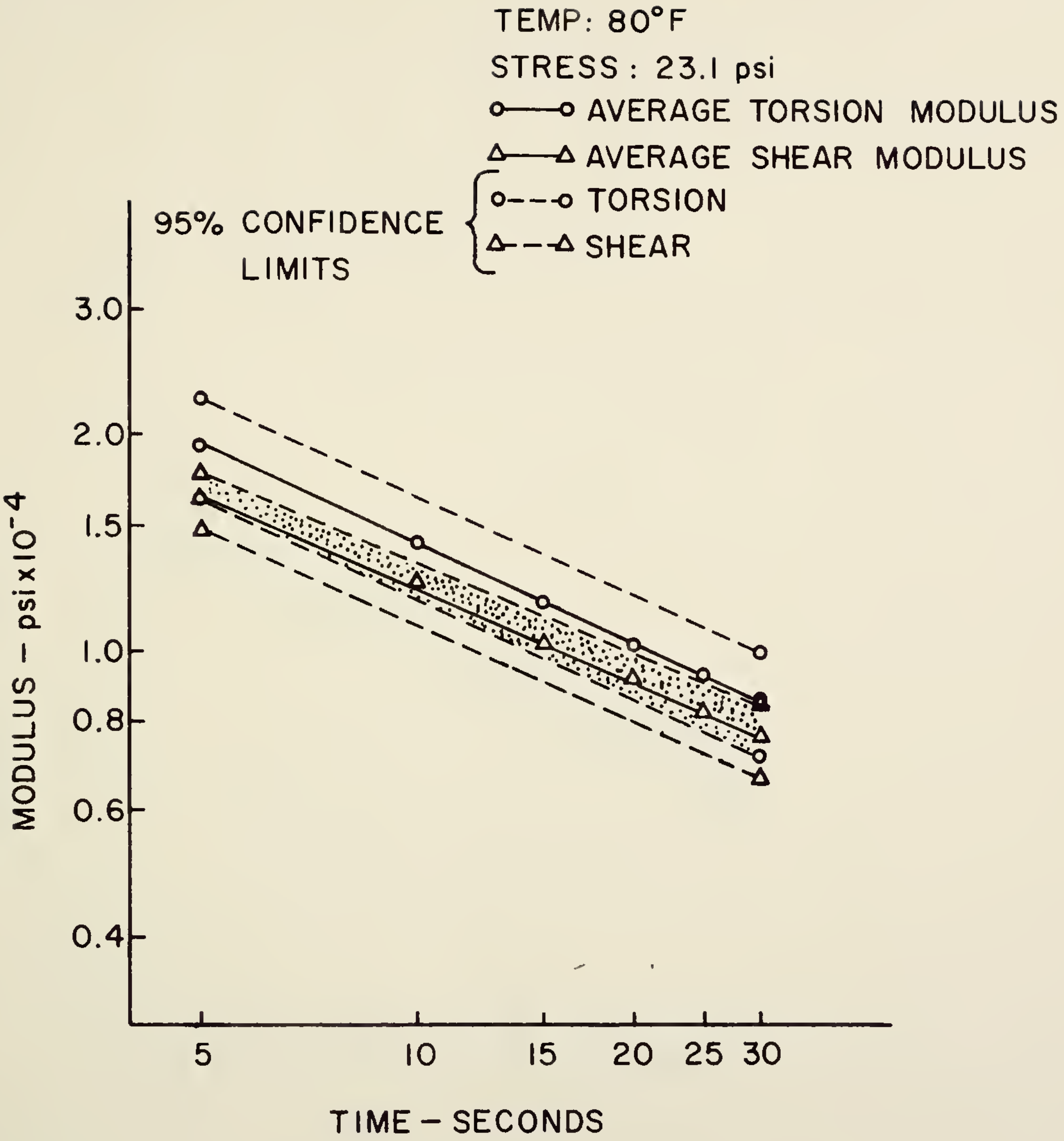

FIGURE 21. COMPARISON OF TORSION AND SHEAR MODULI – 23.1 psi

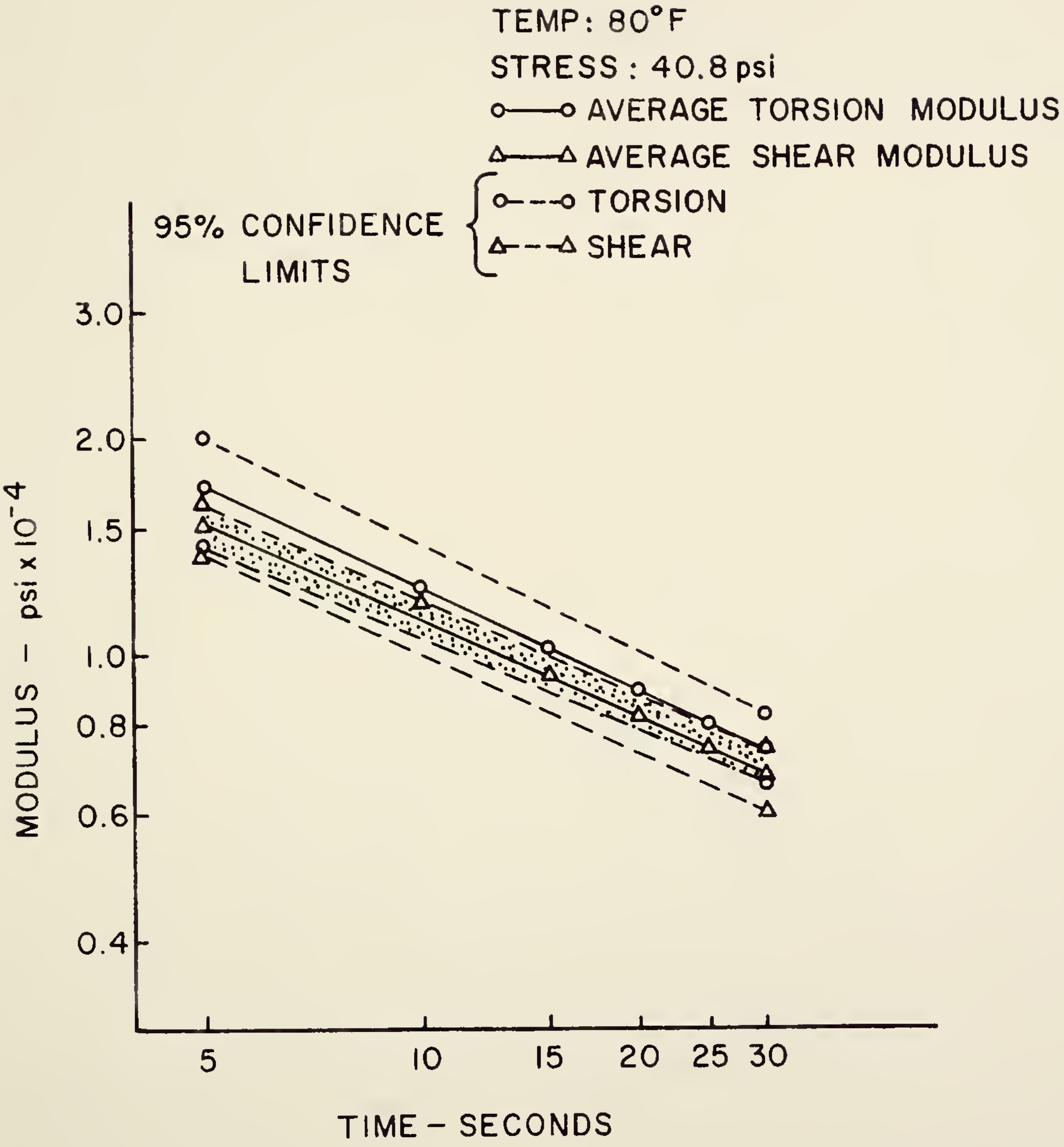

FIGURE 22. COMPARISON OF TORSION AND SHEAR MODULI – 40.8 psi

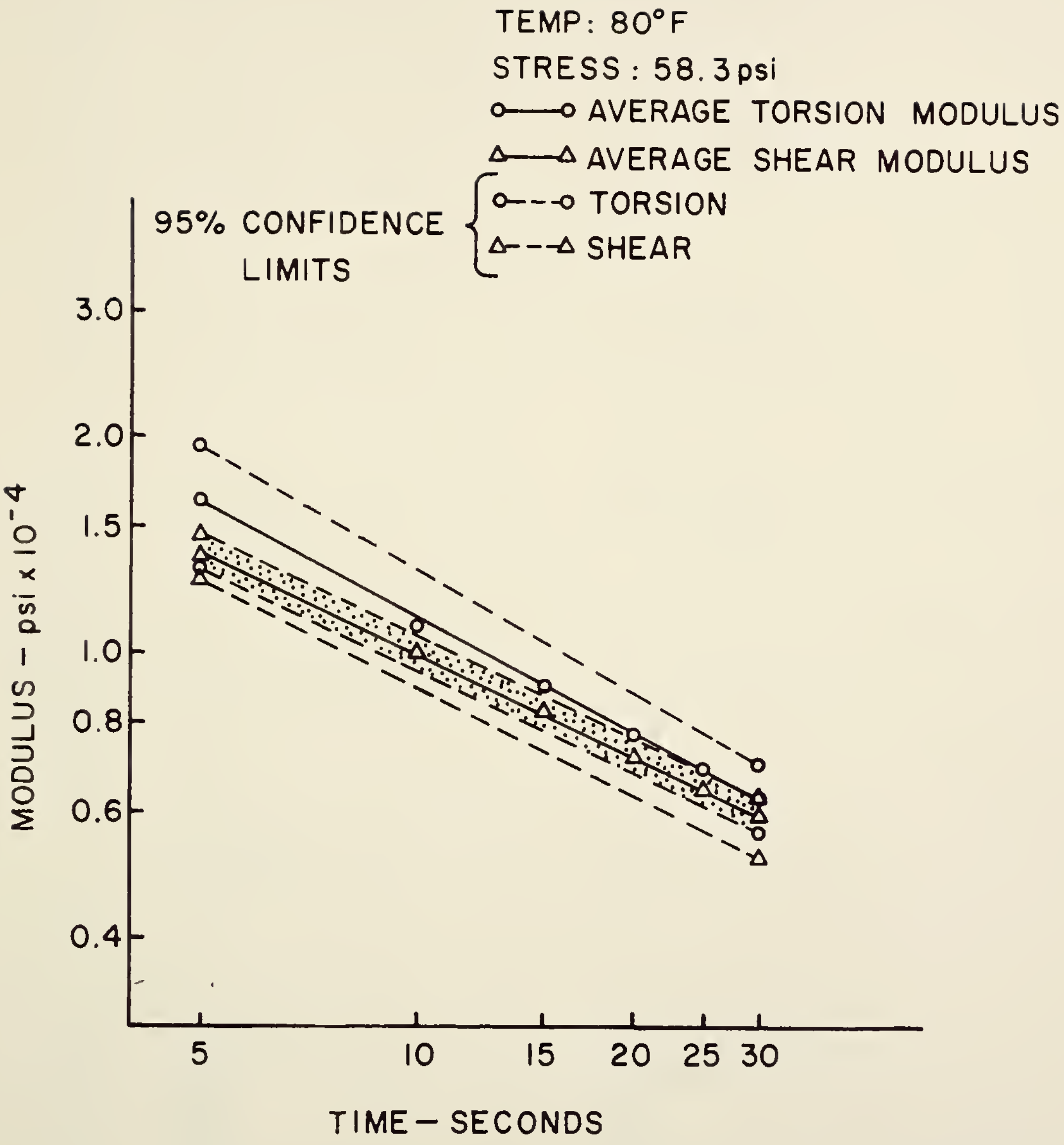

FIGURE 23. COMPARISON OF TORSION AND SHEAR MODULI - 58.3 psi

TABLE 10

Intercepts of Torsion and Shear Moduli for Loading Time of Thirty Seconds
(psi x 10^{-4})

Torsion Test

Stress - psi	Specimen 1	2	3	4	5	6	Avg.
23.1	0.84	0.67	0.90	0.98	0.72	0.98	0.85
40.8	0.80	0.73	0.70	0.77	0.83	0.61	0.74
58.3	0.71	0.72	0.64	0.51	0.54	0.58	0.63

Shear Test

Stress - psi	Specimen 1	2	3	4	5	6	Avg.
23.1	0.69	0.75	0.69	0.92	0.73	0.75	0.75
40.8	0.60	0.74	0.62	0.80	0.66	0.68	0.68
58.3	0.51	0.66	0.59	0.62	0.56	0.60	0.59

TABLE 11

Least Squares Logarithmic Slopes of Torsion and Shear Moduli on Time

Torsion Test

Stress - psi	Specimen 1	2	3	4	5	6	Avg.
23.1	-0.50	-0.41	-0.49	-0.35	-0.56	-0.44	-0.46
40.8	-0.55	-0.42	-0.48	-0.43	-0.47	-0.45	-0.47
58.3	-0.57	-0.46	-0.51	-0.52	-0.51	-0.47	-0.51

Shear Test

Stress - psi	Specimen 1	2	3	4	5	6	Avg.
23.1	-0.51	-0.42	-0.46	-0.39	-0.38	-0.41	-0.43
40.8	-0.50	-0.42	-0.46	-0.48	-0.44	-0.46	-0.46
58.3	-0.50	-0.41	-0.51	-0.45	-0.45	-0.47	-0.47

TABLE 12

95% Confidence Intervals for Shear and Torsion Moduli (psi x 10^{-4})

Torsion Modulus ($X10^{-4}$psi) Stress	5 Seconds	30 Seconds
23.1 psi	1.92 ± 0.31	0.85 ± 0.14
40.8 psi	1.71 ± 0.29	0.74 ± 0.08
58.3 psi	1.64 ± 0.31	0.63 ± 0.07

Shear Modulus ($X10^{-4}$psi) Stress		
23.1 psi	1.61 ± 0.14	0.75 ± 0.09
40.8 psi	1.52 ± 0.13	0.68 ± 0.08
58.3 psi	1.36 ± 0.09	0.59 ± 0.05

SUMMARY OF RESULTS AND CONCLUSIONS

The results and conclusions justified by data obtained in this study are summarized here. The scope of the study included one bituminous mixture, laboratory compacted, tested at three stress and three temperature levels, and for durations of loading up to thirty seconds. It should be recognized that these results and conclusions are known to be applicable only to the materials and testing procedures used in this investigation. Extrapolation of experimental results is not justified without further testing.

1. Six material coefficients exist and may be used for the description of the stress-strain behavior of transversely anisotropic, statistically homogeneous, nonconservative materials subjected to small strains. The coefficients which relate stress to strain are shown below and in the section entitled development of theory as follows:

$$\begin{bmatrix} \epsilon_1 \\ \epsilon_2 \\ \epsilon_3 \\ \epsilon_4 \\ \epsilon_5 \\ \epsilon_6 \end{bmatrix} = \begin{bmatrix} \frac{1}{E_1} & \frac{\mu_{21}}{E_1} & \frac{\mu_{13}}{E_3} & 0 & 0 & 0 \\ \frac{\mu_{21}}{E_1} & \frac{1}{E_1} & \frac{\mu_{13}}{E_3} & 0 & 0 & 0 \\ \frac{\mu_{31}}{E_1} & \frac{\mu_{31}}{E_1} & \frac{1}{E_3} & 0 & 0 & 0 \\ 0 & 0 & 0 & \frac{1}{G_{13}} & 0 & 0 \\ 0 & 0 & 0 & 0 & \frac{1}{G_{13}} & 0 \\ 0 & 0 & 0 & 0 & 0 & \frac{2(1-\mu_{21})}{E_1} \end{bmatrix} \begin{bmatrix} \sigma_1 \\ \sigma_2 \\ \sigma_3 \\ \sigma_4 \\ \sigma_5 \\ \sigma_6 \end{bmatrix}$$

2. The methods of this investigation provide quantitative parameters that relate the common engineering concepts of stress and strain. These parameters can be used in the description, evaluation and design of bituminous mixtures for the prefailure conditions considered in the testing program. Reliability of the parameters was established statistically for material coefficients obtained from shear and torsion tests.

3. It is feasible to determine the values of the six material coefficients by the testing methods utilized in this study. From determinations of the material coefficients, strains can be predicted, temperature and stress dependence of the bituminous mixture can be assessed and a measure of transverse anisotropy can be obtained. Tests include uniaxial compressions tests, direct shear tests, torsion tests and uniaxial compression tests with volume change measurements.

4. For the bituminous mixture tested, stiffnesses in compression were greater in the direction of imposed compaction forces than in orthogonal directions indicating that assumptions of isotropy for bituminous mixtures are questionable. The logarithm of mixture stiffness was found to vary essentially linearly when plotted against the logarithm of time for the time interval from five to thirty seconds. Mixture stiffness also decreased with increasing stresses and test temperatures. Anisotropy appears to be independent of time, for the mixture tested, at each stress level and temperature of the study.

5. A necessary condition for the invariance of the material coefficients was satisfied for the mixture used in this

study. Both torsion and direct shear tests yielded essentially the same values for the shear modulus for three magnitudes of stress applied at the $80^{\circ}F$ test temperature.

6. Poisson's ratios obtained from volumetric measurements and linear measurements did not agree and additional work is necessary to determine accurately the dependence of Poisson's ratios on temperature and applied stress for small strains. Data from volume change measurements indicate that Poisson's ratio is independent of time for the conditions of this test.

7. The strain gage displacement transducer developed for the measurement of deformations was satisfactory for the time, temperature and stress conditions of this study. Instrumentation of the typical element of bituminous material for the purpose of determining the material coefficients, C_{ij}, was completely satisfactory and sufficiently accurate for the boundary conditions utilized during testing.

SUGGESTIONS FOR FURTHER RESEARCH

The research undertaken and completed in this project has exposed other questions and problems that might also be investigated with fruitful results. In this section five specific projects, among others, are proposed.

1. The limitations imposed by instrumentation on the measurement of small strains should motivate additional work on the development of displacement transducers for small deformations. Work on transducers that could be used in conjunction with volume change measurements would assist a more exact definition of Poisson's ratio. A profitable approach might be made by utilizing more recently available stable linear variable differential transformers or transducers made with self-temperature-compensated semiconductor strain gages.

2. This study was concerned with the material coefficients defined from creep moduli. A companion examination of relaxation coefficients and moduli would assist in the optimum utilization of data obtained from this study. Both deformation and recovery occur and may be observed in flexible pavements in service.

3. A study of the effect of mixture variables upon the material coefficients would provide additional bases for using the theory of this study to assist in prediction of mixture

performance.

4. Other variable factors that deserve consideration in future testing are combined stresses and the time interval between loads. The possibility of superposing time, temperature and cycle effects in the constitutive equations for bituminous mixtures should also be investigated.

5. To be ultimately useful, the concepts and data of the laboratory should provide a basis for predicting the field performance of bituminous mixtures. It is suggested that companion studies utilize data and/or experience from this research to investigate the validity of the method proposed in this study for the design of bituminous mixtures used in any layer of a flexible pavement. To this end a field study would be desirable to help assess the usefulness and precision of testing methods proposed here.

6. A larger portion of engineering design and planning is being relegated to electronic computers. It is suggested that one research project might incorporate the conjunction of deterministic material properties obtained in this study and stochastic variables of vehicle weight and headway distribution in a computer program. Simulation of traffic and temperature conditions together with pavement performance can be studied in this way to assist in optimizing the design of bituminous mixtures relative to their expected use.

LIST OF REFERENCES

LIST OF REFERENCES

1. Barden, Laing, "Stresses and Displacements in a Cross-anisotropic Soil," Geotechnique, Vol. 13, No. 3, December, 1963.

2. Beckman Instruments, Inc., Instruction Manual, Type R and Type RC Dynograph Direct Writing Recorder, Schiller Park, Illinois, 1964.

3. Bland, D. R., The Theory of Linear Viscoelasticity, Pergamon Press, New York, 1960.

4. Bolotin, V. V., Nonconservative Problems of the Theory of Elastic Stability, Pergamon Press, New York, 1963.

5. Cady, Walter G., Piezoelectricity, Vol. 1, Dover Publications, New York, 1964.

6. Dove, R. C. and Adams, P. H., Experimental Stress Analysis and Motion Measurement, Charles E. Merrill Books, Columbus, Ohio, 1964.

7. Dorsey, James, Semiconductor Strain Gage Handbooks, BLH Electronics, Waltham, Mass., 1964.

8. Doyle, D. V., Drow, J.T. and McBurney, R. S., "Elastic Properties of Wood," Report No. 1528, Forest Products Laboratory, Madison, Wisconsin, 1956.

9. Durelli, A. J., Phillips, E. A., Tsao, C. H., Introduction to the Theoretical and Experimental Analysis of Stress and Strain, McGraw-Hill, New York, 1958.

10. Eirich, Frederick R., Rheology, Vol. II, Academic Press, New York, 1958.

11. Elliott, H. A., "Three-dimensional Stress Distributions in Hexagonal Aeolotropic Crystals," Proceedings of the Cambridge Philosophical Society, Vol. 44, Part 4, 1948.

12. Espinasse, Margaret, Robert Hooke, Wm. Heineman, Ltd., Toronto, 1956.

13. Everett, F. L., and Miklowitz, J., "Poisson's Ratio at High Temperatures," Journal of Applied Physics, Vol. 15, 1944.

14. Filonenko-Borodich, M., Theory of Elasticity, Peace Publishers, Moscow, 1963.

15. Freudenthal, Alfred, M., The Inelastic Behavior of Engineering Materials and Structures, John Wily & Sons, New York, 1950.

16. Garofalo, F., Malenock, P. R., Smith, G. V., "The Influence of Temperature on the Elastic Constants of Some Commercial Steels," Symposium on Determination of Elastic Constants, ASTM Special Technical Publication No. 129, New York, 1952.

17. Greszczuk, L. B., "Effect of Material Orthotropy on the Directions of Principal Stresses and Strain," Report presented at the Fifth Pacific Area National Meeting of the ASTM, Seattle, 1965.

18. Greszczuk, L. ., "Elastic Constants and Analysis Methods for Filament Wound Shell Structures," Report SM-45849, Douglas Aircraft Company, Santa Monica, California, 1964.

19. Groot, S. R. de, Thermodynamics of Irreversible Processes, North-Holland Publishing Co., Amsterdam, The Netherlands, 1958.

20. Hearmon, R. F. S., An Introduction to Applied Anisotropic Elasticity, Oxford, London, 1961.

21. Jayne, B. A., Suddarth, S. K., "Mechanics of Fibrous Orthotropic Materials," Preprint of paper presented at Fifth Pacific Area National Meeting of the ASTM, Seattle, 1965.

22. Klug, H. P. and Alexander, L. E., X-Ray Diffraction Procedures, Wiley, New York, 1959.

23. Lal, N. B., "Two Dimensional Stress-strain Relationships of a Fine Asphalt-aggregate System," Ph.D. Thesis, submitted to the Faculty of Purdue University, 1965.

24. Lee, A. R. and Markwick, A. H. D., "The Mechanical Properties of Bituminous Surfacing Materials Under Constant Stress," Journal of the Society of the Chemical Industry, London, 1937.

25. Lekhnitskii, S. G., Theory of Elasticity of An Anisotropic Elastic Body, Holden-Day, San Francisco, 1963.

26. Livneh, M. and Shklarsky, E., "The Bearing Capacity of Asphaltic Concrete Carpets," Proceedings International Conference on the Structural Design of Asphalt Pavements, Ann Arbor, Michigan, 1962.

27. Love, A. E. H., A Treatise on the Mathematical Theory of Elasticity, Dover Publications, New York, 1944.

28. Mededelingen, LGM, "De Spanningverdeling in een Homogeen, Anisotroop Elastisch Halfmedium," Vol. 5, No. 2, 1960.

29. Michell, J. H., "The Stress in an Aeolotropic Elastic Solid with an Infinite Plane Boundary," Proceedings of the London Mathematical Society, Vol. 31, London, 1900.

30. Mix Design Methods for Asphalt Concrete, The Asphalt Institute, College Park, Maryland, May, 1963.

31. Monismith, Carl L., Alexander, R. L., and Secor, K. E., "Rheologic Behavior of Asphalt Concrete," Paper prepared for presentation at the Annual Meeting of the Association of Asphalt Paving Technologists, Minneapolis, 1966.

32. Morant, M. J., Introduction to Semiconductor Devices, Addison-Wesley, Reading, Mass., 1964.

33. Nadai, A., Theory of Flow and Fracture of Solids, Vol. 1, McGraw-Hill, New York, 1950.

34. Nijboer, L. W., Plasticity as a Factor in the Design of Dense Bituminous Road Carpets, Elsevier, New York, 1948.

35. Papazian, H. S., "The Response of Linear Viscoelastic Materials in the Frequency Domain with Emphasis on Asphaltic Concrete," Proceedings of the International Conference on the Structural Design of Asphalt Pavements, Ann Arbor, Michigan, 1962.

36. Perloff, W. H. and Moavenzadeh, F., "Deflection of Viscoelastic Medium Due to a Moving Load," Preprint prepared for the Second International Conference on the Structural Design of Asphalt Pavements, 1967.

37. van der Poel, C., "Road Asphalt," in Building Materials, edited by M. Reiner, Interscience, New York, 1954.

38. Polakowski, N. H. and Ripling, E. J., Strength and Structure of Engineering Materials, Prentice-Hall, Englewood Cliffs, N. J., 1966.

39. Puzinauskas, V. P., "Influence of Mineral Aggregate Structure on Properties of Asphalt Paving Mixtures," Paper prepared for presentation at the Highway Research Board 43rd Annual Meeting, Washington, D. C., 1963.

40. Roscoe, K. H. and Schofield, A. N., Discussion in Journal, Soil Mechanics and Foundation Section, American Society of Civil Engineers, January, 1964.

41. Schapery, R. A., "An Approximate Method of Stress Analysis for a Large Class of Problems in Viscoelasticity," Aeronautical and Engineering Science *Report* No. 62-18, Purdue University, 1963.

42. Sokolnikoff, I. S., *Mathematical Theory of Elasticity*, McGraw-Hill, New York, 1946.

43. "Strain Gage *Handbook*," BLH Electronics, Waltham, Mass., 1964.

44. "Stress-strain Relations in Wood and Plywood Considered as Orthotropic Materials," *Report* No. 1503, Forest Products Laboratory, Madison, Wisconsin, 1962.

45. Symposium on Significance of the Tension Test of Metals in Relation to Design, *Proceedings* of the ASTM, Vol. 40, 1940.

46. Todhunter, Isaac and Pearson, Karl, *A History of the Theory of Elasticity and of Strength of Materials*, Dover Publications, New York, 1960.

47. Voigt, Waldemar, *Lehrbuch der Kristallphysik*, Edwards Brothers, Ann Arbor, Michigan, 1946.

48. Williams, M. L., "Structural Analysis of Viscoelastic Materials," AIAA *Journal*, Vol. 2, No. 5, 1964.

49. Wolf, K., "Distribution of Stress in a Half-plane and in a Half-space of Anisotropic Material," *Zeitschrift* für Angewandte Mathematik und Mechanik, Vol. 15, No. 5, 1935.

50. Wood, L. E. and Goetz, W. H., "Rheological Characteristics of a Sand-Asphalt Mixture," *Proceedings*, Association of Asphalt Paving Technologists, Vol. 28, 1959.

51. Zener, Clarence, *Elasticity and Anelasticity of Metals*, University of Chicago Press, Chicago, 1948.

APPENDIX A

APPENDIX A

Notation

This appendix is included to specify the conventions used in defining stresses, strains and various ratios and moduli that are discussed in the main body of the text. Because tensor notation is common in the literature of the theory of elasticity and continuum mechanics, the coordinate axes have been designated x_1, x_2 x_3 rather than x, y, z. Other departures from the engineering notation popularized by Timoshenko and others are evident. The notation utilized here follows closely that recommended as standard by the Institute of Radio Engineers and used by Hearmon (20).

A standard convention in matrix notation is to use the first subscript following a matrix element to designate the number of the row in which the element is located and the second subscript to designate the number of the column in which the element is located. Hence a_{ij} refers to the element a in the i-th row and the j-th column.

The orientation of the coordinate system in which stresses are described is shown in Figure 24. Referenced to this coordinate system is a sketch of the compacted beam of bituminous mixture from which test specimens were prepared.

The stresses shown on the beam illustrate the notation

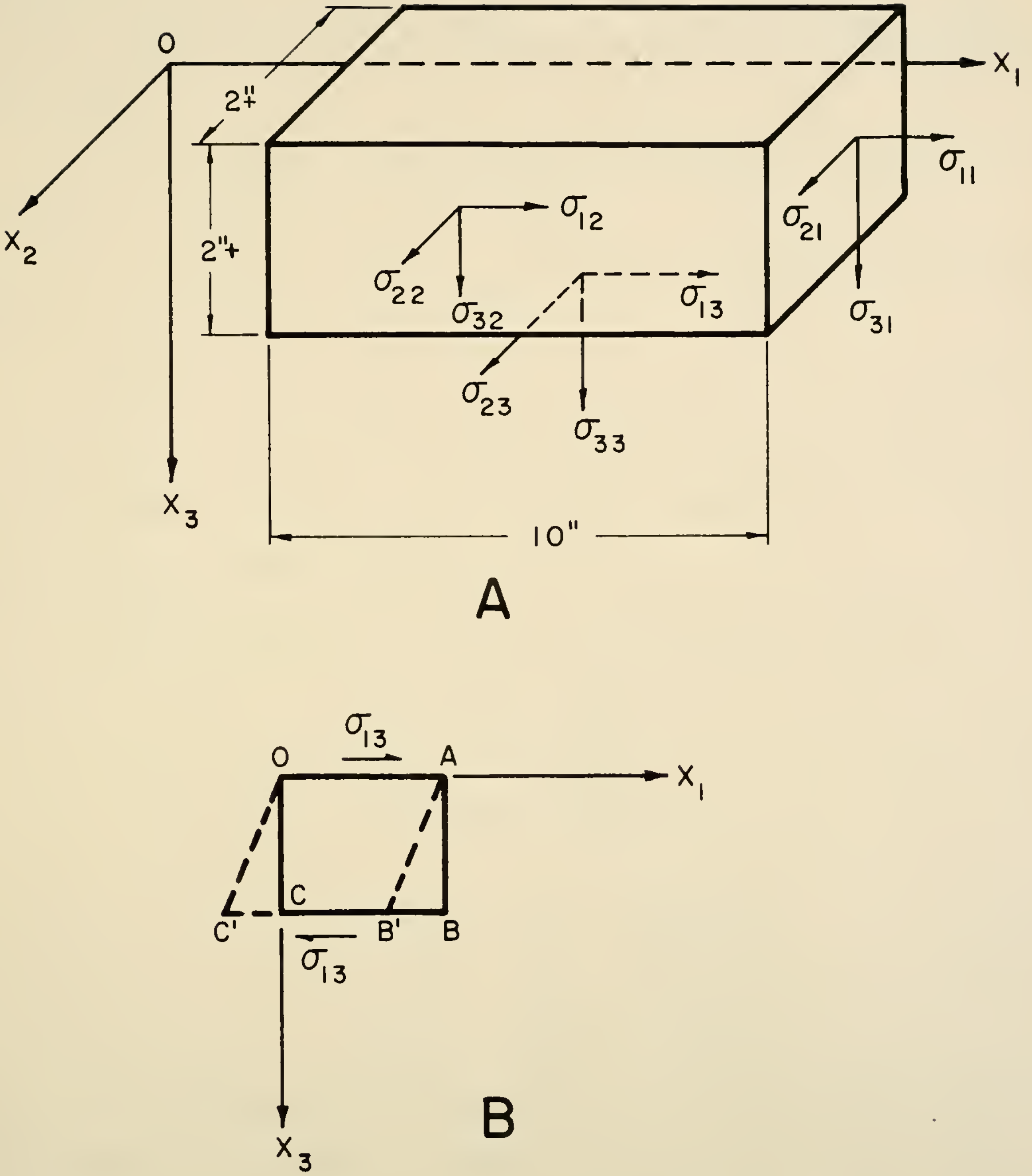

FIGURE 24. ORIENTATION OF BEAM OF
COMPACTED BITUMINOUS MATERIAL
SHOWING NOTATION CONVENTION

convention used throughout the discussion. In general, σ_{ii} are normal components of stress and σ_{ij} $(i \neq j)$ are tangential components.

The strains, ϵ_{ii}, are extensional strains defined as (change in length)/(original length). The components ϵ_{ij} $(i \neq j)$ are shear strains and are defined diagrammatically in the lower portion of Figure 24.

When the shear stress σ_{13} acts as shown in the figure, a distortion occurs in the element causing the unit square ABCO to change into the rhombus AB'C'O. The angles BAB' and COC' are each equal to ϵ_{13}.

In matrix form the stresses and strains are shown as:

$$S = \begin{bmatrix} \sigma_{11} & \sigma_{12} & \sigma_{13} \\ \sigma_{21} & \sigma_{22} & \sigma_{23} \\ \sigma_{31} & \sigma_{32} & \sigma_{33} \end{bmatrix}$$

$$E = \begin{bmatrix} \epsilon_{11} & \frac{1}{2}\epsilon_{12} & \frac{1}{2}\epsilon_{13} \\ \frac{1}{2}\epsilon_{21} & \epsilon_{22} & \frac{1}{2}\epsilon_{23} \\ \frac{1}{2}\epsilon_{31} & \frac{1}{2}\epsilon_{32} & \epsilon_{33} \end{bmatrix}$$

The off-diagonal elements σ_{ij}, $(i \neq j)$ are symmetrical about the diagonal by reason of the condition for zero rotation of the typical element. The double subscripts shown here are used in a contracted form in the main body of the text. Hence the following equivalence relations are defined:

$$\sigma_1 = \sigma_{11} \qquad \sigma_2 = \sigma_{22} \qquad \sigma_3 = \sigma_{33}$$

$$\sigma_4 = \sigma_{23} \qquad \sigma_5 = \sigma_{13} \qquad \sigma_6 = \sigma_{12}$$

$\epsilon_1 = \epsilon_{11}$ $\epsilon_2 = \epsilon_{22}$ $\epsilon_3 = \epsilon_{33}$

$\epsilon_4 = \epsilon_{23}$ $\epsilon_5 = \epsilon_{13}$ $\epsilon_6 = \epsilon_{12}$

The subscript convention for Poisson's ratio involves two numbers. In general, μ_{ij} denotes Poisson's ratio, ϵ_i/ϵ_j, when the stress is directed along the coordinate axis x_j. The time- and temperature-dependent shear modulus is denoted by the letter G, while the moduli defined from normal strains in the x_1 and x_3 directions are designated E_1 and E_3, respectively.

APPENDIX B

APPENDIX B

Materials and Preparation of Specimens

Specimens for compression, shear and torsion tests were prepared from aggregate blended to conform to the grading curve shown in Figure 25. Table 13 shows the sieve analysis and origin of the aggregate used in testing. After being blended in 2200 gram batches, the aggregate was placed in an oven and heated to 325°F.

A 60-70 penetration asphalt cement having the properties shown in Table 14 was used in this study. The asphalt was heated to 325°F and then mixed with the heated aggregate in a mechanical mixer for two minutes. The weight of asphalt cement mixed with the aggregate was 5 percent by weight of the aggregate. After mixing was completed, each batch was put in flat pans and placed in a forced-air draft oven to cure for 24 hours at 140°F.

Compaction of the bituminous mixture was started after the mixture was reheated to 325°F. The heated mixture was placed in two layers in the heated beam mold shown in Figure 26. Each layer was tamped 25 times with a ½-inch diameter, round-end tamping rod.

The mixture in the beam mold was compacted in the kneading compactor by the special tamping foot shown with

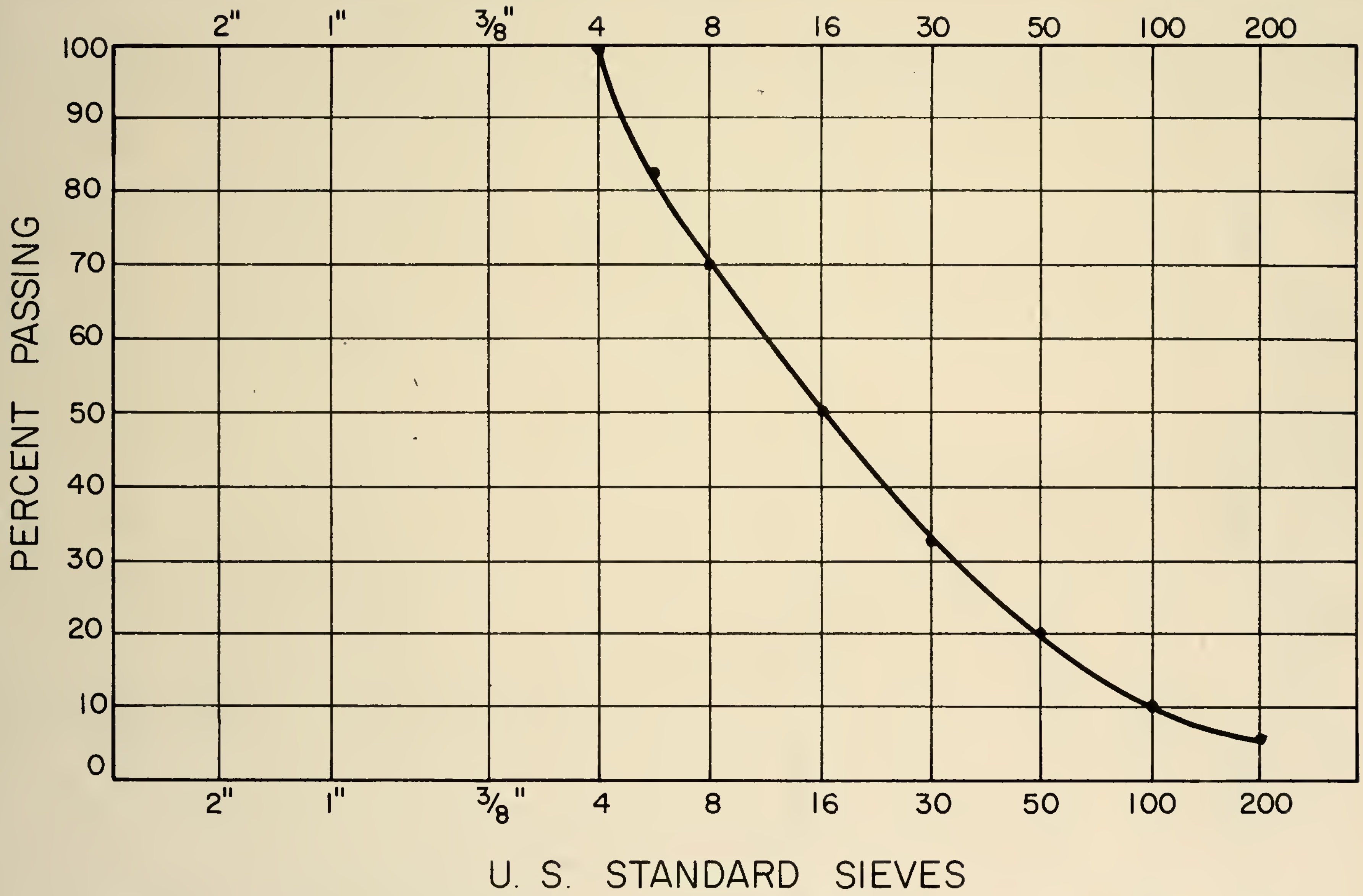

FIGURE 25. GRADATION CURVE FOR BITUMINOUS MIXTURE

TABLE 13

Sieve Analysis of Aggregates

Sieve		Fraction, %	Material
Passing	Retained		
No. 4	No. 6	17	Crushed Greencastle Limestone
No. 6	No. 8	13	" " "
No. 8	No. 16	20	River Terrace Sand (Lafayette)
No. 16	No. 30	17	" " " "
No. 30	No. 50	13	" " " "
No. 50	No. 100	10	" " " "
No. 100	No. 200	5	" " " "
No. 200		5	Greencastle Limestone Filler

TABLE 14

Results of Tests on Asphalt Cement

Specific Gravity @ 77°F	1.036
Softening Point, Ring and Ball, °F	124
Ductility at 77°F, 5 cm/min, cm	200 +
Penetration, 100 grams, 5 sec., 77°F	66
Penetration, 200 grams, 60 sec., 32°F	17
Loss on Heating, 50 grams, 5 hr., 325°F, %	0.01
Penetration of Residue, percent of original	89
Flash Point, Cleveland Open Cup, °F	595
Solubility in CCl_4, percent	99.84

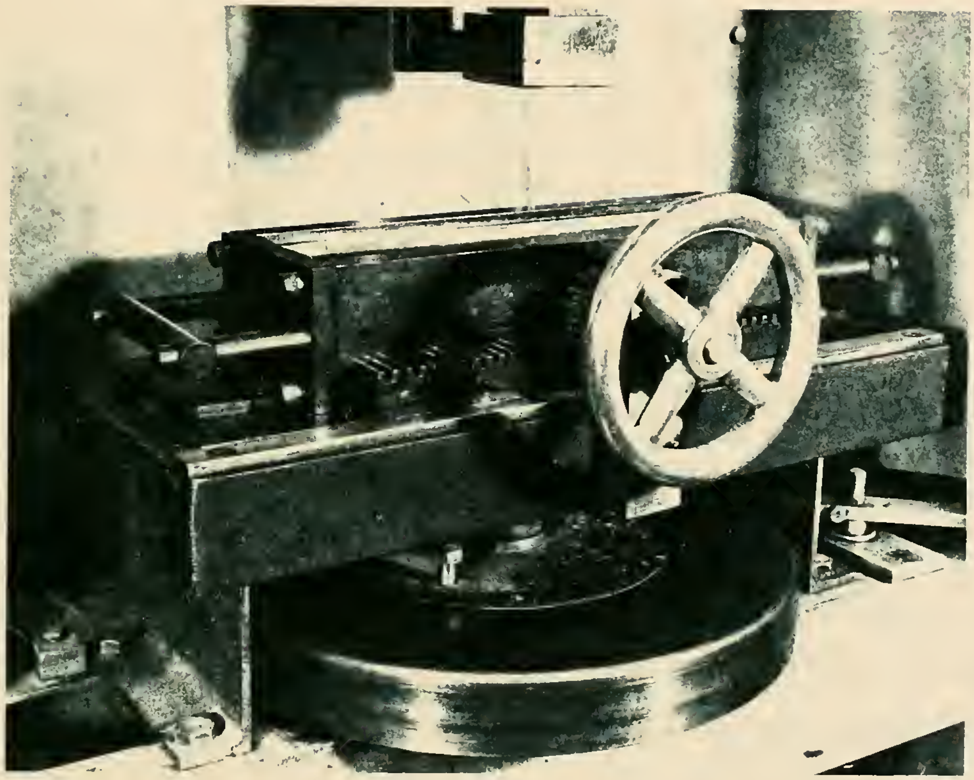

FIGURE 26. MOLD AND TAMPING FOOT FOR COMPACTING BEAM OF BITUMINOUS MIXTURE

the beam mold in Figure 26. The mixture was compacted with the tamping foot by moving the mold back and forth its entire length under the tamping foot four times, using 8 tamps during each one-way traverse, for each of four different compaction pressures. Foot pressures used in compaction were 20, 35, 100 and 120 psi, in that order. After the beam was compacted on its top side according to this procedure, the mold and beam were inverted and the procedure was repeated. Hence, both the top and the bottom of the beam received the same compactive effort.

After the beam was compacted, it was removed from the mold and placed in a forced-air draft oven and cured for 24 hours at a temperature of 140°F for 24 hours. After the curing period, the beam was cooled to room temperature.

The compacted beam was cut into specimens by use of a masonry saw. One-inch pieces were cut from both ends of the beams and wasted. This was done because it was recognized that confinement at the ends of the beam mold might cause compaction conditions to be atypical at these locations.

Specimens for uniaxial compression testing were cut approximately 0.05 inch oversize from the beam by a masonry saw. Final shaping and polishing were accomplished on a lapping wheel using 100 and 800 mesh grinding compounds, respectively. Dimensions of the compression test specimens were controlled to 0.01 inch by utilizing the jig shown in Figures 27 and 28. Final dimensions of the compression test were 1 x 1 x 2.05 inches.

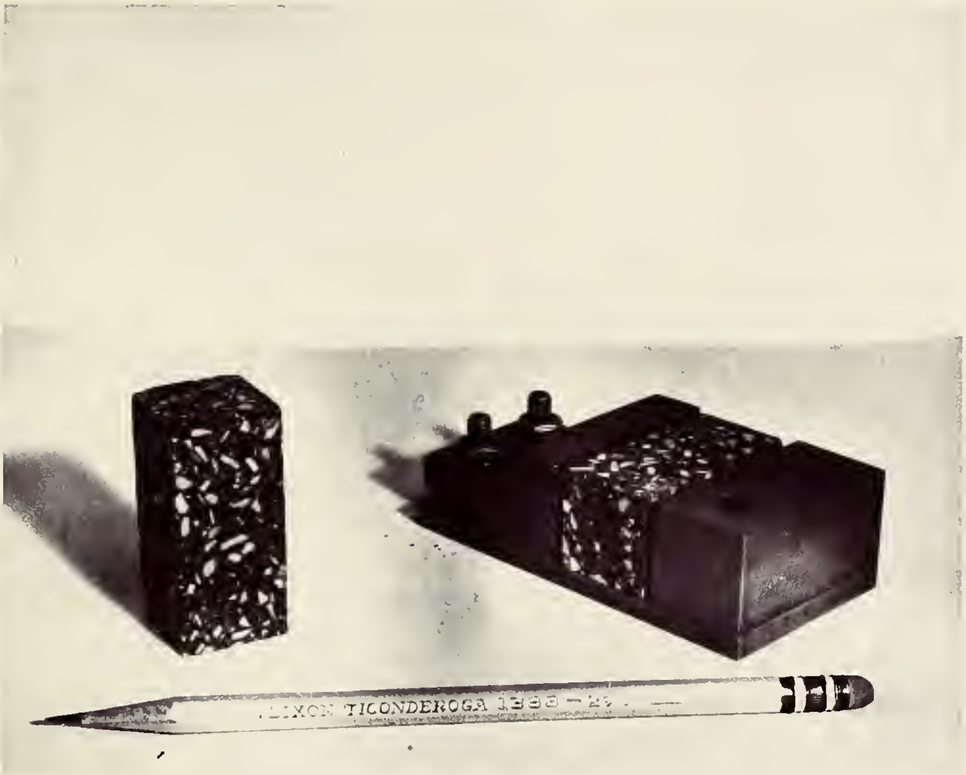

FIGURE 27. UNIAXIAL COMPRESSION SPECIMENS
WITH JIG FOR SIZING

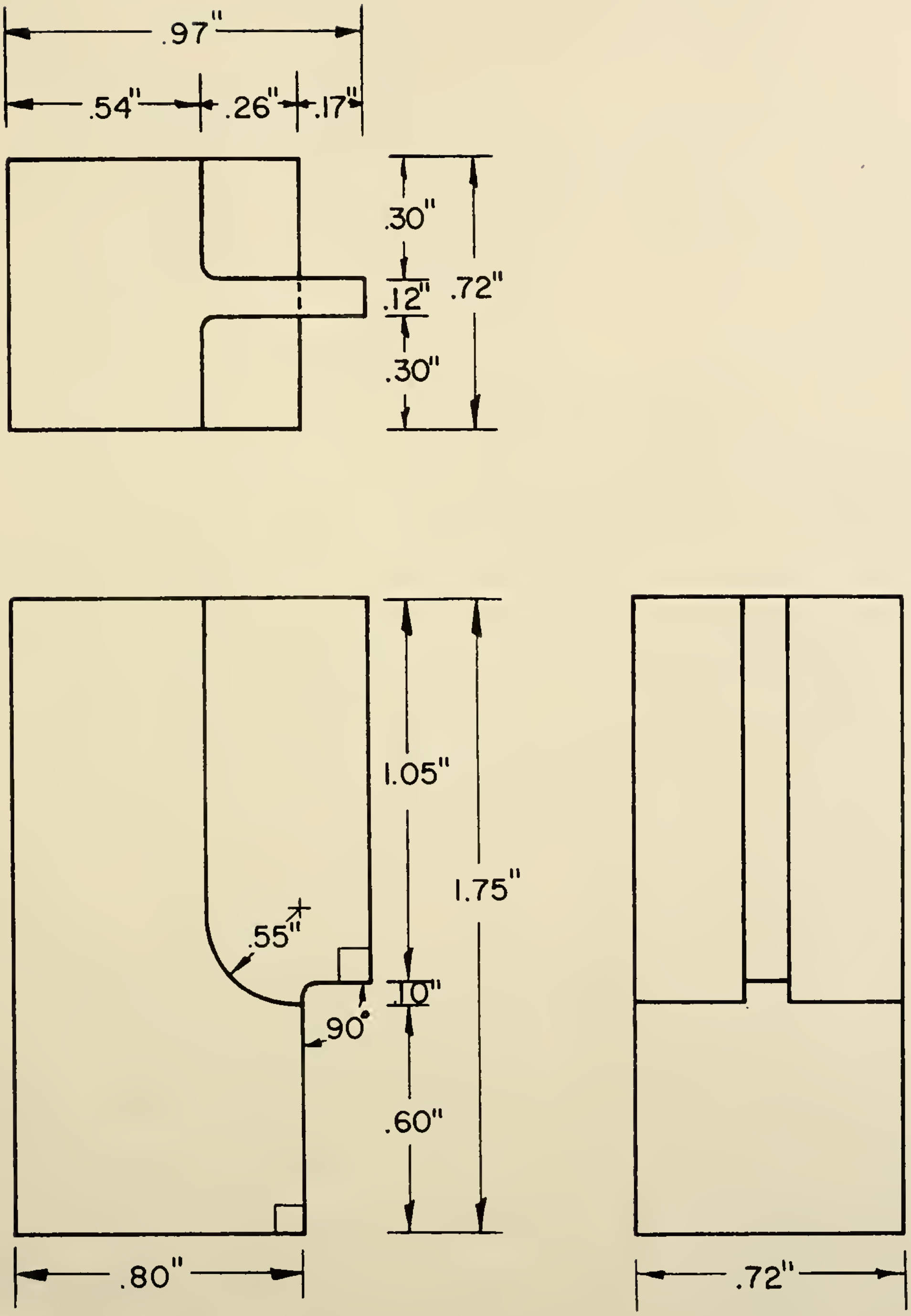

FIGURE 28. JIG FOR SPECIMEN ALIGNMENT

Specimens for shear testing were also cut approximately 0.05 inch oversize from the beam and then ground and polished to test dimensions on a lapping wheel. Final dimensions of the shear test specimens were 1/2 x 1/2 x 2-1/8 inch. The long dimension of the specimen was parallel with the x_1 axis of the beam shown in Figure 24.

Torsion specimens with an outside diameter of 1-1/8 inch were cut from the compacted bituminous mixture and polished on the lapping wheel. The height of the test specimens was 1/2 inch. The axis of the cylindrical torsion specimens was parallel with the x_3 axis of the compacted beam.

After the specimens were polished, they were secured to the specimen holders shown in Figures 5, 8 and 29 by an epoxy formulated from the following components:

Epon (Shell) Resin 828	55% by weight
Epon (Shell) Resin 871	36% by weight
Diethylenetriamine Curing Agent	9% by weight

In some instances Eastman 910 adhesive was used to secure specimens to holders. When the epoxy had hardened, the specimens were placed in the constant temperature room for at least 4 hours prior to testing. Each specimen was tested on the test stand shown in Figure 30. Compression and shear specimens were bolted to the steel plate fixed on the surface of the test stand while the torsion specimens were tested on the frame over the concrete base. Test loads were applied for 30 seconds and load magnitudes were 23.1, 40.8 and 58.3 psi respectively. Test loads for shear and torsion testing

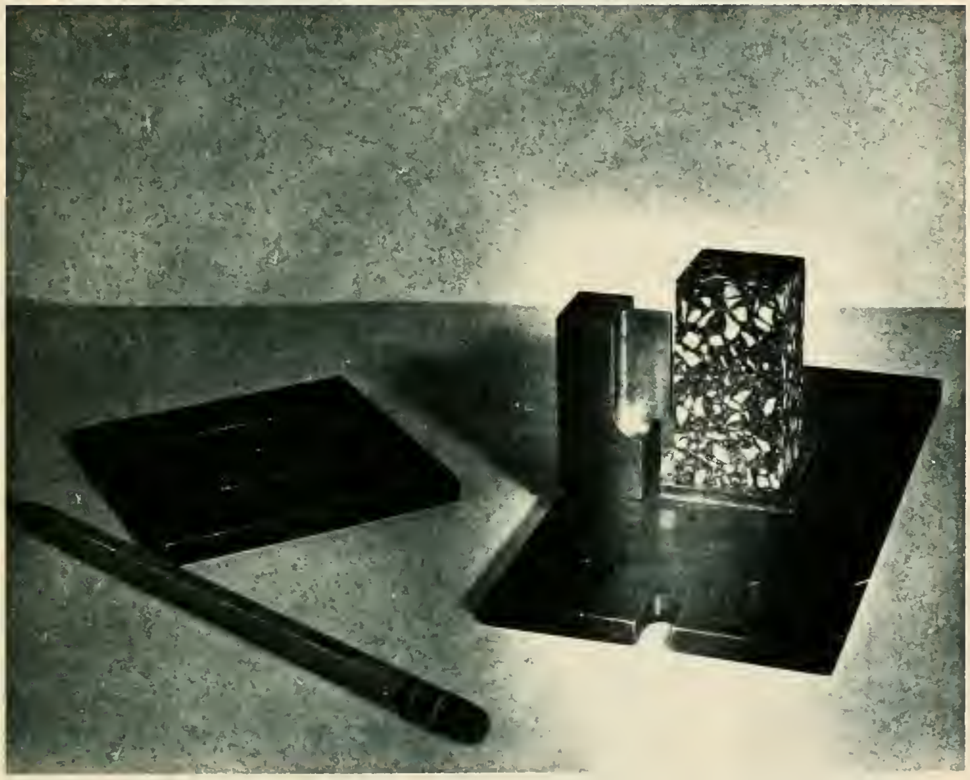

FIGURE 29. UNIAXIAL COMPRESSION SPECIMEN
WITH BASE, TOP AND ALIGNMENT JIG

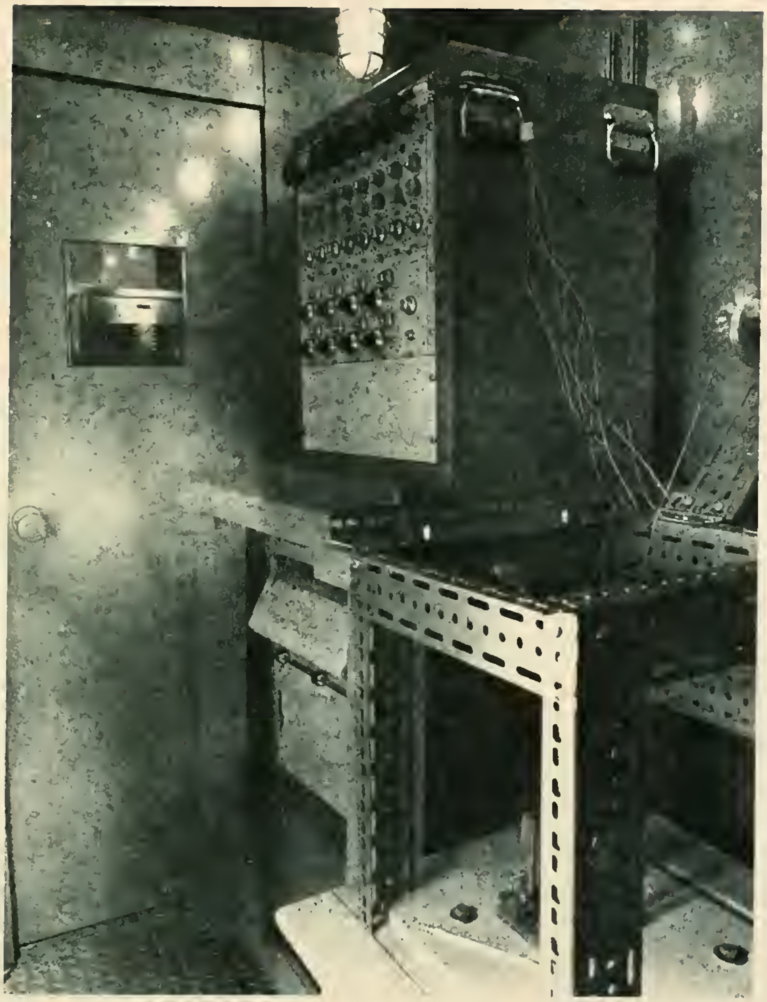

FIGURE 30. INTERIOR OF CONSTANT TEMPERATURE ROOM SHOWING TEST STAND AND RECORDER

were applied by lead weights acting through a wire and pulley arrangement. Compression loads were applied by lead weights resting on a shaft that was seated on the spherical bearing piece shown in Figure 3. The three stresses were applied to specimens at temperatures of 70, 80 and 90°F.

Instrumentation developed for measurement of deformation of the specimens is described in Appendix C.

APPENDIX C

APPENDIX C

Instrumentation

Instrumentation was designed with consideration of the hypothesis that a typical element of bituminous material would exhibit transverse anisotropy. As described in an earlier section, coefficients for transverse anisotropy are measureable in uniaxial compression tests in two orthogonal directions and in shear tests. The measurement of time-dependent strains in both longitudinal and transverse directions was required. From a review of literature and preliminary laboratory investigation, strains of the order of 1×10^{-3} and 1×10^{-4}in/in were expected in the longitudinal and transverse directions, respectively.

The need for a continuous record of time-dependent displacement precluded the use of optical gages or dial gages because considerable time and labor would be involved in collecting data by these means. In addition, physical discomfort involved in reading this type of gage at elevated or depressed temperatures motivated the decision to record deformations electronically (2).

Because it appeared possible to obtain resolution of the small strains that were anticipated by means of a strain gage transducer, instrumentation was developed to measure deformations

by this mode of measurement.

Sample calculations shown in Table 15 illustrate typical magnitudes of loads and strains that were expected in a cantilever type displacement transducer made from a metal beam.

The thin metal beam was used at first with semiconductor strain gages that were required to measure the small strains indicated by the sample calculations. Silicon extrinsic semiconductor gages of the p-type were used initially. Because the output voltage of semiconductor gages is very sensitive to temperature changes, temperature compensation techniques had to be considered.

Initially, two p-type semiconductor gages were used in adjacent arms of a Wheatstone bridge, as shown in Figure 31. This was done to compensate for temperature changes by well-known (6, 7) circuitry techniques. After initial testing in an insulated enclosure in a constant temperature room, it was found that the gages did not give an accurate measurement of strain. The discrepancy was apparently caused by the steep slope of the apparent strain vs. temperature curve for p-type gages (32).

To improve the characteristics of the transducer with respect to temperature stability, metal foil gages were used on plastic beams. Polystyrene plastic was used for the beams and the strain gages were bonded with Eastman 910 adhesive and moistureproofed with a silicon gage-coating compound. A schematic drawing of the transducer and the circuitry involved are shown in Figure 31 and a photograph of a transducer is

TABLE 15

Sample Calculations for Cantilever Transducer

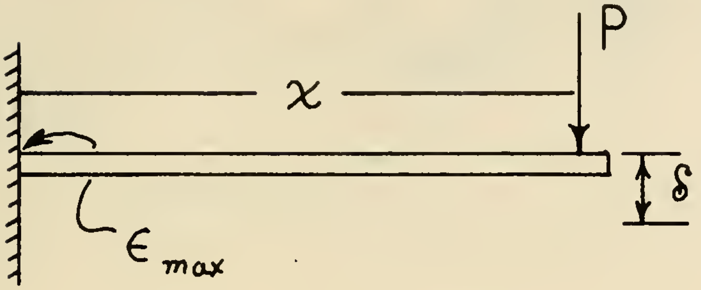

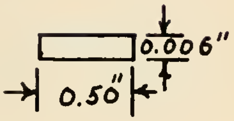

Given: Steel cantilever beam as shown.

Find: P, ϵ_{max} for $\delta = 0.001"$, $X = 2"$, $E = 2.5 \times 10^6$ psi.

$$\delta = \frac{Px^3}{3EI} \quad \text{OR} \quad P = \frac{3EI(.001)}{x^3}, \text{ WHERE } I = \frac{(.50)(.006)^3}{12}$$

$$P = \frac{3(2.5)\times10^6(.5)(.006)^3(.001)}{(8)(12)}$$

$$P = \underline{\underline{8.4 \times 10^{-6}\text{ LB.} = 3.8 \times 10^{-3}\text{ GRAMS}}}$$

DEFLECTION FORCE

$$\sigma_x = E\epsilon_x = \frac{Mc}{I} = \frac{Pxc}{I}$$

$$\epsilon_x = \frac{Mc}{EI} = \frac{Pxc}{EI} = \frac{3EI\delta}{x^2}\,\frac{c}{EI}$$

$$\epsilon_x = \frac{(.003)\cdot c}{x^2} = \frac{(.003)^2}{4} = \frac{9}{4} \times 10^{-6}$$

$$\epsilon_x = \underline{\underline{2.2 \times 10^{-6}\text{ IN./IN}}}$$

STRAIN

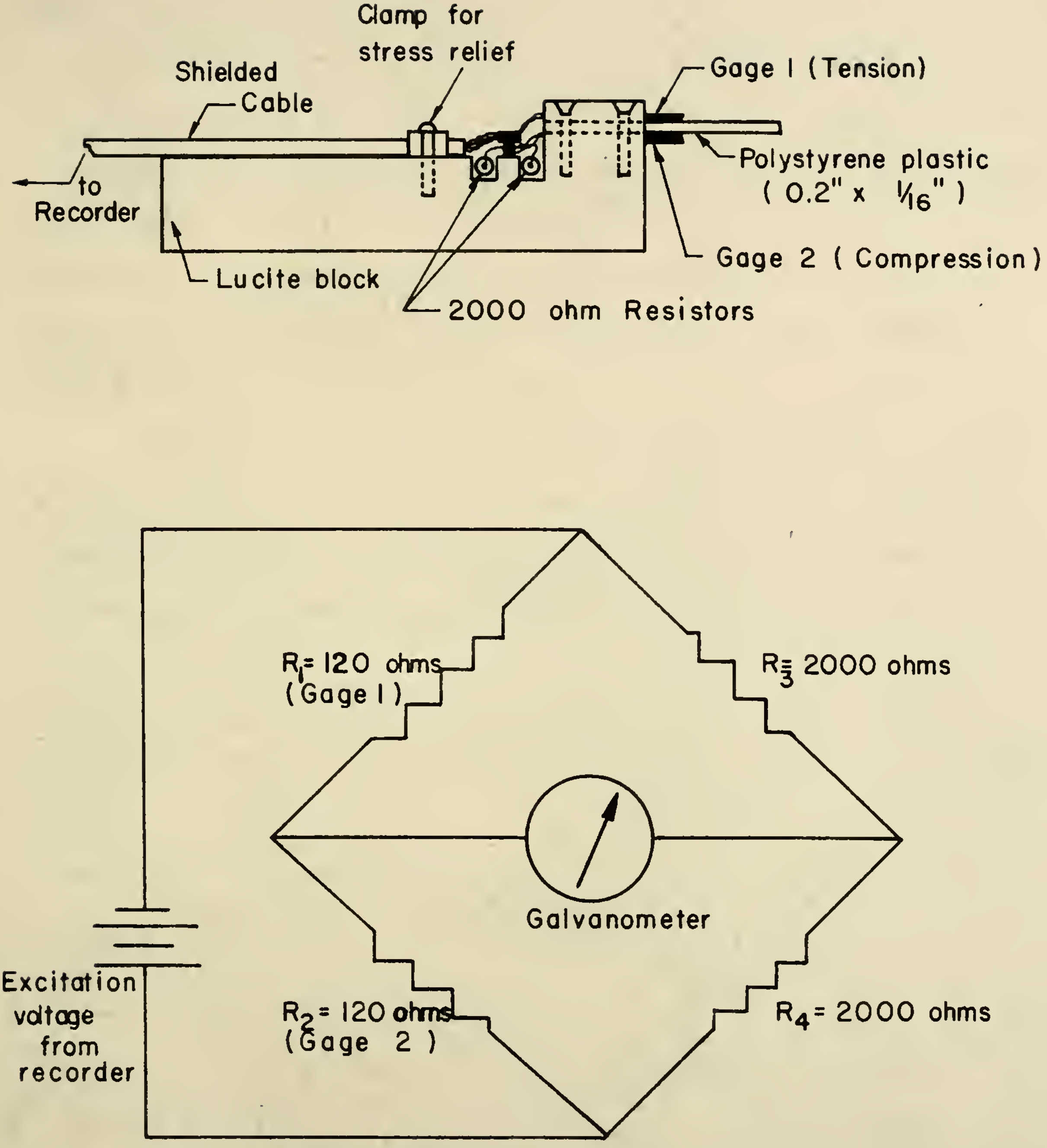

When bridge is balanced, $\frac{R_1}{R_2} = \frac{R_3}{R_4}$

FIGURE 31. SCHEMATIC DIAGRAM OF DISPLACEMENT TRANSDUCER AND WHEATSTONE BRIDGE

shown in Figure 32.

Changes in output voltage from the displacement transducers were amplified and recorded on an eight-channel electronic recorder. Calibration of the transducers was effected by deflecting the end of the cantilever beam with a micrometer and relating this displacement to the magnitude of the pen displacement of the recorder. A typical calibration sheet for some transducers is shown in Table 16.

Transducers were held in place by brass holders secured to the metal surface of the test stand by magnets which were attached to the brass holders by Eastman 910 adhesive. A holder is shown in the photograph of Figure 9.

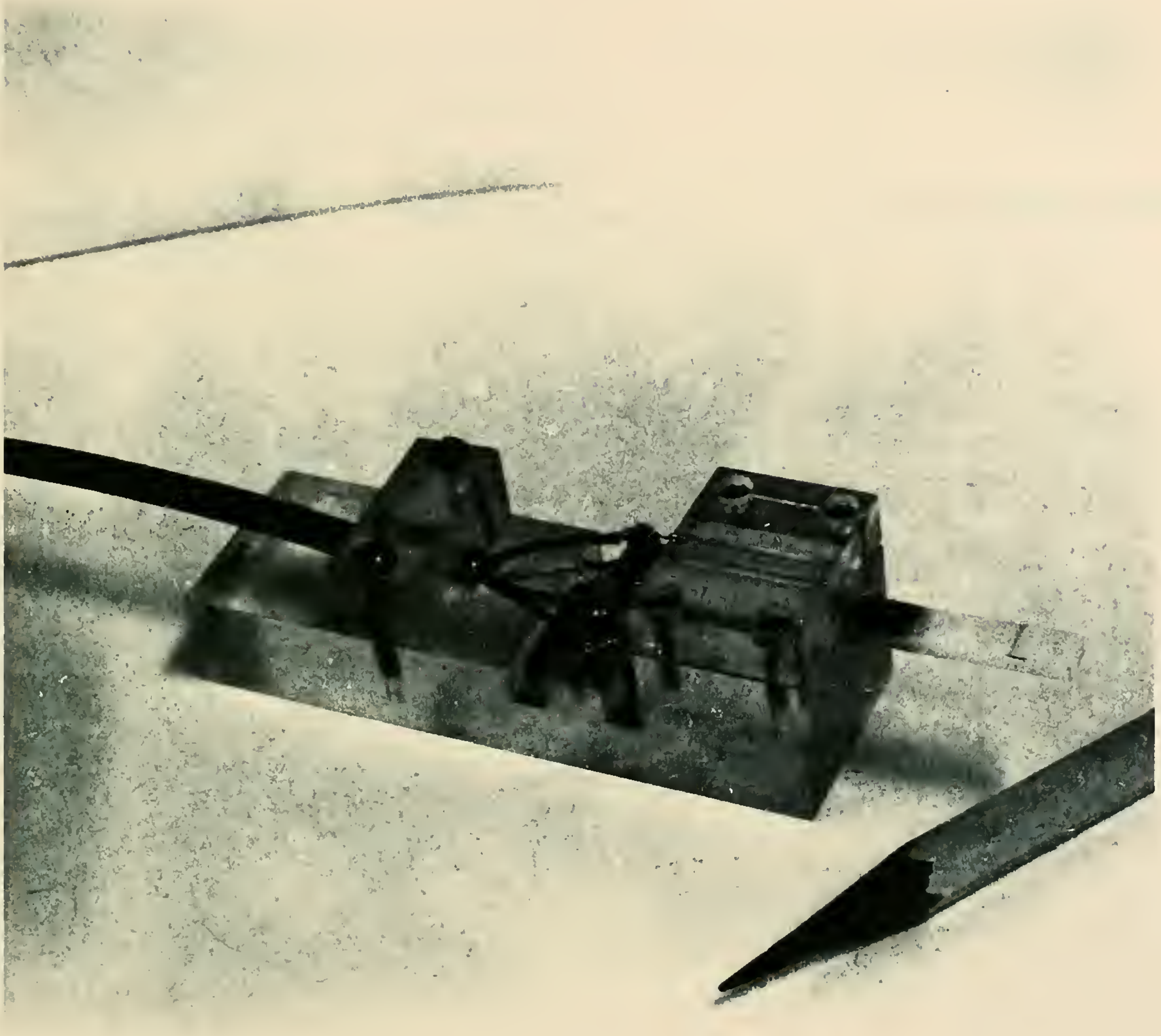

FIGURE 32. DISPLACEMENT TRANSDUCER

TABLE 16

Typical Format for Transducer Calibration (Metal Foil Strain Gages)

Temperature: 75°F
Power amplifier setting: x.02
Preamplifier setting, mv/cm: 2
Beam Displacement, 0.0001 inch: 20

Channel	Gage Length, in.	Pen Displacement,mm.
1	1	25
	3/4	38
4	1	25
	3/4	47
5	1	30
	3/4	47
6	1	34
	3/4	53
7	1	28
	3/4	47
8	1	31
	3/4	53

APPENDIX D

APPENDIX D

TABLE 17

Stiffness Moduli $(\mathrm{x}10^{-4}\mathrm{psi})$

Compression Axis: X_1, 70°F

Time (sec)	23.1 psi	40.8 psi	58.3 psi
5	17.6	15.5	12.9
10	13.4	12.2	9.8
15	11.1	10.1	8.3
20	9.7	9.0	7.3
25	8.6	8.1	6.6
30	7.9	7.4	6.2

Compression Axis: X_3, 70°F

Time (sec)	23.1 psi	40.8 psi	58.3 psi
5	38.5	21.5	30.7
10	27.5	15.6	21.2
15	22.9	13.1	17.4
20	19.4	11.8	15.3
25	17.6	10.7	13.9
30	16.3	10.1	12.9

Compression Axis: X_1, 80°F

Time (sec)	23.1 psi	40.8 psi	58.3 psi
5	10.22	9.52	9.80
10	7.75	7.28	6.98
15	6.70	6.35	5.83
20	5.88	5.71	5.32
25	5.40	5.35	4.90
30	5.11	5.04	4.55

Compression Axis: X_3, 80°F

Time (sec)	23.1 psi	40.8 psi	58.3 psi
5	10.22	9.52	9.80
10	7.75	7.28	6.98
15	6.70	6.35	5.83
20	5.88	5.71	5.32
25	5.40	5.35	4.90
30	5.11	5.04	4.55

TABLE 17 (cont'd.)

Compression Axis: X_1, 90°F

Time (sec)	23.1 psi	40.8 psi	58.3 psi
5	6.48	6.86	7.24
10	4.85	5.07	5.45
15	4.05	4.27	4.66
20	3.60	3.81	4.18
25	3.23	3.43	3.77
30	3.03	3.26	3.57

Compression Axis: X_3, 90°F

Time (sec)	23.1 psi	40.8 psi	58.3 psi
5	8.44	9.80	12.20
10	5.72	6.86	8.53
15	4.73	5.71	7.25
20	4.06	4.91	6.32
25	3.65	4.42	5.80
30	3.35	4.04	5.45

APPENDIX D

TABLE 18

Shear Moduli ($x10^{-4}$psi)

70°F

Time (sec)	23.1 psi	40.8 psi	58.3 psi
5	2.77	3.12	2.23
10	2.42	2.45	1.74
15	2.16	2.02	1.58
20	1.94	1.80	1.44
25	1.76	1.63	1.32
30	1.62	1.56	1.22

80°F

Time (sec)	23.1 psi	40.8 psi	58.3 psi
5	1.76	1.89	1.75
10	1.39	1.49	1.36
15	1.21	1.22	1.19
20	1.07	1.14	1.06
25	0.97	1.07	0.98
30	0.93	1.01	0.91

90°F

Time (sec)	23.1 psi	40.8 psi	58.3 psi
5	0.88	1.01	1.02
10	0.59	0.74	0.76
15	0.47	0.62	0.63
20	0.41	0.54	0.54
25	0.37	0.49	0.48
30	0.35	0.45	0.42

APPENDIX E

APPENDIX E

If stresses are expressed in Taylor's series as functions of several variables (strains):

$$S = K_0 E_0 + K_1 E_1 + \dots$$

If only small strains are considered then

$$S = K_0 E_0 + K_1 E_1$$

When initial strains are neglected this reduces to

$$S = KE$$

The inverse relation $E = K^{-1}S$ exists if the strains are single-valued; hence the relation $E = Cs$ results. This is Cauchy's generalized expression of Hooke's law.

VITA

VITA

Herbert William Busching was born on January 19, 1935, in Chicago, Illinois. He attended the grammar schools of that city and Roselle, Illinois. His high school education was completed at Palatine Township High School, Palatine, Illinois, in June, 1953.

The author completed his undergraduate education at Valparaiso University, Valparaiso, Indiana, in June, 1958. He majored in mathematics and civil engineering and received the Bachelor of Arts degree and the Bachelor of Science in Civil Engineering degree.

After graduation the author was employed by the Indiana State Highway Department for approximately three years. During this time he also served with active and reserve components of the U. S. Army.

In September, 1961, the author returned to school at Purdue University to pursue studies in highway materials. He received the Master of Science in Civil Engineering degree from Purdue in June, 1963. He continued his studies at Purdue in September, 1963, as a graduate assistant.

Mr. Busching is a citizen of the United States. He is married and the father of three children.